A Model for the PTX Properties of H_2O-NaCl

by

Allen Bradley Atkinson Jr.

Thesis submitted to the Faculty of
Virginia Polytechnic Institute and State University
as partial fulfillment of the requirements
for the degree of

MASTER OF SCIENCE
in
GEOLOGICAL SCIENCES

Robert J. Bodnar, Chair
Cahit Coruh
Christine Anderson-Cook

July 16, 2002
Blacksburg, Virginia

Keywords: H_2O-NaCl, fluid inclusions, PTX, vapor pressure, statistical regression analysis, phase equilibria

A MODEL FOR THE PTX PROPERTIES OF H_2O-NaCl

by

Allen Bradley Atkinson Jr.

Robert J. Bodnar, Chair
Dept. of Geological Sciences, Virginia Tech

ABSTRACT

In many geologic environments, fluids have compositions that are approximated by the H_2O-NaCl system. When minerals grow in the presence of such fluids, some of the solution is trapped in the growing mineral as fluid inclusions. The salinity, temperature of homogenization, and pressure of homogenization are required to predict the trapping conditions of the fluid inclusion. In the laboratory the salinity and the temperature of homogenization of the trapped fluid are easily determined however, the pressure of homogenization cannot be determined directly, and must be calculated from an equation of state.

A statistical model that relates the vapor pressure of H_2O-NaCl to the fluid temperature and composition has been developed. The model consists of equations that predict the vapor pressure of H_2O-NaCl from the eutectic temperature (–21.2ºC) to 1500ºC and for all compositions between the pure end-members. The model calculates the vapor pressure based on the composition (wt% NaCl) and the temperature of homogenization, which can be directly obtained from laboratory studies of fluid inclusions. This information in turn can be used to construct the isochore, or line of constant volume, along which the fluid inclusion was trapped. Finally the isochore can be used to determine the temperature and pressure at which the host mineral of the fluid inclusion was trapped.

Dedication

I wish to dedicate this project to my Grandmother "Nana" Mabel Light. She has been a strong influence in my education. Without her help and determination to see me succeed in life, none of this would have happened. Thank you Nana.

Acknowledgments

I wish to thank Dr. Robert J. Bodnar for advising me through this study. I would like to also thank my committee members Dr. Cahit Coruh and Christine M. Anderson-Cook for their help and input into the model development. I would like to thank Alyaa Zahran of the Department of Statistics at Virginia Tech for programming help and guidance in learning and understanding the SAS statistical program that was used for constructing the model. I owe a large debt of gratitude to my family and friends who have supported me throughout my college career.

TABLE OF CONTENTS

List of Figures

List of Figures

List of Tables

A Model for the PTX Properties of H_2O-NaCl

ABSTRACT

In many geologic environments, fluids have compositions that are approximated by the H_2O-NaCl system. When minerals grow in the presence of such fluids, some of the solution is trapped in the growing mineral as fluid inclusions. The salinity, temperature of homogenization, and pressure of homogenization are required to predict the trapping conditions of the fluid inclusion. In the laboratory the salinity and the temperature of homogenization of the trapped fluid are easily determined however, the pressure of homogenization cannot be determined directly, and must be calculated from an equation of state.

A statistical model that relates the vapor pressure of H_2O-NaCl to the fluid temperature and composition has been developed. The model consists of equations that predict the vapor pressure of H_2O-NaCl from the eutectic temperature (–21.2ºC) to 1500ºC and for all compositions between the pure end-members. The model calculates the vapor pressure based on the composition (wt% NaCl) and the temperature of homogenization, which can be directly obtained from laboratory studies of fluid inclusions. This information in turn can be used to construct the isochore, or line of constant volume, along which the fluid inclusion was trapped. Finally the isochore can be used to determine the temperature and pressure at which the host mineral of the fluid inclusion was trapped.

INTRODUCTION

Saline aqueous solutions are common in a wide variety of geologic environments, ranging from seawater (Brown et al., 1995) and basinal brines (Collins, 1975) through deep crustal fluids associated with granulite grade metamorphism (Touret, 1986; Newton et al., 1998) to silicic igneous plutons (Roedder and Bodnar, 1997). When minerals precipitate in these environments some of the fluid is trapped as inclusions (Roedder, 1984). In order to interpret microthermometric data obtained from these fluid inclusions requires information on the pressure, volume, temperature, and composition (PVTX) properties of the fluid. Various workers have shown that PVTX properties of more complex saline aqueous solutions are often more dependent upon salinity than chemical composition, and that the PVTX properties of the fluid are reasonably well approximated by the system H_2O-NaCl (Bodnar, 1983; Zhang and Frantz, 1987).

The H_2O-NaCl system is an example of a binary system in which the solubility curve does not intersect the critical curve (Morey, 1957). The H_2O-NaCl system is characterized by a large region of PTX space in which fluid immiscibility, represented by coexisting higher salinity liquid and lower salinity vapor, is possible (Figure 1). The H_2O-NaCl liquid-vapor two-phase region is bounded by the liquid-vapor curve for pure H_2O, that extends from the triple point of pure water (TP H_2O: T = 0.01ºC, P = 0.006 bar) to the critical point of H_2O (CP H_2O: T = 374.1ºC, P = 220 bars); the ice-liquidus

(L+V+I) or ice melting curve that extends from the triple point of H_2O to the eutectic point (E, I+L+V+Hydrohalite (HH); T = -21.2°C, P ≈ 0.001 bars); the locus of liquid-vapor-hydrohalite triple points (L+V+HH) which extends from the eutectic to the peritectic point, (P, L+V+Halite (H) +HH; T = 0.1°C, P ≈ 0.004 bars); the locus of liquid-vapor-halite triple points (L+V+H) that extends from the peritectic (P) to the NaCl triple point (TP NaCl: T = 801ºC, P ≈ 1 bar); the NaCl liquid-vapor curve that extends from the NaCl triple point to the NaCl critical point (CP NaCl: T ≈ 3327ºC, P ≈ 235 bars). Finally, the liquid-vapor field is bounded by the locus of critical points that extends from the critical point of H_2O to the critical point of NaCl (Figure 1). Within the region of PT space bounded by these various phase surfaces, a given bulk composition may exist as either a single phase liquid or single phase vapor, or may split into two coexisting phases (Sourirajan and Kennedy, 1962; Bodnar et al., 1985a).

Figure 2 shows a representative cooling path for an H_2O-NaCl fluid inclusion that was trapped in the liquid field at Tf, Pf and which homogenizes to the liquid phase. Once trapped, the fluid inclusion will follow the isochore until it intersects the liquid-vapor curve corresponding to the inclusion salinity (Th, Ph; Figure 2). When the isochore intersects the liquid-vapor curve, a vapor bubble will nucleate and grow as the inclusion continues to cool along the liquid-vapor curve. In the laboratory this process can be reversed by heating the inclusion and observing phase changes under the microscope. The homogenization temperature is easily determined in this manner; but the pressure at homogenization (Ph) cannot be directly measured. However, if the inclusion salinity is known, the pressure at Th may be obtained from one of several sources that describe vapor pressures of H_2O-NaCl solutions. Then, the formation conditions (Tf, Pf; Figure 2) can be estimated by calculating the inclusion isochore as described by Bodnar and Vityk (1994).

Experimental data for the H_2O-NaCl system are extensive, with the majority of the data for temperatures below 500ºC. Only a few studies (c.f., Keevil, 1942; Sourirajan and Kennedy, 1962; Urusova, 1974, 1975; Bodnar et al., 1985a; Knight and Bodnar, 1989;) report experimental data for PVTX properties of H_2O-NaCl above 500ºC. Various empirical and theoretical models have been published that describe the PTX properties of H_2O-NaCl (Carlson et al., 1960; Haas, 1976; Pitzer and Pabalan, 1986; Knight and Bodnar, 1989; Anderko and Pitzer, 1993; Bodnar, 1993; Bodnar and Vityk, 1994; Thiéry and Dubessy, 1998). While these and other models adequately describe the PTX properties of H_2O-NaCl, they have limited applicability to fluid inclusion studies because they describe only a limited portion of the system H_2O-NaCl and/or require input not easily obtained by microthermometric analysis of fluid inclusions.

The goal of this study was to develop a model to predict the vapor pressures of H_2O-NaCl solutions as a function of temperature and salinity, using only data easily obtainable through microthermometric analyses of fluid inclusions. This has been accomplished using previously published PTX data for H_2O-NaCl (Table 1).

SOURCES OF PTX DATA FOR H_2O-NaCl

Hundreds of studies have been published describing the PTX properties of H_2O-NaCl. Most of these studies cover only a limited range of PTX space, most report data for only two of the three (PTX) parameters, and very few studies provide data for temperatures

above 500°C. PTX data published before the mid-1970s have been summarized in Potter et al. (1975) and Potter (1978). Some of the more recent PTX data that are relevant to the present study are described below. In the discussion to follow, we first describe those PTX data that define the limits of the liquid + vapor field in the H_2O-NaCl system, followed by those data for vapor pressures of H_2O-NaCl within the two-phase field. Published experimental, theoretical, and empirical data for the H_2O-NaCl system are listed in Table 1. Data used to develop the model described here are marked with an asterisk (Table 1).

Liquid + Vapor Phase Envelope Data

H_2O liquid + vapor (L + V) Curve

Numerous studies have been published that describe vapor pressures along the H_2O liquid + vapor (L + V) curve. In this study we have elected to use the vapor pressures reported by Haar et al. (1984), which is based on a rigorous evaluation and statistical analysis of available PVT data for H_2O (L +V, Figure 1).

Locus of liquid + vapor + ice (L + V + I) triple points

Addition of salt to H_2O results in lowering of the freezing temperature and lowering of the vapor pressure of the H_2O-NaCl liquid + vapor + ice (L + V + I) triple points. As a result, the triple points migrate from the triple point of H_2O (TPH_2O) to lower temperature and pressure with increasing salinity, ending at the eutectic (E; Figure 1). While there have been many studies that have measured the depression of the freezing temperature as a function of salinity, very few workers have determined the vapor pressure along the locus of liquid + vapor + ice triple points. Potter et al. (1978) measured the freezing point of five different H_2O-NaCl solutions and combined these results with previously published data to develop an equation describing freezing point depressions of H_2O-NaCl. More recently, Hall et al. (1988) conducted an experimental study that corrected the higher salinity results published by Potter et al. (1978). Using data from Hall et al. (1988), Bodnar (1993) developed an equation that describes the salinity of H_2O-NaCl liquids as a function of the final ice melting temperature. None of these studies provided data on the vapor pressure along the liquid + vapor + ice phase boundary. However, Burruss and Hollister (1979) report a vapor pressure for the H_2O-NaCl eutectic (T = -21.2ºC, liquid + vapor + ice + hydrohalite) of 0.001 bars, which is essentially identical to the vapor pressure (0.00094 bars) for water ice at this same temperature (Fisher, 1988). Also, Bodnar (2001) noted that equilibrium vapor pressures along the liquid + vapor + ice curve for aqueous solutions having a range of compositions and salinities is approximated by the vapor pressure of pure water ice at the same temperature. Therefore, TX data from Bodnar (1993) were paired with data for the vapor pressure of ice from Fischer (1988) to generate PTX data for the L + V + I curve (Figure 1).

Locus of liquid + vapor + hydrohalite (L + V + HH) triple points

For salinities greater than that at the eutectic point (23.2 wt%), and lower than that at the peritectic point (26.2 wt%; T = 0.1°C), the solid phase in equilibrium with liquid + vapor is hydrohalite, $NaCl \bullet 2H_2O$ (L + V + HH; Figure 1). For vapor pressures along the locus

of liquid + vapor + hydrohalite triple points, we assumed a linear relationship between the pressure at the eutectic (0.001 bars) and that at the peritectic (0.004 bars), and interpolated between these two temperatures to calculate the pressure along the L + V + HH curve.

Locus of liquid + vapor + halite (L + V + H) triple points

Numerous workers have published data for NaCl solubility under vapor-saturated conditions, i.e., along the liquid + vapor + halite (L + V + H) curve. Older data (early 1900's) are summarized in the International Critical Tables published by the National Research Council (1928). Pre-mid-1970s data are summarized in Potter et al. (1975) and Potter (1978). Those studies that cover a significant temperature (and salinity) range and also provide vapor pressure data include Keevil (1942), Sourirajan and Kennedy (1962), Haas (1976), Potter et al. (1977), Pitzer and Pabalan (1986), and Sterner et al. (1988). Morey and Chen (1956) published PT data along the H_2O-NaCl vapor-saturated solubility curve, but did not provide information on the composition. Sterner et al. (1988) developed an empirical relationship for salinity as a function of the halite dissolution temperature along the L + V + H curve, and also presented vapor pressures along the solubility curve.

In this study, data from Keevil (1942), Haas (1976), Sterner et al. (1988) and Bischoff and Pitzer (1989) were used to model the three-phase liquid + vapor + halite curve in the H_2O-NaCl system. The triple point of NaCl (T = 801°C, P = 0.0005 bars) reported by Pitzer and Pabalan (1986) was also used.

NaCl liquid + vapor (L + V) curve

Ewing and Stern (1974) experimentally determined the PTX properties of NaCl along the liquid-vapor curve up to 967°C. These data were combined with PT data for the critical point of NaCl (T ≈ 3327°C, P ≈ 235 bars; CPNaCl, Figure 1) from Carlson et al. (1960) to model PT conditions along the NaCl liquid + vapor curve (L-V NaCl, Figure 1).

Locus of H_2O-NaCl critical points

Ölander and Liander (1950), Carlson et al. (1960), Sourirajan and Kennedy (1962), Khaibullin and Borisov (1966), Urusova (1974), Bischoff and Pitzer (1989) and Knight and Bodnar (1989) have published critical point data for the system H_2O-NaCl. Marshall and Jones (1974) and Marshall (1990) also present critical data for H_2O-NaCl solutions as a function of temperature, however, the critical pressure was not included in their study.

The critical data from Bischoff and Pitzer (1989) show good agreement with the data of Knight and Bodnar (1989) and Khaibullin and Borisov (1966), and the TX projection of the Knight and Bodnar data show good agreement with the theoretical TX projection of Marshall (1990). Data from Bischoff and Pitzer (1989), Knight and Bodnar (1989) and Khaibullin and Borisov (1966) were used along with data for the critical point of NaCl from Carlson et al. (1960) to constrain the location of the H_2O-NaCl critical curve. Data from Ölander and Liander (1950) were not used to define the critical curve because these data differ significantly from the other studies.

Critical data for H_2O-NaCl are available for compositions up to 30 wt% NaCl, and for pure NaCl. This leaves a gap between 30 and 100 wt% NaCl, corresponding to

temperatures from 820° and 3327°C. To generate data to constrain the locus of critical points between 30 and 100 wt% NaCl, equation 1 from Knight and Bodnar (1989) was used to define the TX conditions up to 21 wt% NaCl (584°C). Note that the location of the critical curve for compositions greater than 30wt% NaCl is not constrained by experimental data and is only used to define an end-point for liquid-vapor curves in this study. Then, a smooth curve was drawn connecting the lower salinity (and lower temperature) with the pure NaCl critical point. The shape of the curve was drawn to be consistent with the locus of critical points shown schematically in Figure 1. The TX curve determined in this manner is shown in Figure 3, and is described by the following relationship from 21 to 100 wt% NaCl:

$$T(^{o}C) = 586.5 - (20.647 * X) + (1.119 * X^2) - (6.369x10^{-4} * X^3)$$

where X is salinity in weight percent. The TX projection of the critical curve determined in this manner is shown on Figure 3.

Critical pressures were generated using equation 4 from Knight and Bodnar (1989) for salinities up to and including 20 wt% NaCl. The shape of the curve was drawn to be consistent with the locus of critical points shown schematically in Figure 1. The PT curve determined in this manner is shown in Figure 4, and is described by the following relationship from 20 to 100 wt% NaCl:

$$P(bars) = -2074 + (418 * T_K) - (9.8 * T_K^2)$$

where T_K is equal to temperature (in Kelvins) divided by 100. The PT projection of the critical curve using temperatures and pressures calculated as described above is shown on Figure 4.

Data within the two-phase (liquid + vapor) field

Numerous workers have published PTX data for H_2O-NaCl within the two-phase liquid + vapor field (L + V, Figure 1). Pre-mid-1970s data are summarized in Potter et al. (1975) and Potter (1978). Most of these studies are limited to low temperatures (< 200° - 300°C). Sourirajan and Kennedy (1962), Fabuss and Korosi (1966), Khaibullin and Borisov (1966), Urusova and Ravich (1971), Urusova (1975), Haas (1976), Bodnar et al. (1985a), Bischoff et al. (1986), and Bischoff and Pitzer (1989) have published liquid + vapor phase equilibrium and/or vapor pressure data for H_2O-NaCl that cover a wide range of temperatures and salinities.

Data from Fabuss and Korosi (1966), Khaibullin and Borisov (1966), Haas (1976), Bodnar et al. (1985a) were all in reasonably good agreement and were used in model development. Bischoff and coworkers (Bischoff et al., 1986; Bischoff and Rosenbauer, 1988; Bischoff and Pitzer, 1989; Bischoff, 1991) conducted a series of experimental and theoretical studies of PVTX properties of H_2O-NaCl from 300º to 500ºC and from 58 to 581.8 bars. These data are in agreement with other published experimental data for H_2O-NaCl except those of Sourirajan and Kennedy (1962), which showed higher vapor pressures than the trend presented by Bischoff and Pitzer (1989). Data from Sourirajan and Kennedy (1962) were not used in model development because compositions of the liquid phase are not given, except for liquids on the three-phase (L + V + H) curve and these data are from Keevil (1942). Data from Urusova (1975) and Urusova and Ravich (1971) were not used in model development.

High temperature, high salinity region
Very few data are available for temperatures above 500ºC (Carlson et al., 1960; Urusova, 1974, 1975; Bodnar et al., 1985a; Pitzer and Pabalan, 1986; Knight and Bodnar, 1989). Keevil (1942) presents data for salinities up to 77 wt% NaCl (646.2°C) along the liquid + vapor + halite curve, and Bodnar et al. (1985a) present limited data within the liquid + vapor field up to 1000°C (72.9 wt% NaCl). Ewing and Stern (1974) present data along the NaCl liquid + vapor curve to 967°C. Thus, no data are available to constrain the model between about 1000° and 3327°C (the critical temperature of NaCl). Due to the lack of data in this large region of PTX space, the liquid + vapor curves predicted in early versions of the predicted crossing isopleths in the high temperature region in violation of thermodynamic constraints on phase equilibria (Pichavant et al., 1982; Ramboz et al., 1982).

To eliminate this problem, synthetic data points were generated for use in model development by drawing smooth isoplethal curves from the L + V + H triple point curve to the locus of critical points (Figure 4). Incorporating these data into the regression model described below resulted in predicted vapor pressures that are consistent with the inferred topology of the H_2O-NaCl system (c.f., Pitzer, 1984; Pitzer and Pabalan, 1986; Anderko and Pitzer, 1993). Moreover, these high temperature predictions merged smoothly with available lower temperature data. However, it should be recognized that the isopleths for salinities greater than about 70 wt% and/or temperatures greater than about 1000°C are unconstrained by experimental data.

MODEL DEVELOPMENT

The goal of this study was to develop a mathematically simple empirical model describing the relationship between vapor pressure of H_2O-NaCl solutions as a function of temperature and salinity. A prime consideration was that the model should be "user friendly" to facilitate and encourage its use. While the accuracy of vapor pressure prediction was certainly important, this was not the most important criterion used to evaluate the success of the model. [We do not wish to minimize the importance of accuracy in research. The decision to sacrifice maximum accuracy in return for a topologically correct model that covers the complete range of PTX conditions encountered in crustal and upper mantle environments is based on the fact that natural inclusions rarely contain only H_2O-NaCl. Thus, the uncertainty in predicted inclusion formation pressures resulting from inaccuracy of the model is considered to be small compared to errors associated with natural fluid compositional variations.] As such, the goal was to produce a "reasonably accurate" numerical model that predicts the correct topology for the H_2O-NaCl system. Specifically, the model was required to have the following monotonicity characteristics (Figure 5):

- At any temperature T, the vapor pressure P of a solution with a salinity $X + \Delta X$ is lower than the vapor pressure of a solution with a salinity X.
- The critical temperature of a solution with a salinity $X + \Delta X$ is higher than the critical temperature of a solution with a salinity X.

- For a given salinity, the vapor pressure at temperature T + ΔT is greater than the vapor pressure at temperature T.

This topology is consistent with the colligative properties of electrolyte solutions (freezing point depression, vapor pressure lowering and boiling point elevation) (Barrow, 1973). An important implication of these constraints is that no two liquid isopleths may intersect (of course, a liquid isopleth and a vapor isopleth may intersect; Bodnar et al. 1985).

Data for PTX properties of H_2O-NaCl were compiled and examined for consistency within individual data sets and between data sets. When there was disagreement between data sets, the various data sources were evaluated to determine which data were more correct. When a satisfactory explanation for the differences could not be identified, those data that were more consistent with larger data sets or which were more generally accepted by the scientific community were used. Data from Sourirajan and Kennedy (1962) showed considerable difference from most other published sources with exception of Keevil (1942). Anderko and Pitzer (1993) presented vapor pressure data for critical conditions that were elevated compared to other studies and did not fit the trend for the locus of critical points when compared to PTX data reported by other authors. The data that were excluded from the regression analysis accounted for less than 2% of all the data listed in Appendix A.

Experimental PTX data as well as some previously compiled data (c.f., Haas, 1976; Haar et al., 1984) were assembled and evaluated for consistency with the other published data (Table 1). Data that did not fit the overall data trend were removed and not used in the regression model. A complete list of all data used in the regression analysis is presented in Appendix A.

Weighted linear regression analysis was used to model the vapor pressure of H_2O-NaCl with a seventh-order polynomial equation. This order of polynomial with all cross-product terms of T and X was selected because it balanced relative simplicity with quality of fit to the data. The model was designed to fit the equation parameters with the form:

$$\mathrm{Log}_{10}(P) = B_{00} + B_{01}X + B_{10}T + B_{11}X*T + B_{20}T^2 + B_{12}T*X^2 \ldots + B_{07}X^7 + B_{70}T^7 + \Sigma$$

where P = vapor pressure in bars, T = temperature in Kelvins/100, X = weight percent NaCl/100, B_{ij} = fitting parameters for the terms, T^i and X^j, estimated by using weighted least squares regression, Σ = errors (0, σ^2 W), 0 represents central location of residuals, σ^2 = variance (spread) of residuals, and W = weight ((1.0001-X)/1.0001)*(2.5/T). The weighting function W is more dependent upon salinity than temperature. This gave salinities with lower concentrations and at lower temperatures a higher weight. This method of weighting was used because of the greater coverage of experimental PTX data that define the lower temperature, lower salinity portion of the H_2O-NaCl liquid + vapor region. Converting pressures to the $\log_{10}$ scale minimized errors associated with the six order of magnitude of variation in pressure over the temperature and composition range studied. That is, errors appeared to be proportional to the response value (multiplicative error), so reducing the range in magnitude of the response variable (P) reduced fitting

errors at higher pressure. By giving different weights to the data, a better fit was obtained at lower temperatures and salinities.

Model development to determine which terms to include in the final model utilized a stepwise, backward elimination regression approach. The model results were compared to published data and evaluated by examining differences from the published results.

The goal of this study was to produce a relatively simple model describing the PTX behavior of H_2O-NaCl over the range of PTX conditions encountered in the earth's crust. The initial model tested was a simple first order equation. Vapor pressures predicted by the model were compared with published values. Progressively higher order models were considered and for each model that was evaluated, percent errors $((\{Vp_{published} - Vp_{predicted}\}/Vp_{published})x\ 100)$ and the fit "monotonicity rules" described above were examined. A further criterion for success was that the model results must predict the correct topology of the H_2O-NaCl system as described above. We defined a successful model as one that predicted vapor pressures within ± 5% of the known (or experimental) value for at least 90% of the data. If the model failed to meet the fit criteria for the residuals (90% of errors within ± 5%) and topology restrictions, a higher order polynomial was tested. Finally, success was evaluated based on the percentage of the predicted values with large errors (>5%) that fell within the temperature and composition range (50º - 1000ºC, 0 – 90 wt% NaCl) corresponding to most fluid inclusions formed at crustal PTX conditions. That is, a larger error was considered to be acceptable in that region of PTX space where few fluid inclusions are trapped, which also corresponds to the PTX region in which there are few data to constrain the model. This process continued until all criteria were satisfied and any further increase in the order of the polynomial equation did not substantially improve the overall fit of the model.

In evaluating the quality of fit of the model, it is important to remember that over the range of temperature (-21.2º to 1500ºC) and salinity (0 – 100 wt% NaCl) that the model applies, the vapor pressure varies by 6 orders of magnitude (from about 0.001 bars at the H_2O-NaCl eutectic to about 2400 bars at the maximum on the locus of critical points). Thus, a 1 bar error for a vapor pressure of 1000 bars is small in an absolute sense and as a percentage error, where as the same 1 bar error for a vapor pressure of 0.1 bar is small in an absolute sense but very large in a relative sense. For this reason, both the absolute error and the percentage error were considered in evaluating the degree of fit. Finally, it should be noted that the main goal of this effort was to produce a simple model to predict vapor pressures of H_2O-NaCl to interpret microthermometric results from fluid inclusions. Specifically, the vapor pressure at homogenization simply represents the trapping pressure for inclusions trapped in a boiling (immiscible) system, or the starting pressure (P) and temperature (T) for the isochore for an inclusion trapped in the single-phase liquid field. As very few (none?) natural inclusions have homogenization temperatures below about 25ºC, or have salinities greater than about 90 wt% NaCl, relatively larger errors in these regions were considered to be acceptable. Thus, while the final model predicts reasonably accurate vapor pressures in that part of the H_2O-NaCl system that is most applicable to fluid inclusion studies (50º < T < 1000ºC, 0 < X < 90 wt% NaCl), somewhat larger errors result outside of this range as described below. Finally, the predicted vapor pressure was evaluated for general adherence to the topology rules for the H_2O-NaCl system as mentioned above.

The original plan was to develop a single equation that would predict vapor pressures for H_2O-NaCl over the range of PTX conditions encountered in the earth's crust. However, this approach was abandoned when it was found that one *simple* equation would not represent H_2O-NaCl PTX phase equilibria over the entire liquid-vapor region and satisfy the required monotonicity conditions. It was then decided to use two equations to represent H_2O-NaCl PTX equilibria, one below the critical temperature of H_2O (374.1ºC, Equation 1; Table 2) and one above (Equation 3; Table 4). The equations reasonably predict the vapor pressures of H_2O-NaCl from –21.2º to 1500ºC, but a slight discontinuity in slope was found where the equations merged at 374°C. A third equation (Equation 2; Table 3) was developed to produce a smooth merger between equations 1 and 3 (Figure 6) as described below. Note that the region above 1500°C, where no experimental data exist, is not described by any of the equations.

Equation 1 adequately describes vapor pressures from –21.2º to 374ºC (Equation 1, Table 2). The equation has an R^2 value of approximately 1.000. The R^2 is the fraction of the variability of the response, pressure, explained by the model (Montgomery and Peck, 1992). The high temperature equation (Equation3; Table 4) predicts vapor pressures for H_2O-NaCl solutions between 350ºC and 1500ºC and with an R^2 of approximately 0.9983.

Although, the low temperature (Equation 1) and high temperature (Equation 3) equations adequately represent the experimental data (i.e., the residuals are within the acceptable limits), a minor discontinuity in slopes was observed where the equations joined. A third equation (Equation 2, Table 3) was developed to span the temperature range where the low and high temperature equations converge to remove the discontinuity. The merge equation covers the temperature range 300º-484ºC and has an R^2 of approximately 1.000. The merge equation was developed using the predicted values from equations 1 and 3 between 250º and 500ºC. An equation of the same form as that used for the low temperature (Equation 1) and high temperature (Equation 3) equations was used. The merge equation (Equation 2) joins smoothly with the low temperature equation at 300°C, and with the high temperature equation at 484°C, resulting in a smooth continuous vapor pressure curve up to 1500°C or the critical temperature, whichever is lower. Figure 7 shows the comparison of predicted pressures where equations 1 and 2 merge at 300ºC, and Figure 8 shows the comparison of predicted pressures where equations 2 and 3 merge at 484ºC. Selected isopleths spanning the temperature range where the low and high temperature equations join are shown on Figure 9.

COMPARISON OF PREDICTED AND EXPERIMENTAL VALUES

Figure 10 is a summary histogram showing the agreement between predicted vapor pressures and published data. According to Figure 10, 90% of the predicted values are within ± 5% of published values. All of the data from National Research Council (1928), Fabuss and Korosi (1966), Haas (1976), Haar et al. (1984) and Bodnar (1993, using the vapor pressure of H_2O-ice from Fisher, 1988) are predicted within ± 5% by the model. Most of the data from Khaibullin and Borisov (1966) Keevil (1942) Sourirajan and Kennedy (1962) and Knight and Bodnar (1989) are predicted within ± 10% by the model. Most of the data from Bodnar et al. (1985a), Bischoff and Pitzer (1989), and the single

data point from Carlson et al. (1960) show poorer agreement with model predictions, differing by more than ± 10%. Data from Sourirajan and Kennedy (1962) are included in Figure 10, because data from Sourirajan and Kennedy are often used to interpret microthermometric results from fluid inclusions even though these data were not used in model construction.

Figure 11 compares the predicted vapor pressure for a composition of 20 wt% NaCl with published data for this same composition (Khaibullin and Borisov, 1966; Urusova and Ravich, 1971; Urusova, 1974,1975; Haas, 1976; Bischoff and Pitzer, 1989; Knight and Bodnar, 1989) and shows good agreement between the predicted and published pressures with exception to Urusova (1974). Figure 12 is a comparison of predicted and published data showing close agreement for critical points of H_2O-NaCl solutions with exception of Sourirajan and Kennedy (1962). Figure 13 compares predicted and published vapor pressures along the liquid + vapor + ice curve. Figure 14 compares predicted and published vapor pressures along the liquid + vapor + halite curve and shows close agreement between the predicted and published data. Figure 15 compares predicted and published vapor pressures along the pure H_2O liquid + vapor curve.

PREDICTED PHASE EQUILIBRIA AND APPLICATIONS

Due to the ~6 order of magnitude range in pressure in going from the eutectic (P = 0.001 bar) to the maximum on the critical locus (P ≈ 2400 bar), it is not possible to show all calculated PTX data on a single diagram. As a result, phase relations predicted by the model are shown in a series of PT diagrams (Figures 16 - 23). PX relationships are shown in Figures 24 and 25, and Figure 26 is a TX projection predicted by the model.

Application of the model described here to interpret results from fluid inclusion studies can best be described with a few examples. Consider a two-phase (liquid + vapor) fluid inclusion that has an ice melting temperature of -6.6°C and a homogenization temperature of 250°C. According to Bodnar (1993), an ice melting temperature of -6.6°C corresponds to a salinity of 10 wt% NaCl. Using the model developed here, the vapor pressure curve for 10 wt% NaCl has been calculated and is shown on Figure 27. Using the technique described by Bodnar (1983) and Bodnar et al. (1985b), the inclusion described above is estimated to contain 17 volume percent vapor at room temperature. During heating, the bubble will shrink and disappear at the homogenization temperature of 250°C, and the internal pressure in the inclusion at homogenization will be 37 bars. If there is evidence that the fluid inclusion was trapped in a boiling system, then the homogenization temperature and pressure are equal to the trapping temperature and pressure. If no evidence of boiling is observed, then the inclusion was trapped at some temperature and pressure along the isochore that originates at 250°C and extends into the one-phase liquid field (Figure 27). The inclusion isochore has a slope of 13.9 bars/°C (Bodnar and Vityk, 1994). Thus, if the inclusion were trapped at 350°C, the trapping pressure would be 1427 bars (Figure 27).

As another example, consider a two-phase (liquid + vapor) fluid inclusion that has a hydrohalite melting temperature of –8.6°C and a homogenization temperature of 400°C. According to data from Sterner et al. (1988), a hydrohalite melting temperature of –8.6°C corresponds to a salinity of 25 wt% NaCl. The vapor pressure curve for 25 wt% NaCl

has been calculated and is shown on Figure 28. Using the technique described by Bodnar (1983) and Bodnar et al. (1985b), the inclusion described above is predicted to contain 28 volume percent vapor at room temperature. During heating, the bubble will shrink and disappear at the homogenization temperature of 400°C, and the internal pressure in the inclusion at homogenization will be 224 bars. As described in the previous example, if the fluid inclusion was trapped in a boiling system, then the homogenization temperature and pressure are equal to the trapping temperature and pressure. If no evidence of boiling is observed, then the inclusion was trapped at some temperature and pressure along the isochore that originates at 400°C and extends into the one-phase liquid field (Figure 28). The inclusion isochore has a slope of 8.9 bars/°C (Bodnar and Vityk, 1994). Thus, if the inclusion were trapped at 600°C, the trapping pressure would be 2004 bars.

For a final example, consider a three-phase (liquid + vapor + halite) fluid inclusion that has a halite melting temperature of 323°C and a homogenization temperature of 600°C. According to Sterner et al. (1988), the solubility of NaCl in water at 332°C is 40 wt%. The vapor pressure curve for 40 wt% NaCl has been calculated and is shown on Figure 29. During heating, the halite will shrink and disappear at 323°C, while the bubble will disappear at 600°C. The internal pressure in the inclusion at homogenization will be 603 bars. As described in the previous example, if the fluid inclusion was trapped in a boiling system, then the homogenization temperature and pressure are equal to the trapping temperature and pressure. If no evidence of boiling is observed, then the inclusion was trapped at some temperature and pressure along the isochore that originates at 600°C and extends into the one-phase liquid field (Figure 29). The inclusion isochore has a slope of 7.5 bars/°C (Bodnar and Vityk, 1994). Thus, if the inclusion were trapped at 800°C, the trapping pressure would be 2102 bars (Figure 29).

SUMMARY

The system H_2O-NaCl is a binary H_2O-salt system that can be used as a suitable analog for understanding the PTX conditions of more complex saline-aqueous solutions, which are found in a wide range of geologic crustal environments. H_2O-NaCl filled inclusions yield information about formation (trapping) conditions that can be inferred from measurements taken from microthermometric studies. PTX conditions for the liquid + vapor region range from 0.001 to ≈ 2400 bars, –21.2º to ≈ 3327ºC and 0 to 100 wt% NaCl.

Previous PTX studies of the system H2O-NaCl have been summarized within this study. Numerous studies have focused on the PTX phase equilibria of H_2O-NaCl, with most experimental data at or below 500ºC. Most previous theoretical and empirical models have presented methods to determine the PTX conditions of H_2O-NaCl solutions and do not allow calculation of vapor pressures with measurements taken directly from microthermometric phase equilibria studies. This study has empirically determined the PTX relations of the system H_2O-NaCl for temperatures up to 1500ºC and for salinities ranging from 0 to 100 wt% NaCl with predicted pressures up to ≈ 2400 bars. This model will be useful for fluid inclusion research because it will allow vapor pressure calculation from microthermometric data observed from phase equilibria changes. The model predicts vapor pressures for saline-aqueous filled fluid inclusions from

microthermometric measurements directly obtained from fluid inclusion heating and freezing studies.

References:

Anderko A, Pitzer KS (1993) Equation-of-state representation of phase equilibria and volumetric properties of the system NaCl-H_2O above 573K. *Geochim. Cosmochim. Acta*, **57**, 1657-1680.

Barrow GM (1973) Physical Chemistry: third edition W. P. Orr and L. Warner. New York, NY: McGraw-Hill pp. 787.

Bischoff JL (1991) Densities of liquids and vapors in boiling NaCl-H_2O solutions: A PVTX summary from 300º to 500ºC. *Amer. J. Sci.*, **291**, 309-338.

Bischoff JL, Pitzer KS (1989) Liquid-vapor relations for the system NaCl-H_2O: summery of the PTX surface from 300º to 500ºC. *Amer. J. Sci*., **289**, 217-248.

Bischoff JL, Rosenbauer RJ (1988) Liquid-vapor relations in the critical region of the system NaCl-H_2O from 380º to 415ºC: A refined determination of the critical point and two-phase boundary of seawater. *Geochim. Cosmochim. Acta*, **52**, 2121-2126.

Bischoff JL, Rosenbauer RJ, Pitzer KS (1986) The system NaCl-H_2O: Relations of vapor-liquid near the critical temperature of water and of vapor-liquid-halite from 300º to 500ºC. *Geochim. Cosmochim. Acta*, **50**, 1437-1444.

Bodnar RJ (1983) A method of calculating fluid inclusion volumes based on vapor bubble diameters and P-V-T-X properties of inclusion fluids. *Econ. Geology*, **78**, 535-542.

Bodnar RJ (1993) Revised equation and table for determining the freezing point depression of H_2O-NaCl solutions. *Geochim. Cosmochim. Acta*, **57**, 683-684.

Bodnar RJ (1995) Experimental determination of the PVTX properties of aqueous solutions at elevated temperatures and pressures using synthetic fluid inclusions: H_2O-NaCl as an example. *Pure & Appl. Chem*., **67**, 873-880.

Bodnar RJ (2001) PTX phase equilibria in the H_2O-CO_2-salt system at Mars near-surface conditions. In *Lunar and Planetary Science XXXII*, Abstract # 1689, Lunar and Planetary Institute, Houston (CD-ROM).

Bodnar RJ, Burnham C W, Sterner SM (1985a) Synthetic fluid inclusions in natural quartz. III. Determination of phase equilibrium properties in the system H_2O-NaCl to 1000ºC and 1500 bars. *Geochim. Cosmochim. Acta*, **49**, 1861-1873.

Bodnar RJ, Reynolds TJ and Kuehn CA (1985b) Fluid inclusion systematics in epithermal systems. *In.* Geology and Geochemistry of Epithermal Systems, BR

Bodnar RJ, Vityk MO (1994) Interpretation of Microthermometric data for H_2O-NaCl fluid inclusions. In: De Vivo B. and Frezzoti M. L. (eds) *Fluid Inclusions in Minerals: Methods and Applications*. Blacksburg, VA: Virginia Tech, pp. 117-130.

Brown E, Colling A, Park D, Phillips J, Rothery D, Wright J (1995) Seawater: Its composition, properties and behaviour, second edition. Pergamon, Walton Hall, Milton Keynes MK7 6AA. 168 pp.

Burruss RC, Hollister LS (1979) Evidence from fluid inclusions for a paleogeothermal gradient at the geothermal test well sites, Los Alamos, New Mexico. *J. Volcanology and Geothermal Research*, **5**, 163-177.

Carlson CM, Eyring H, Ree T (1960) Significant structures in liquids, III. Partition function for fused salts. *Proceedings of the National Academy of Sciences of the United States of America*, Vol. 46, No. 3. (Mar. 15, 1960), pp. 333-336.

Collins AG (1975) Geochemistry of oilfield waters, Elsevier Scientific Publishing Co., New York, 496 pp.

Ewing CT, Stern KH (1974) Equilibrium vaporization rates and vapor pressures of solid and liquid sodium chloride, potassium chloride, potassium bromide, cesium iodide, and lithium fluoride. *J. Physical Chem.,* **78**, 1998-2005.

Fabuss BM, Korosi A (1966) Vapor pressures of binary aqueous solutions of NaCl, KCl, Na_2SO_4, and $MgSO_4$ at concentrations and temperatures of interest in desalination processes. *Desalination,* **1**, 139-148.

Fisher G (ed) (1988) Landolt-Bornstein, Numerical Data and Functional Relationships in Science and Technology, Volume 4, Subvolume b, Physical and Chemical Properties of Air, Springer-Verlag, Heidelberg.

Haar L, Gallagher TS, Kell GS (1984) NBS/NRS Steam Tables: Thermodynamic and transport properties and computer programs for vapor and liquid states in SI units. Hemisphere, Washington, DC, 120 p.

Haas JL, Jr. (1976) Thermodynamic properties of the coexisting phases and thermochemical properties of the NaCl component in boiling NaCl solutions. Preliminary steam tables for NaCl solutions. Geol. Surv. Bull. 1421-B, 1-71.

Hall DL, Sterner SM, Bodnar RJ (1988) Freezing point depression of NaCl-KCl-H_2O solutions. Econ. Geology, **83**, 197-202.

Keevil NB (1942) Vapor pressures of aqueous solutions at high temperatures. *J. Amer. Chem. Soc.*, **64**, 841-850.

Khaibullin Kh, Borisov NM (1966) Experimental investigation of the thermal properties of aqueous and vapor solutions of sodium and potassium chlorides at phase equilibrium. *Teplofizika Vysokikh Temperatur*, **4**, p. 518-523 (English translation, p.489-494).

Knight CL, Bodnar RJ (1989) Synthetic fluid inclusions: IX. Critical PVTX properties of NaCl-H_2O solutions. *Geochim. Cosmochim. Acta*, **53**, 3-8.

Marshall WL (1990) Critical curves of aqueous electrolytes related to ionization behaviour: new temperatures for sodium chloride solutions. *J. Chem. Soc. Faraday Trans.*, **86**, 1807-1814.

Marshall WL, Jones EV (1974) Liquid-vapor critical temperatures of aqueous electrolyte solutions. *J. Inorg. Nucl. Chem.*, **36**, 2313-2318.

Montgomery DC, Peck EA (1992) Introduction to Linear Regression Analysis. New York: Wiley.

Morey GW (1957) The solubility of solids in gases. *Econ. Geol.*, **52**, 225-251.

Morey GW, Chen WT (1956) Pressure-temperature curves in some systems containing water and a salt. *Amer. Chem. Soc. J.*, **78**, 4249-4252.

National Research Council (1928) International critical tables of numerical data, physics, chemistry, and technology: New York, McGraw-Hill, v. **3**. 444 p.

Newton RC, Aranovich LYa, Hansen EC, Vandenheuvel BA (1998) Hypersaline fluids in Precambrian deep-crustal metamorphism**.** *Precambrian Research (1998).*, **91**, 41-63.

Ölander A, Liander H (1950) The phase diagram of sodium chloride and steam above the critical point. *Acta Chim. Scand.*, **4**, 1437-1445.

Pichavant M, Ramboz C, Weisbrod A (1982) Fluid immiscibility in natural processes: use and misuse of fluid inclusion data. I. Phase equilibria analysis – a theoretical and geometrical approach. Chemical Geology, **37**, 1-27.

Pitzer, K. S. (1984) Ionic fluids. J. Physical Chemistry, **88**, 2689-2697.

Pitzer KS, Pabalan RT (1986) Thermodynamics of NaCl in steam. *Geochim. Cosmochim. Acta*, **50**, 1445-1454.

Potter RW II, Shaw DR, Haas JL Jr. (1975) Annotated bibliography of studies on the density and other volumetric properties for major components in geothermal waters 1928-74. *Geol. Surv. Bull.*, **1417**, 1-78.

Potter RW II, Brown DL (1977) The volumetric properties of aqueous sodium chloride solutions from 0º to 500ºC at pressures up to 2000 bars based on a regression of available data in the literature. *Geol. Surv. Bull.*, **1421-C**, 1-36.

Potter RW II, Babcock RS, Brown DL (1977) A new method for determining the solubility of salts in aqueous solutions at elevated temperatures. *J. Research U.S. Geol. Survey*, **5**, 389-395.

Potter RW II (1978) Bibliography of the PVTXE properties of the binary system H_2O-NaCl., U.S. Geological Survey Open-file report, **78-549**, 1-34.

Potter RW II, Clynne MA, Brown DL (1978) Freezing point depression of aqueous sodium solutions. Econ. Geology, **73**, 284-285.

Ramboz C, Pichavant M, Weisbrod A (1982) Fluid immiscibility in natural processes: use and misuse of fluid inclusion data II. Interpretation of fluid inclusion data in terms of immiscibility. Chemical Geology, **37**, 29-48.

Roedder E (1984) Fluid Inclusions. *Mineral. Soc. Amer. Reviews in Mineralogy.*, **12**, 644p.

Roedder E, Bodnar RJ (1997) Fluid inclusion studies of hydrothermal ore deposits. In: Barnes H. L. (ed) *Geochemistry of Hydrothermal Ore Deposits third edition*. New York, NY: John Wiley, pp. 657-697.

Rosenbauer RJ, Bishcoff JL (1987) Pressure-composition relations for coexisting gases and liquids and the critical points in the system NaCl-H_2O at 450, 475, and 500ºC. *Geochim. Cosmochim. Acta*, **51**, 2349-2354.

SAS (2001) Version 8.12. SAS Institute, Cary, NC.

Sourirajan S, Kennedy GC (1962) The system H_2O-NaCl at elevated temperatures and pressures. *J. Amer. Chem. Soc.*, 260, 115-141.

Sterner SM, Hall DL, Bodnar RJ (1988) Synthetic fluid inclusions. V. Solubility relations in the system NaCl-KCl-H_2O under vapor-saturated conditions. *Geochim. Cosmochim. Acta*, **52**, 989-1005

Thiéry R, Dubessy J (1998) Description of vapour-liquid phase equilibria of the H_2O-NaCl system between 100 and 900ºC with a thermodynamic model based on the Mean Spherical Approximation. *Eur. J. Mineral.*, **10**, 1151-1165.

Touret J (1986) Fluid inclusions in rocks from the lower continental crust. Dawson, J. B., D. A. Carswell, J. Hall, and K. H. Wedepohl (eds.) *The Nature of the Lower Continental Crust, Geological Society Special Publication*, **24**, 161-172.

Urusova MA (1974) Phase equilibria and thermsodynamic characteristics of solutions in the system NaCl-H_2O and NaOH-H_2O at 350º-550ºC. *Russian J. Inorg. Chem*., **19**, 944-950.

Urusova MA (1975) Volume properties of aqueous solutions of sodium chloride at elevated temperatures and pressures. *Zhur. Neorgan. Khim*., **20**, 3103-3110.

Urusova MA, Ravich MI (1971) Vapor pressure and solubility in the system NaCl-H_2O at 350º and 400ºC: *Zhur. Neorgan. Khim*., **16**, 2881-2883.

Zhang Yi-G, Frantz JD (1987) Determination of the homogenization temperatures and densities of supercritical fluids in the system NaCl-KCl-$CaCl_2$-H_2O using synthetic fluid inclusions. *Chemical Geology*, **64**, 335-350.

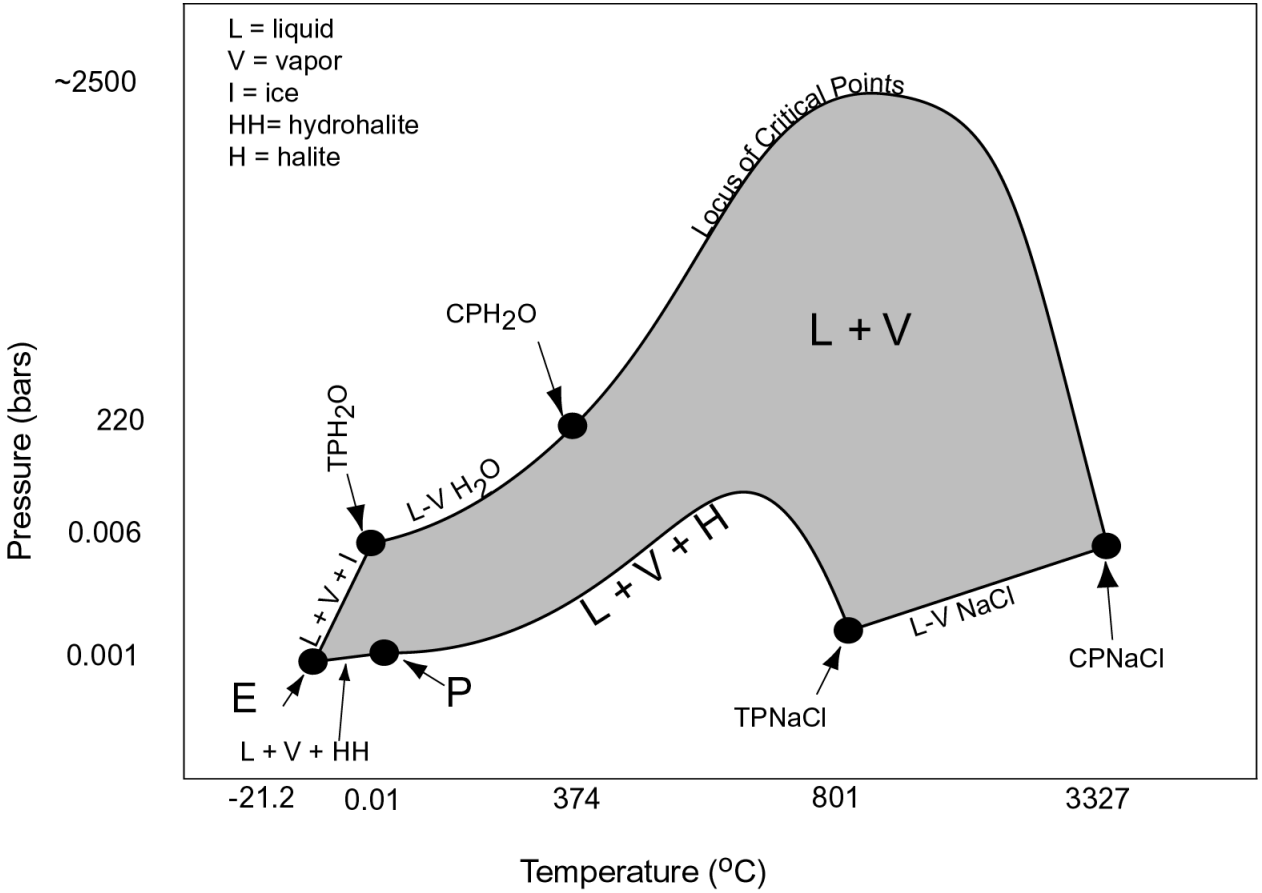

Figure 1. Distorted, schematic PT projection of the H_2O-NaCl liquid-vapor envelope. TP_{H_2O} = H_2O triple point (T = 0.01°C, P = 0.006 bar); CP_{H_2O} = H_2O critical point (T = 374.1°C, P = 220 bars); TP_{NaCl} = NaCl triple point (T = 801°C, P = approx. 1 bar); CP_{NaCl} = NaCl critical point (T = approx. 3327°C, P = approx. 235 bars); E = eutectic point (L + V + I + HH, T = -21.2°C, P = 0.001 bar, 23.2 wt% NaCl); P = peritectic point (L + V + HH + H, T = 0.1°C, P = 0.004 bar, 26.2 wt%NaCl). Within the shaded region, fluid immiscibility to produce a high salinity liquid in equilibrium with a lower salinity vapor is possible (modified from Bodnar et al., 1985).

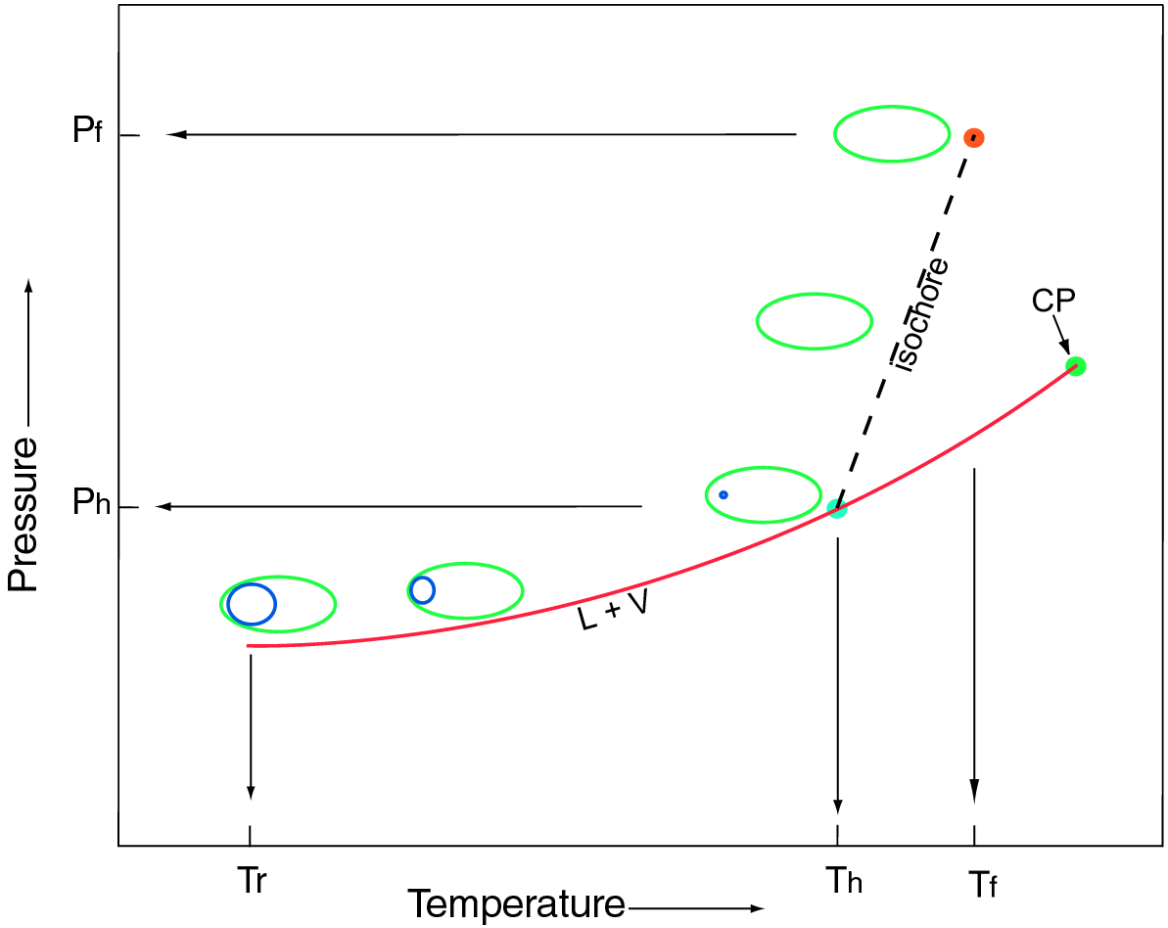

Figure 2. Schematic representation showing a typical cooling path followed by a liquid-rich fluid inclusion. The single phase inclusion trapped at Tf, Pf follows the isochore (dashed line) to the liquid-vapor curve (L + V), at which point a vapor bubble nucleates. With continued cooling the inclusion follows the liquid-vapor curve and the vapor to liquid ratio increases (modified from Bodnar, 1995).

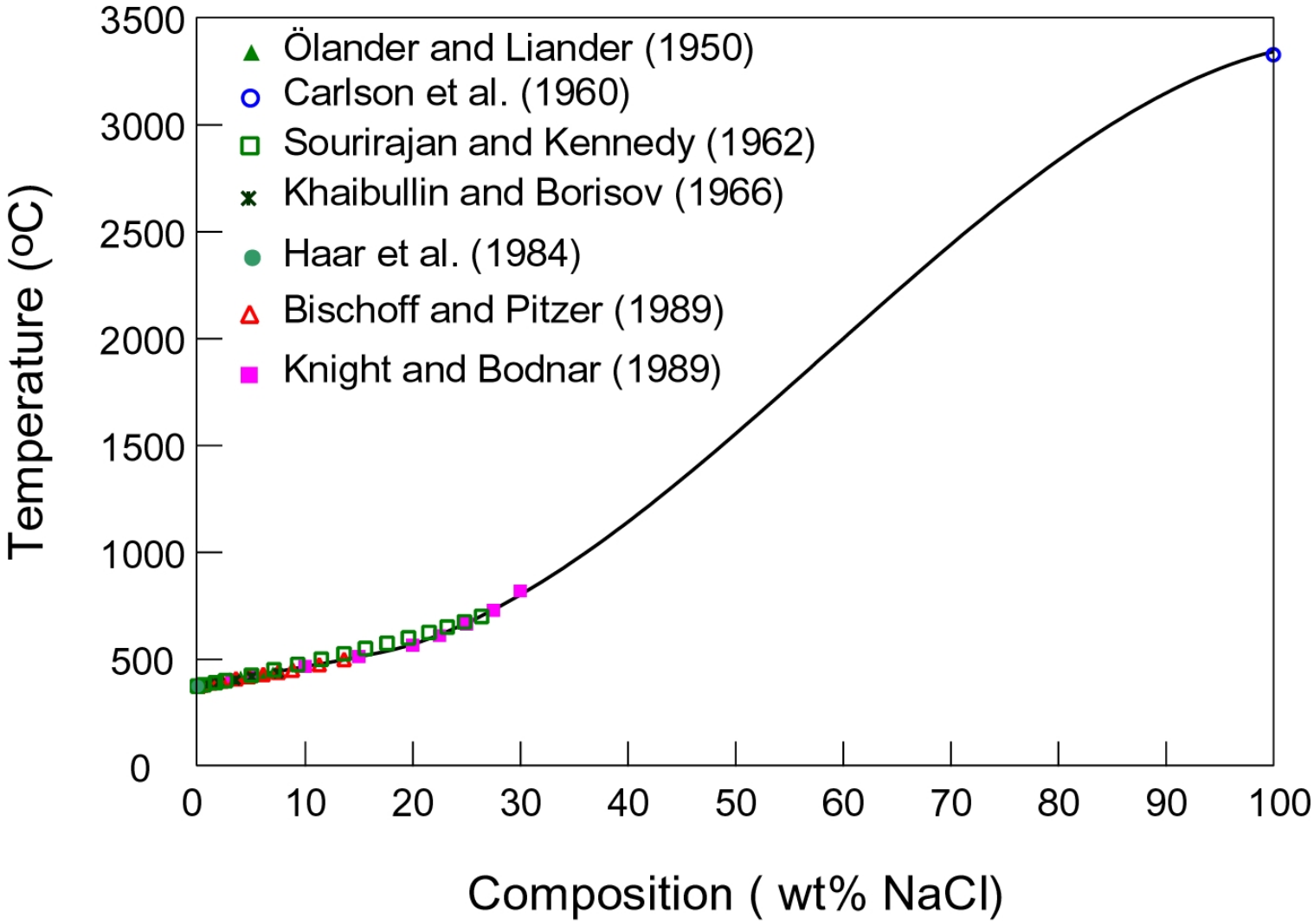

Figure 3. TX projection of critical locus showing published critical point data.

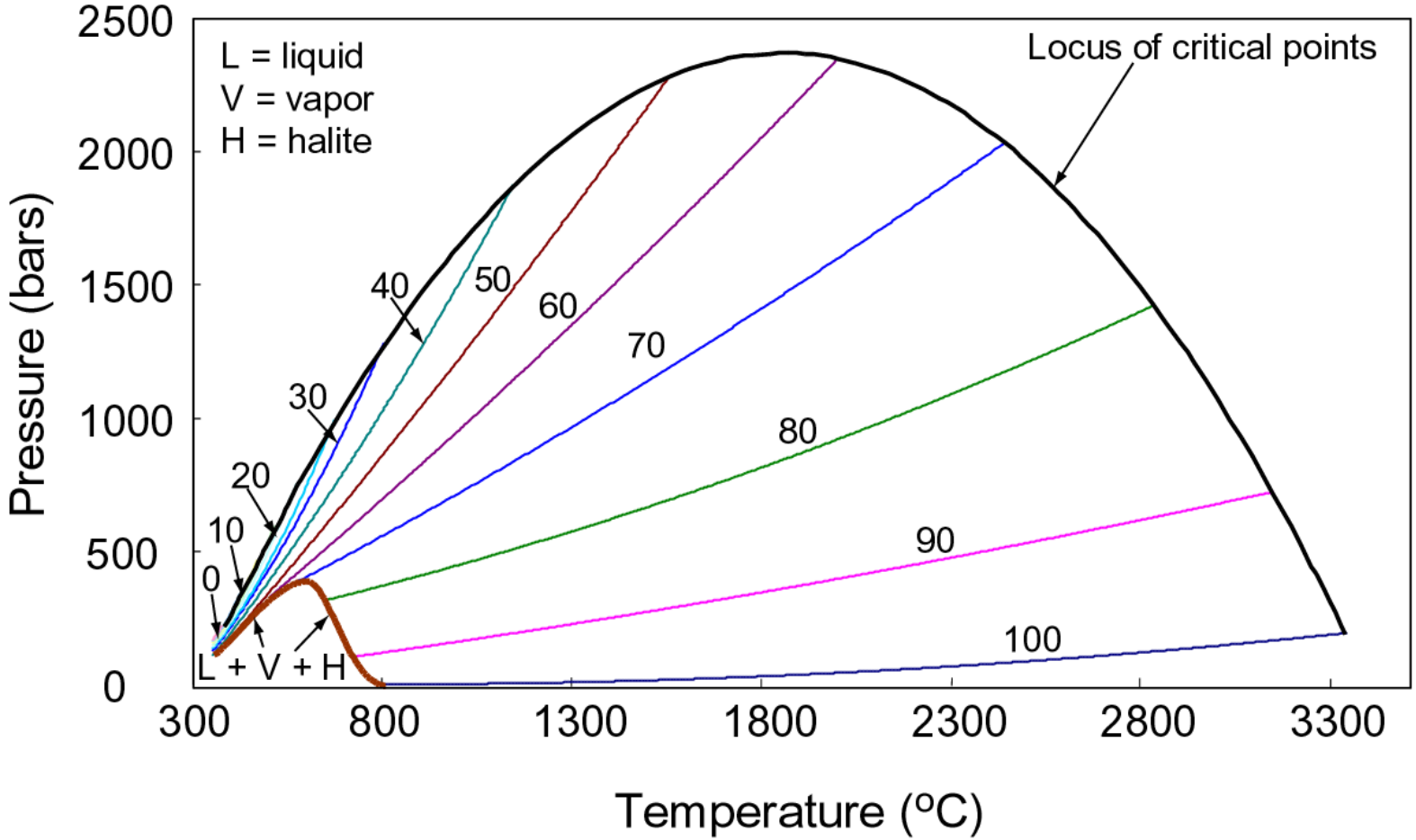

Figure 4. PT projection of the high temperature, high salinity portion of the H_2O-NaCl system, isopleths shown in wt% NaCl. Also shown is the locus of critical points, and the liquid + vapor + halite (L + V + H) curve for the system H_2O-NaCl.

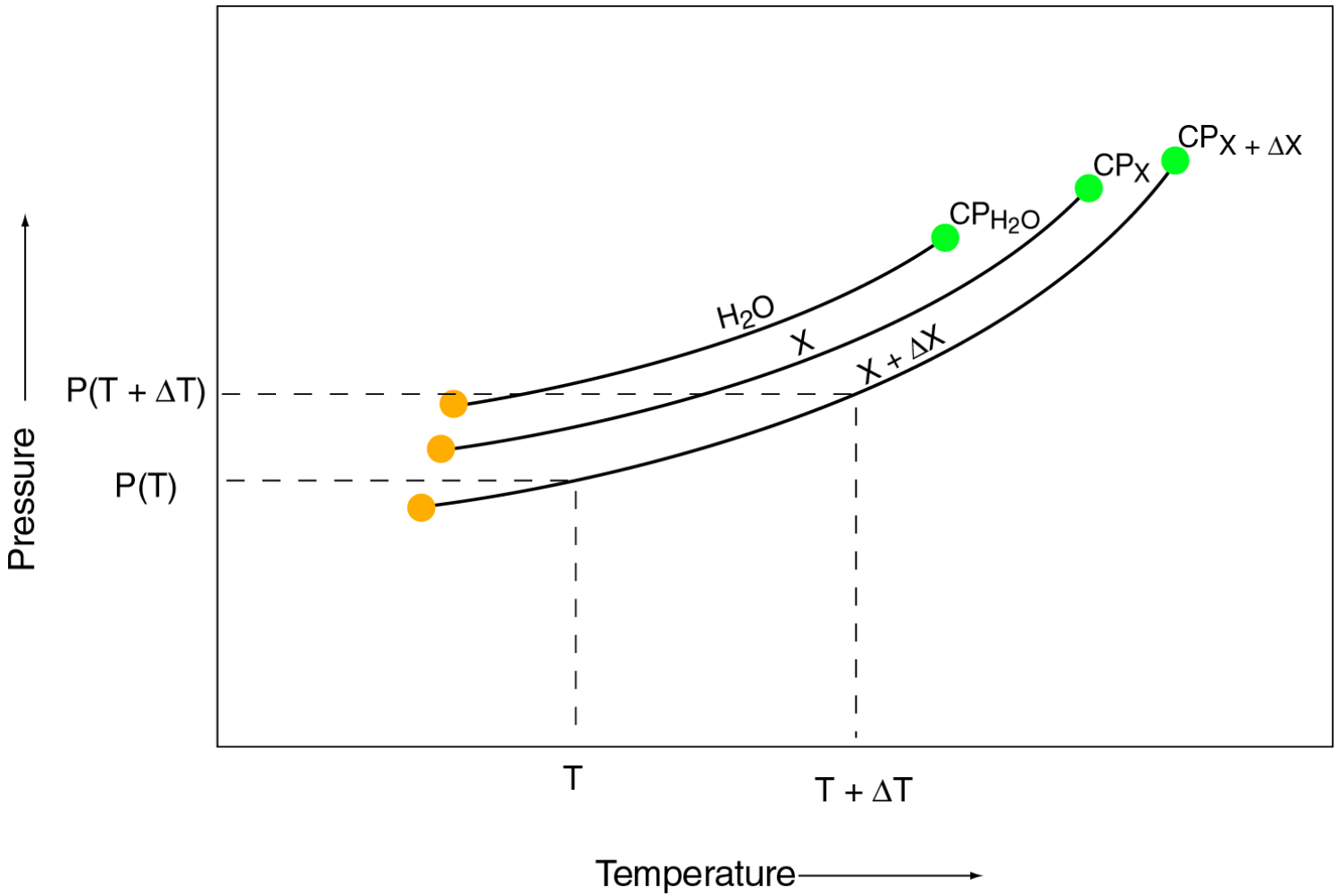

Figure 5. Schematic PT projection showing the relationship of H_2O-NaCl isopleth location change in postion as a function of temperature (T) and composition (X).

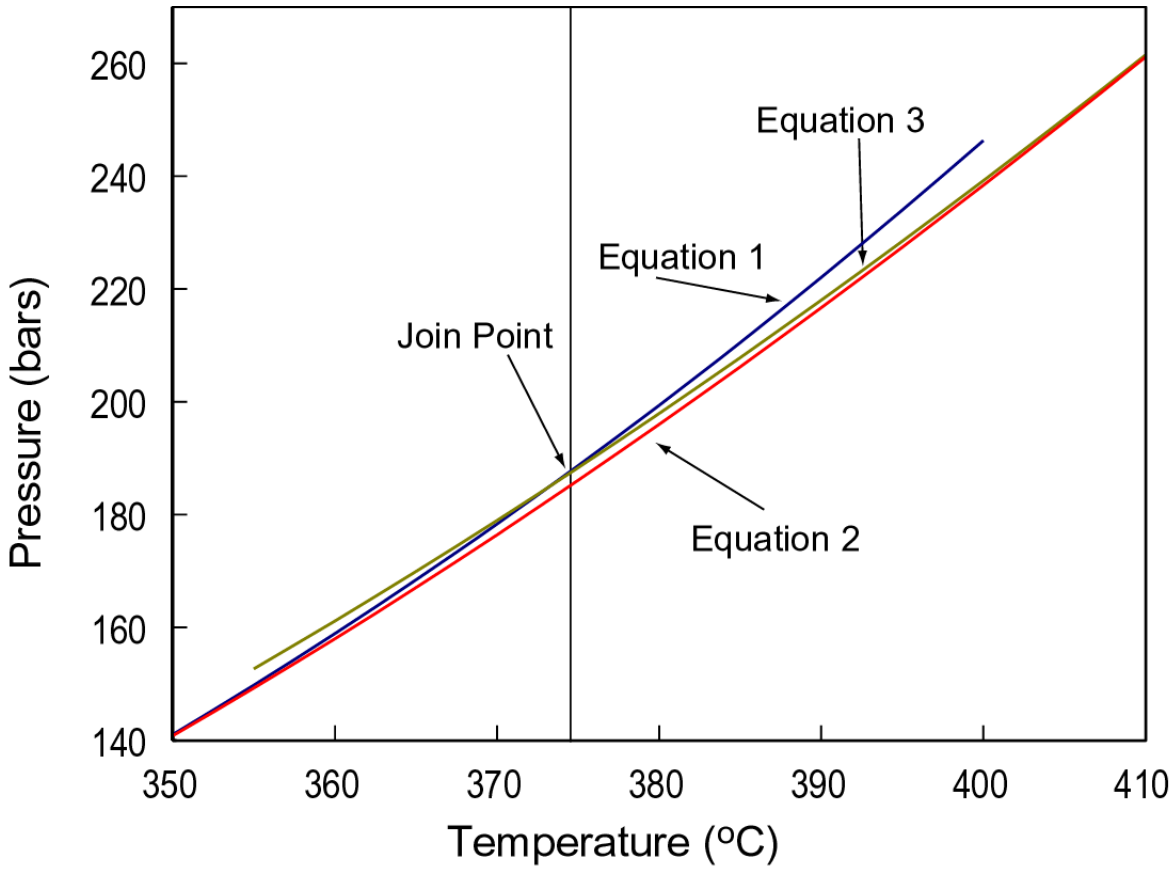

Figure 6. PT projection showing the relationships between the low temperature equation (Equation 1), the high temperature equation (Equation 3) and the merge equation (Equation 2). The vertical line represents the join at 374°C where there is a slight discontinuity between equations 1 and 3. That is, the slope dp/dt predicted by equation 1 is different than that predicted by equation 3.

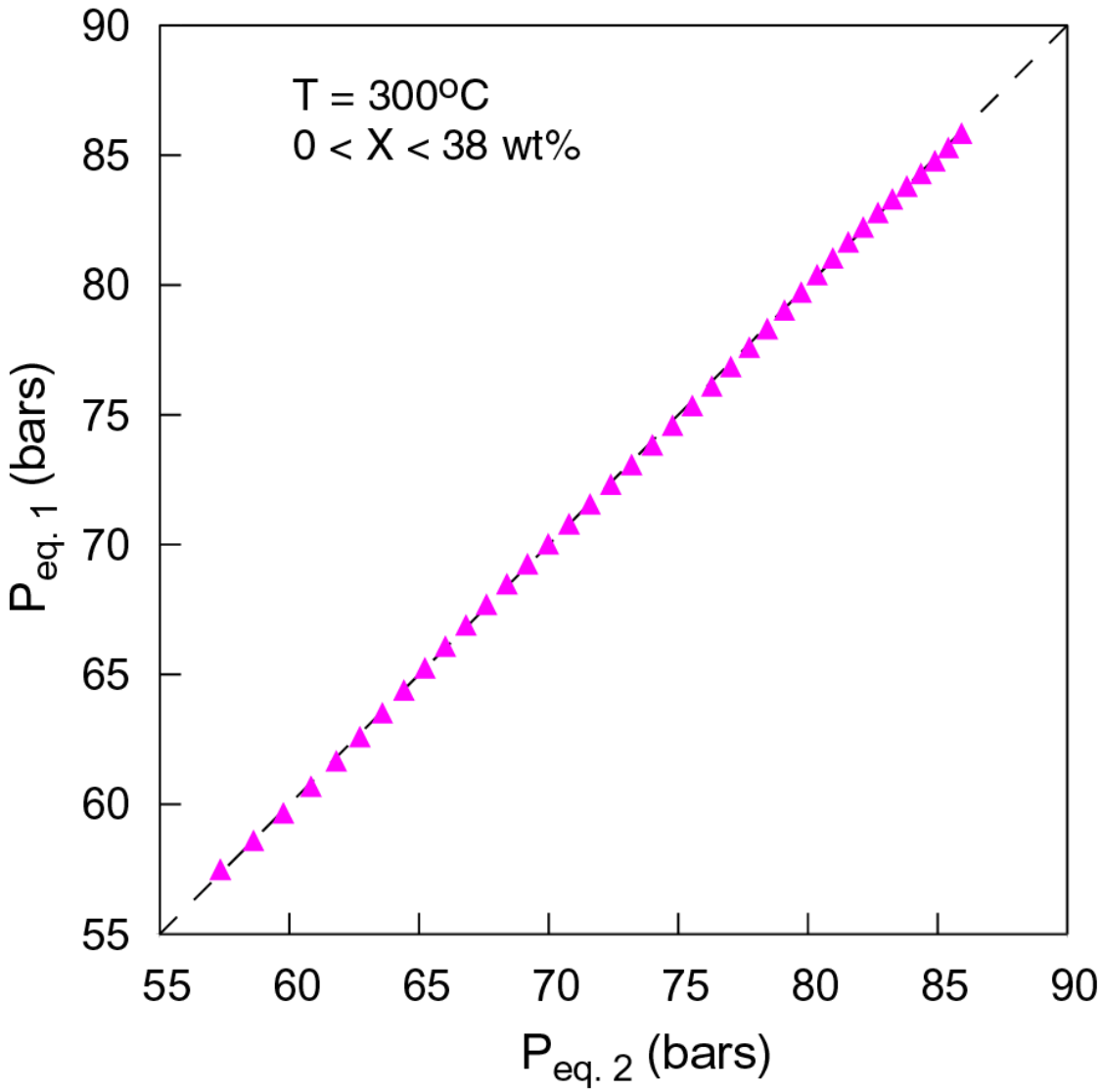

Figure 7. Comparison of pressures predicted by the low temperature equation (eq. 1) and those predicted by the merge equation (eq. 2) as a function of salinity at 300°C where the model changes from eq. 1 to eq. 2 to calculate vapor pressures of H_2O -NaCl solutions. The differences are < 0.3% over the entire salinity range.

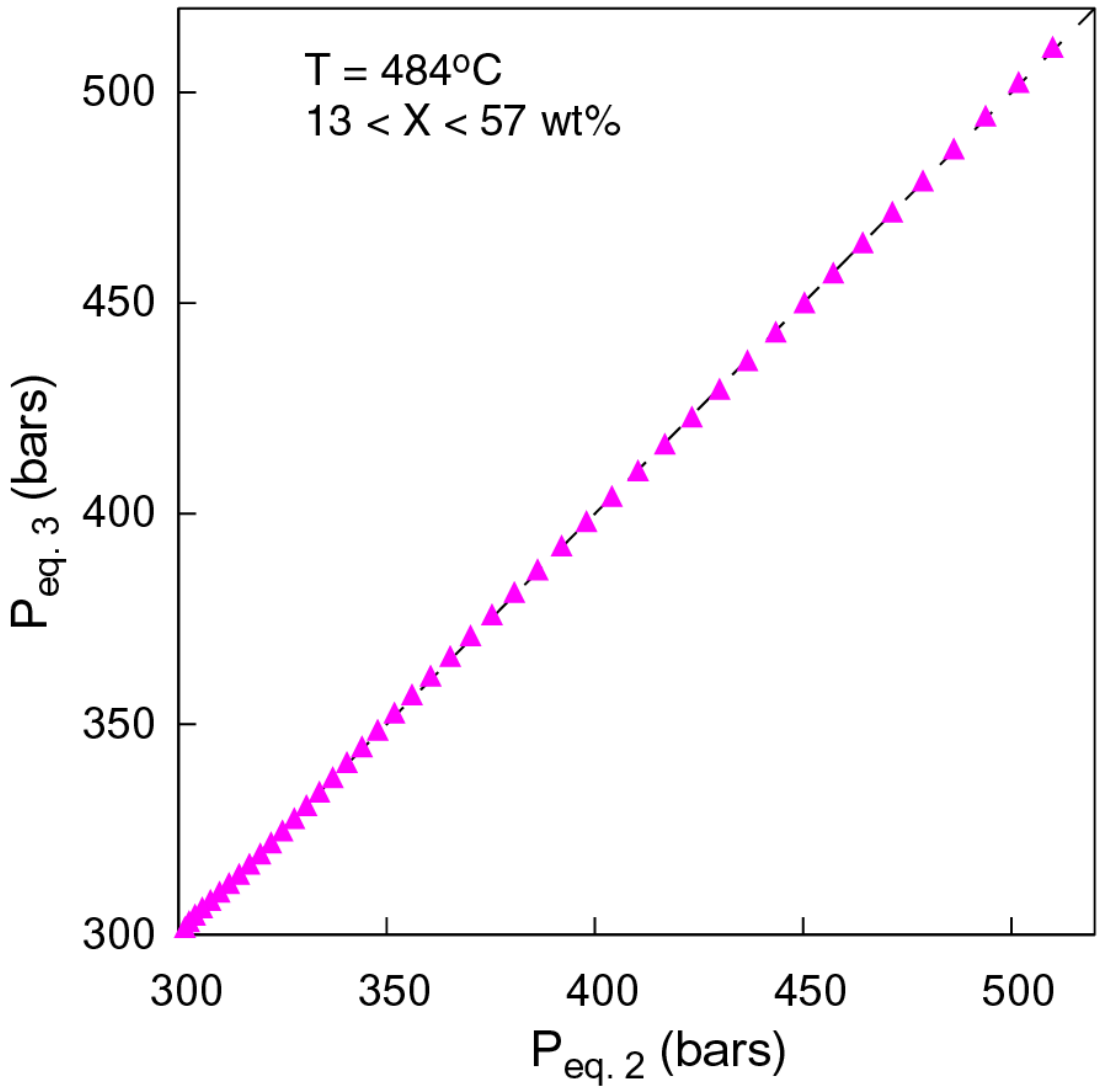

Figure 8. Comparison of pressures predicted by the high temperature equation (eq. 3) and those predicted by the merge equation (eq. 2) as a function of salinity at 484°C where the model changes from eq. 3 to eq. 2 to calculate vapor pressures of H_2O -NaCl solutions. The differences are < 0.3% over the entire salinity range.

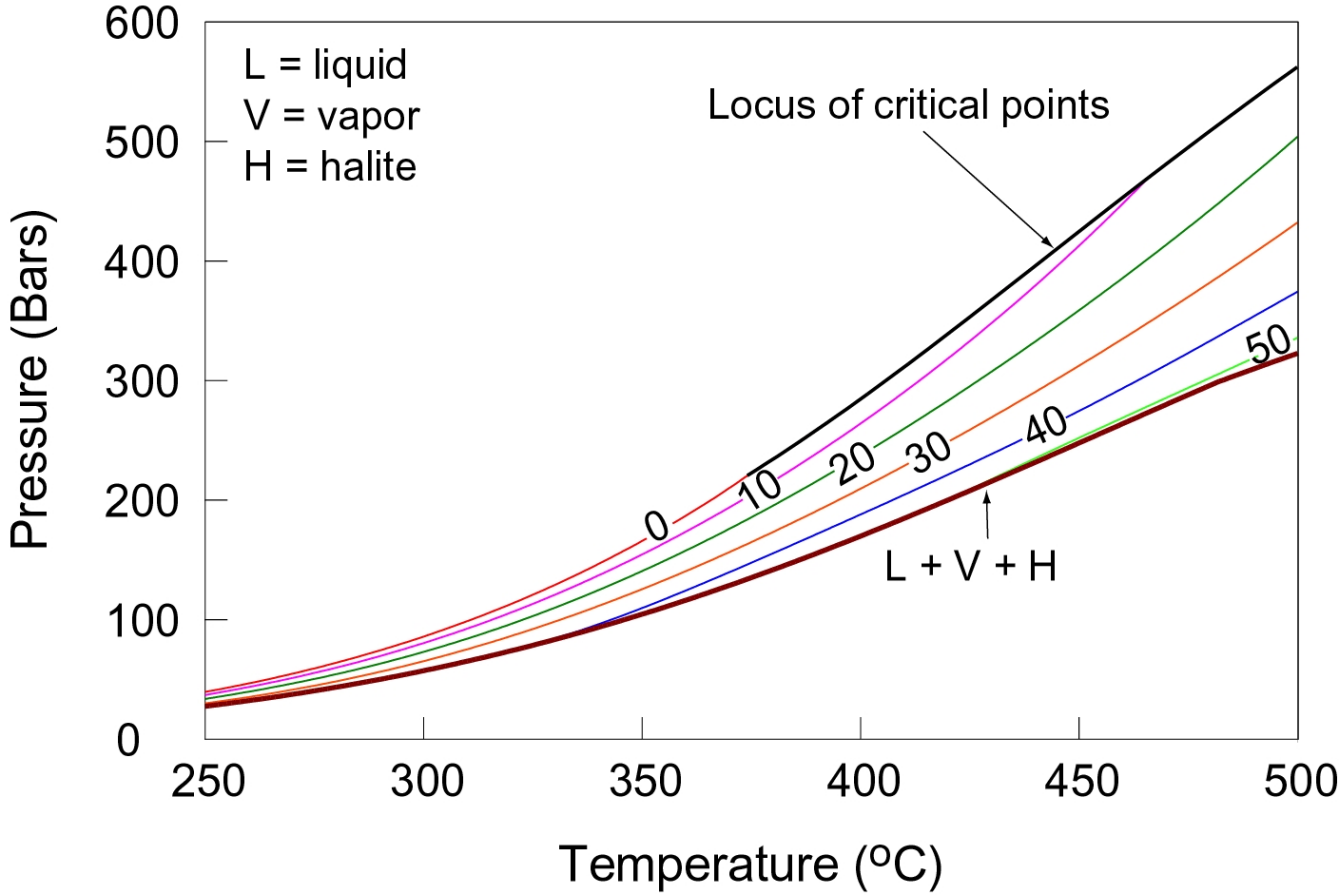

Figure 9. PT projection of isopleths (labeled in wt% NaCl) for the region where low temperature and high temperature equations are joined by the merge equation. Also shown are the liquid + vapor + halite (L + V + H) curve and locus of critical points.

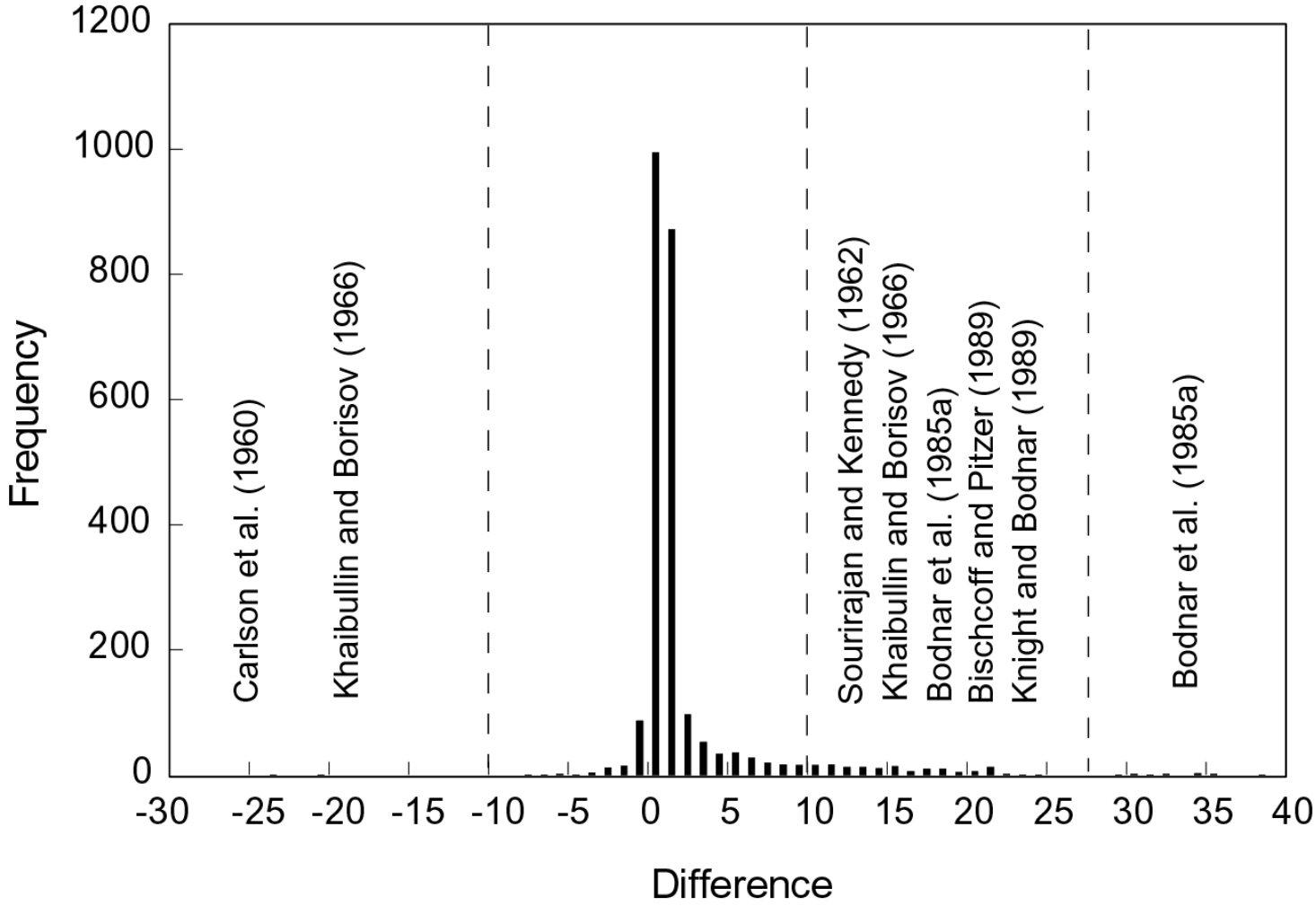

Figure 10. Difference between published data and vapor pressures predicted by the model.

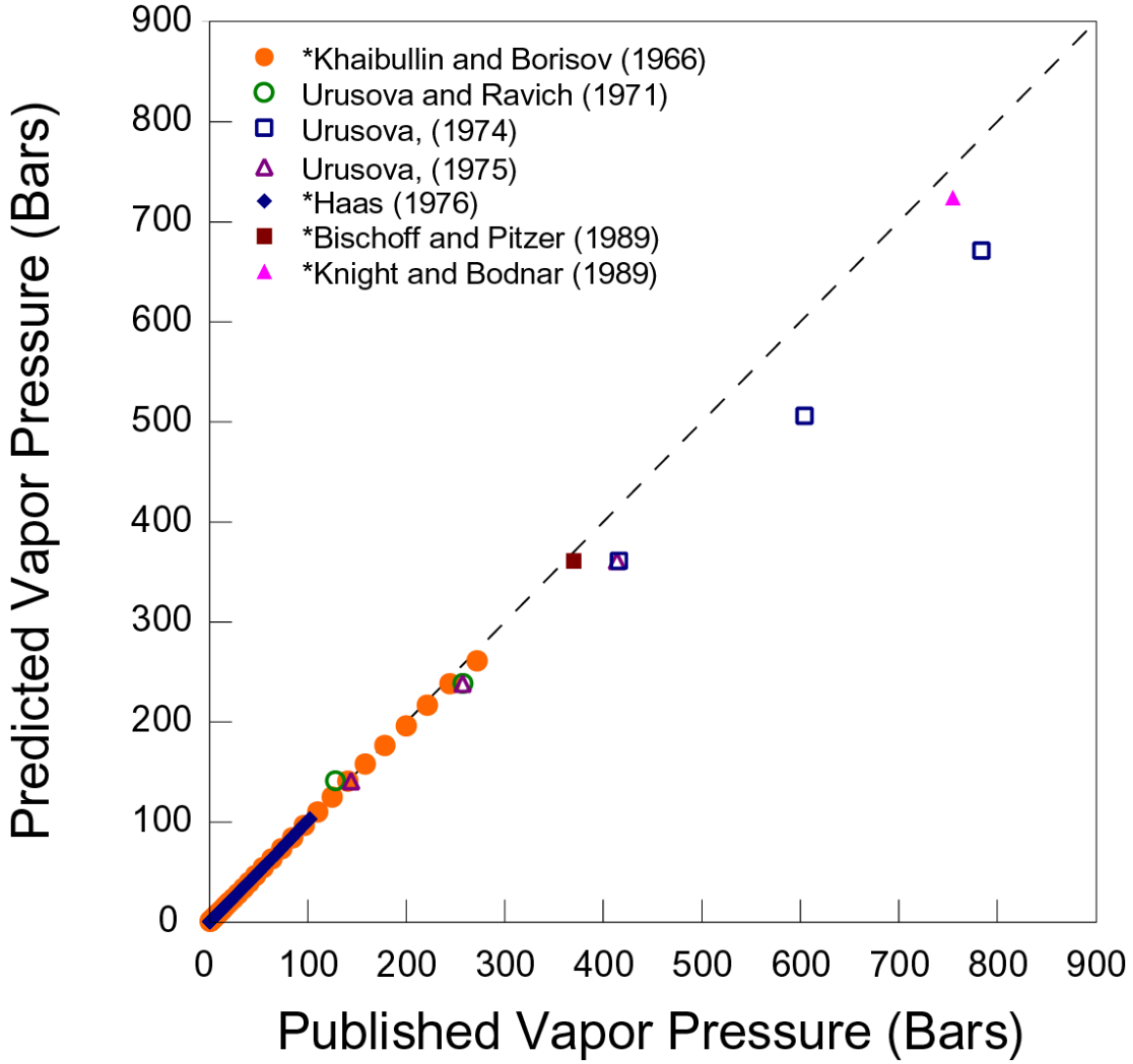

Figure 11. Comparison of predicted vs. published vapor pressures for a composition of 20 wt% NaCl. Authors noted with an asterisk were used in the regression analysis.

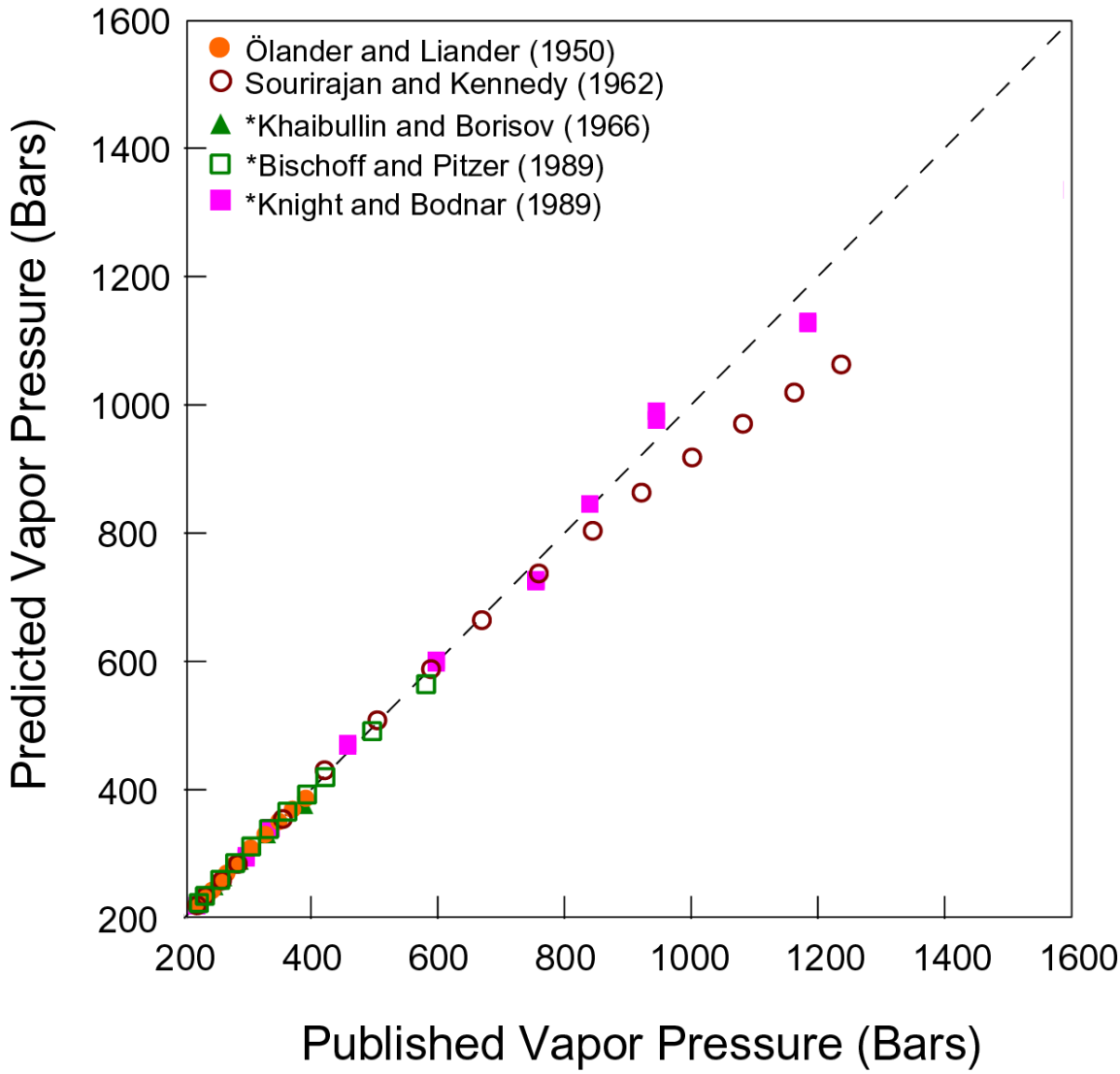

Figure 12. Comparison of predicted vs. published vapor pressures along the H_2O-NaCl locus of critical points. Authors noted with an asterisk were used in the regression analysis.

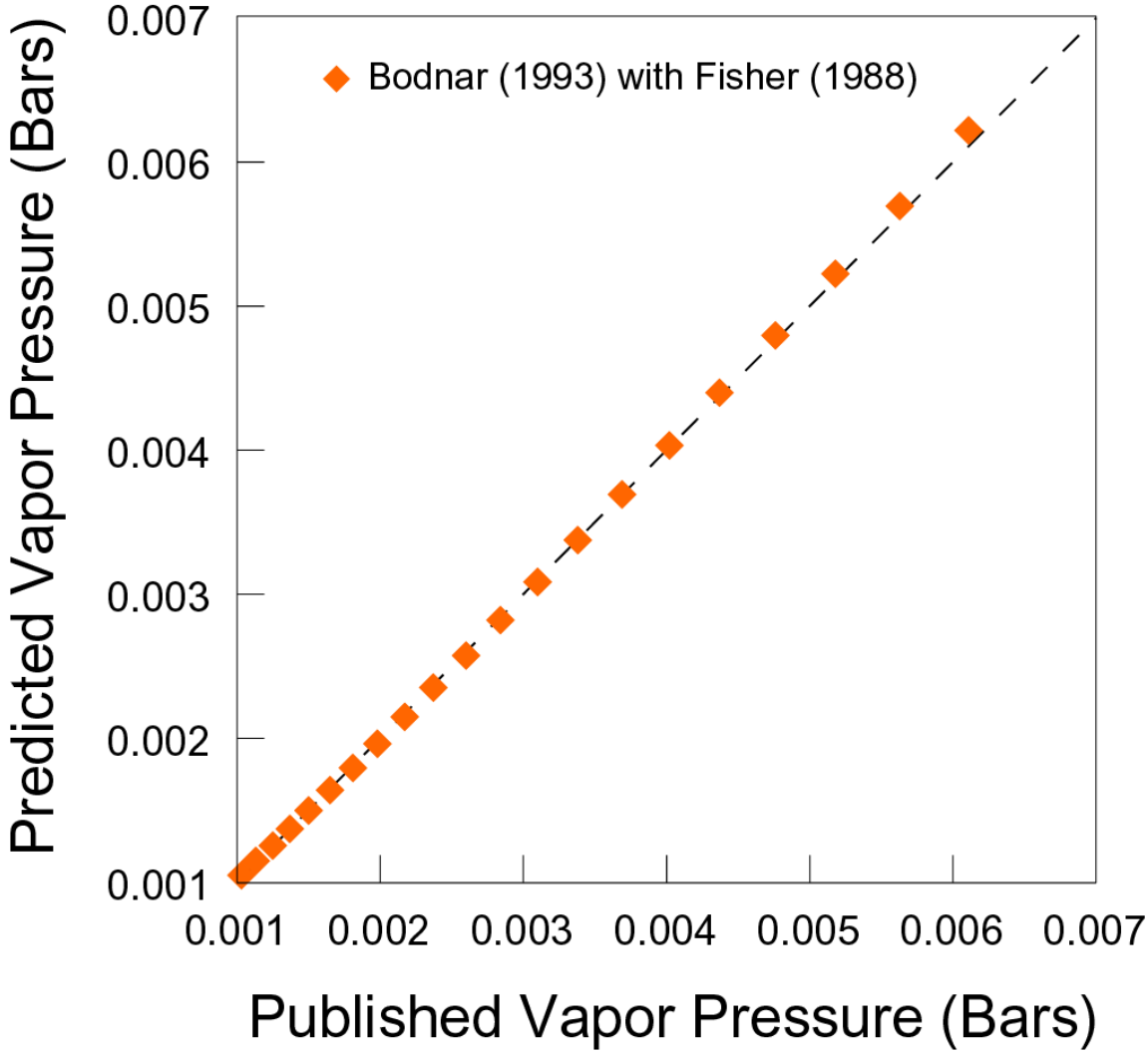

Figure 13. Comparison of predicted vs. published vapor pressures along the liquid + vapor + ice curve in the H_2O-NaCl system.

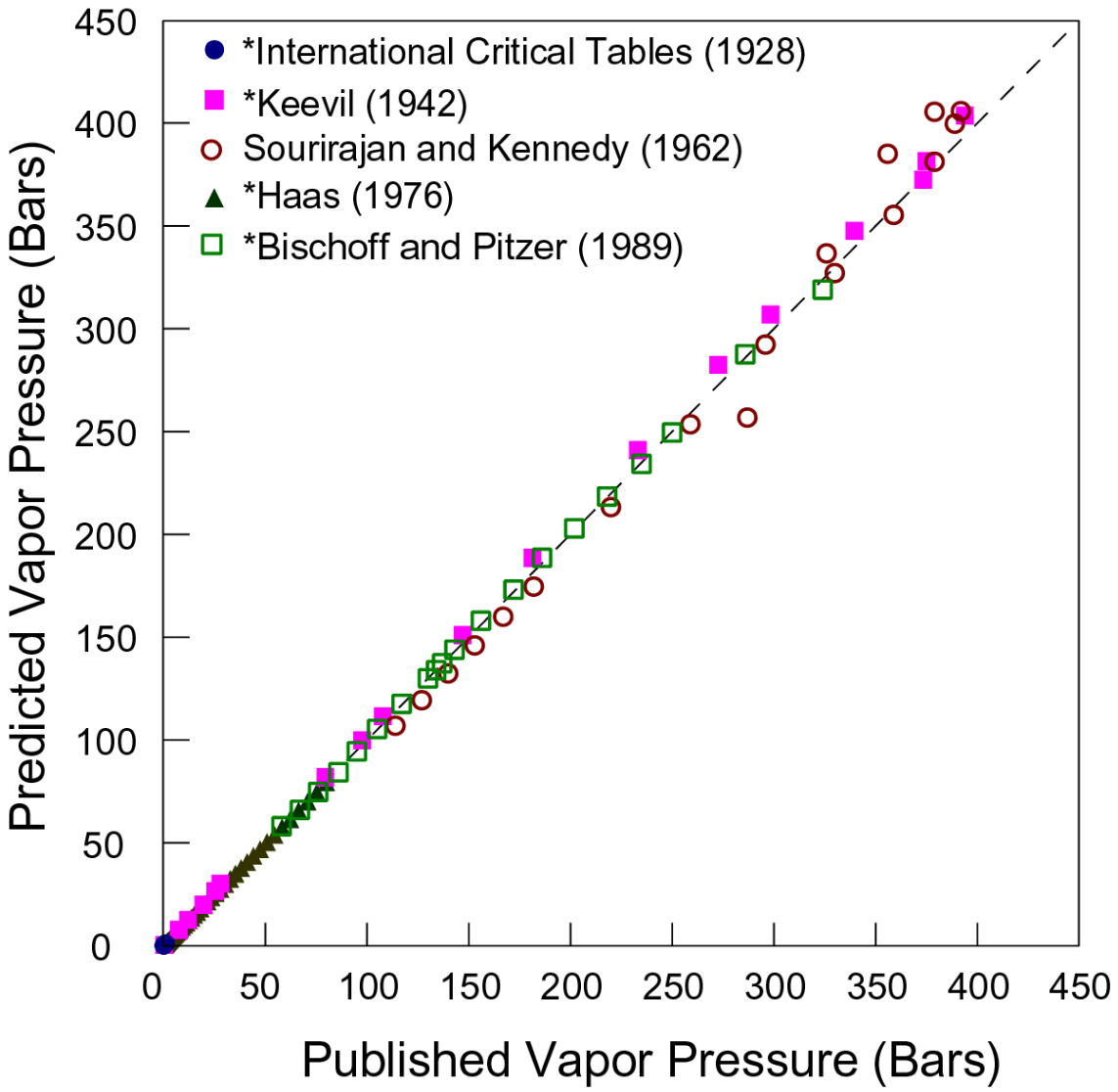

Figure 14. Comparison of predicted vs. published vapor pressures along the liquid + vapor + halite curve in the H_2O-NaCl system. Authors noted with an asterisk were use in the regression analysis.

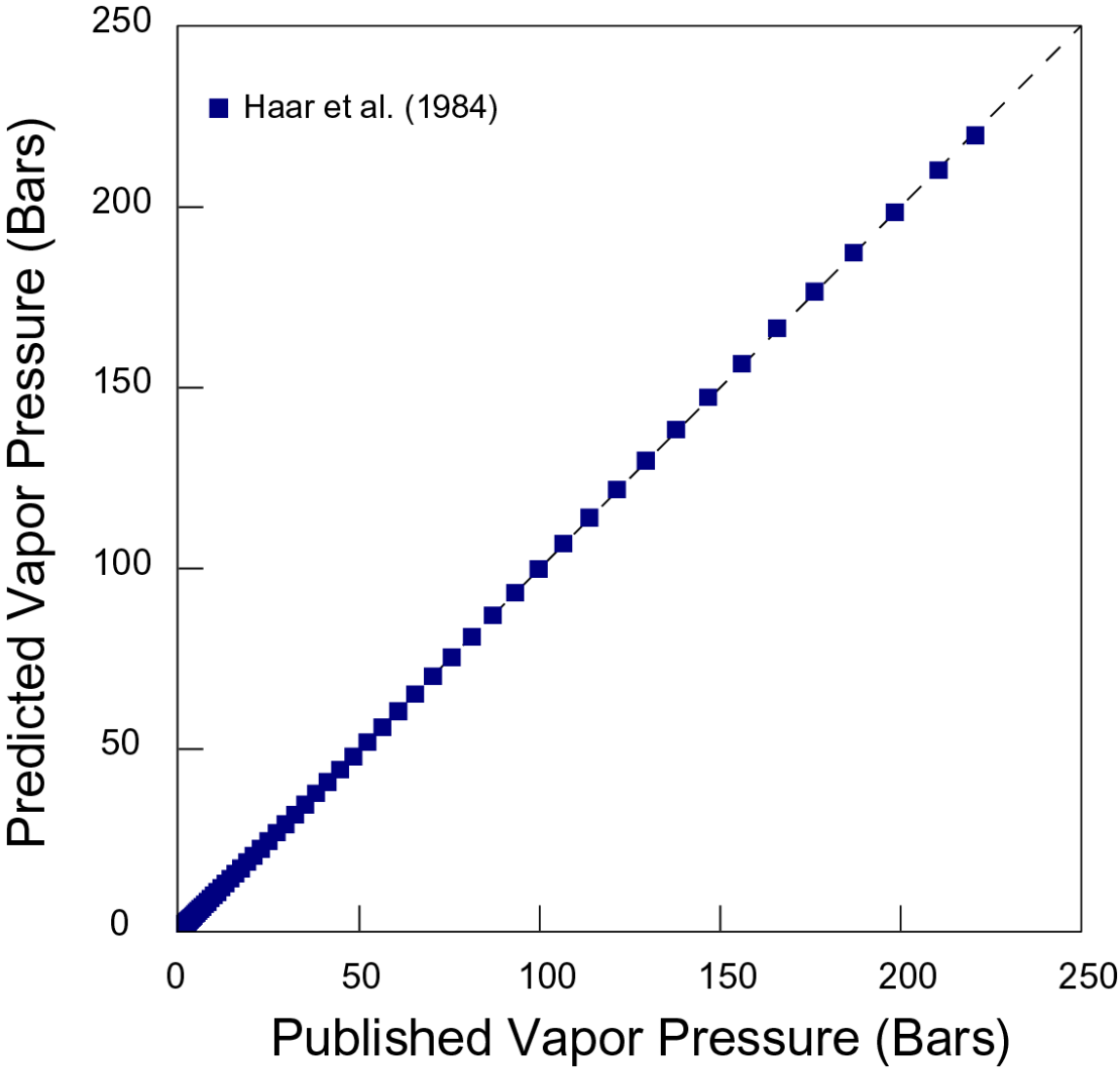

Figure 15. Comparison of predicted vs. published vapor pressures along the H_2O liquid + vapor curve.

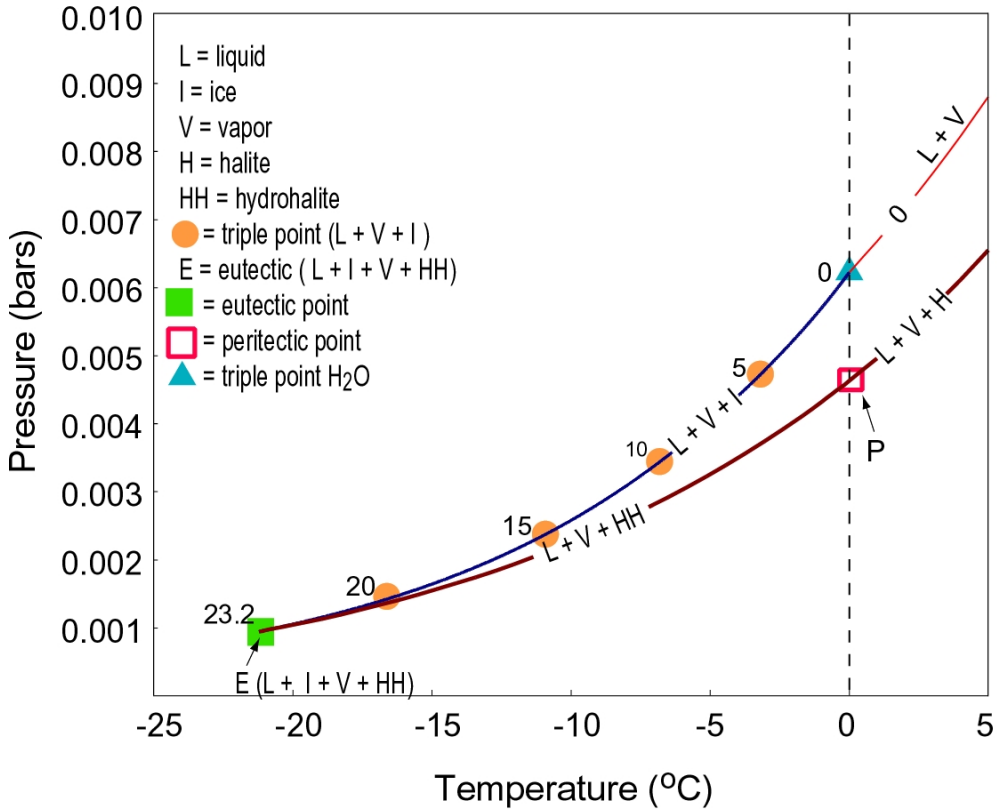

Figure 16. PT plot of the locus of ice triple points (L + V + I) for salinities from pure H_2O (0) to the eutectic composition (23.2 wt%). Also shown is the locus of hydrohalite triple points (L + V + HH) and a portion of thelocus of halite triple points (L + V + H). The line labeled 0, L + V represents the pure water liquid-vapor curve that starts at the pure water triple point (0, ▲) and extends to higher temperatures and pressures. The higher temperature area to the left of the dashed line represents the range of temperature overlap with the next PT diagram.

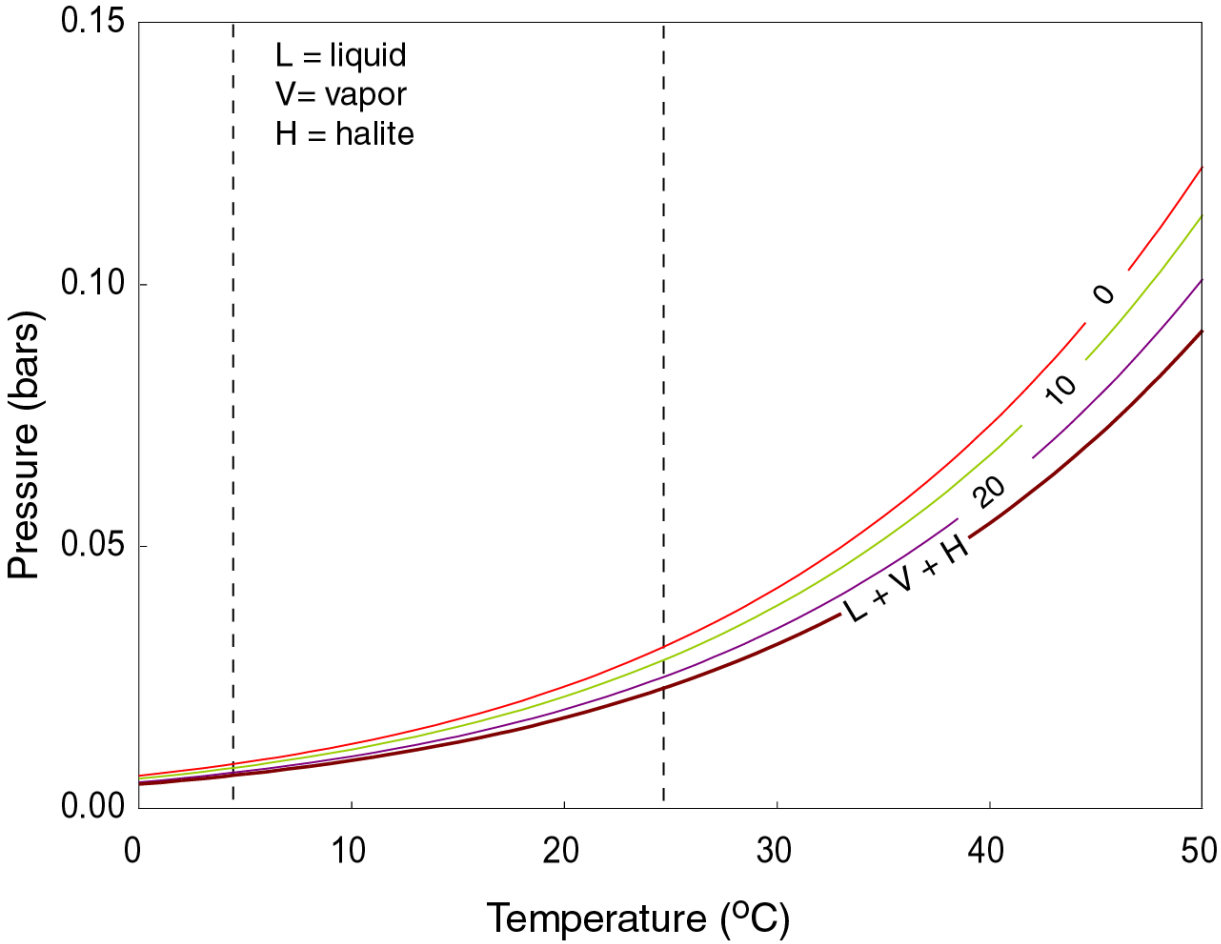

Figure 17. PT projection of isopleths for H_2O-NaCl (labeled in wt% NaCl) over the temperature range 0° - 50°C. The lower temperature and higher temperature dashed lines represent the maximum temperature of the previous P-T diagram, and the minimum temperature of the following P-T diagram, respectively.

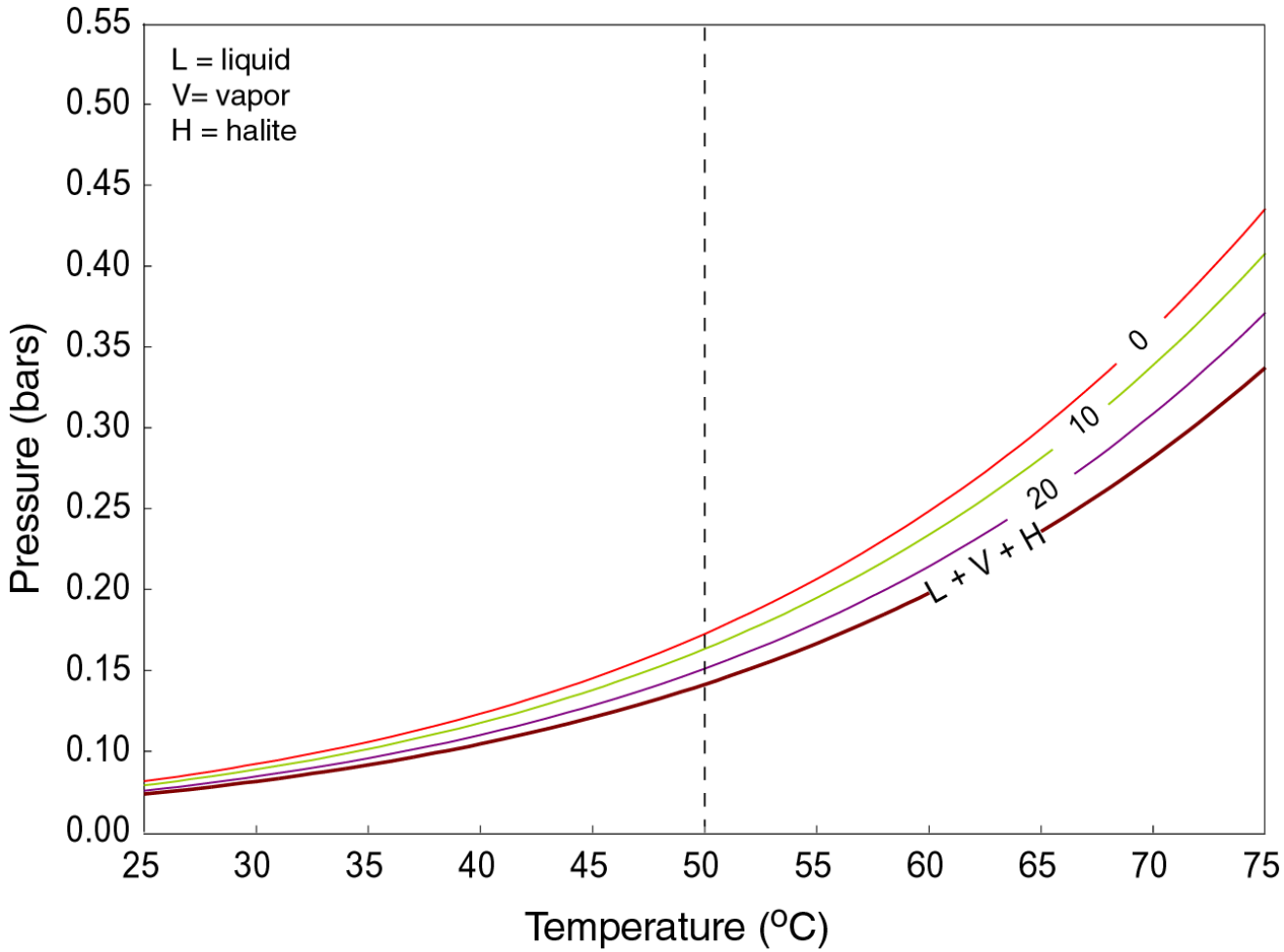

Figure 18. PT projection of isopleths for H_2O-NaCl (labeled in wt% NaCl) over the temperature range 25° - 75°C. The dashed line represents the maximum temperature shown on the previous diagram, and the minimum temperature on the following diagram.

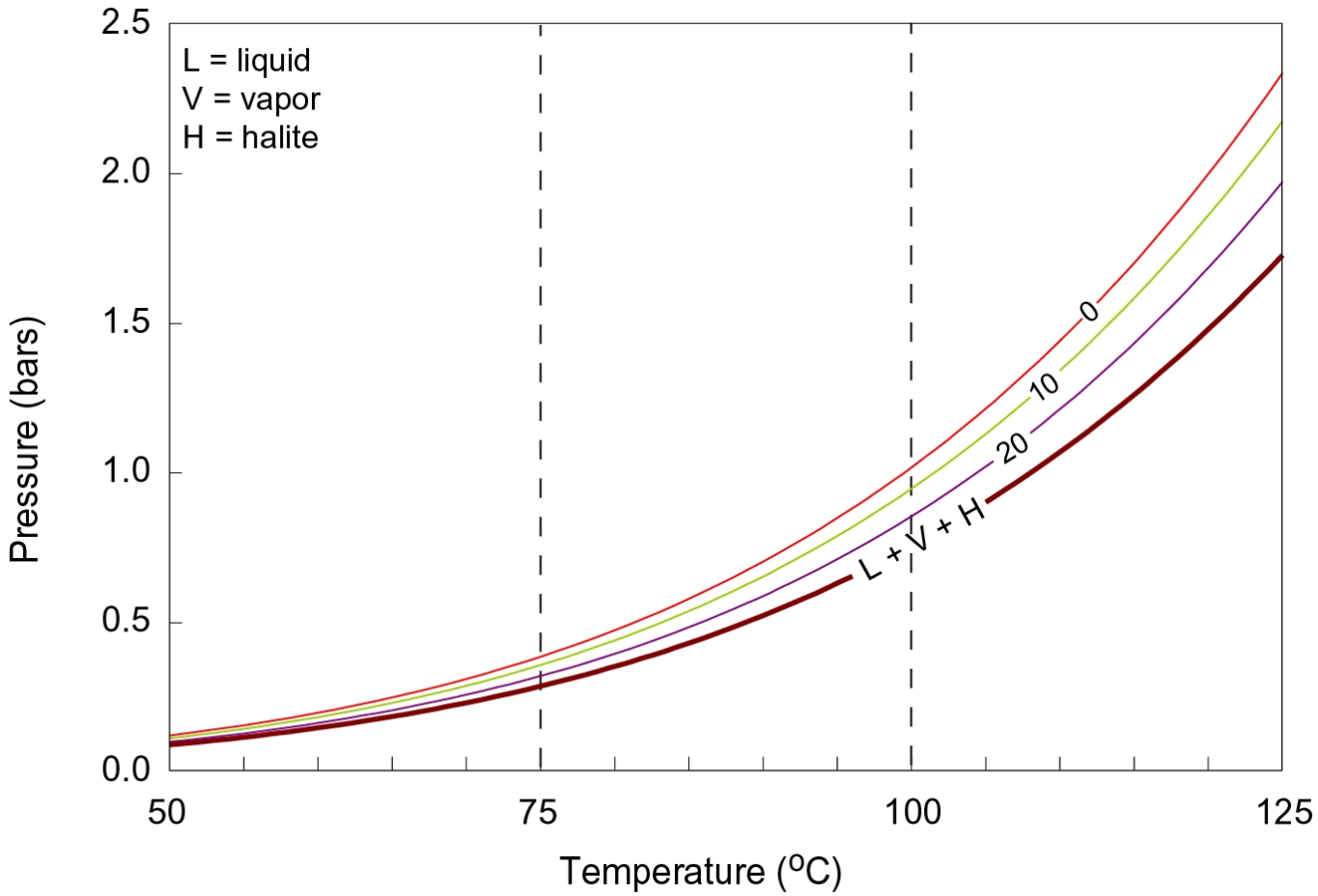

Figure 19. PT projection of isopleths for H_2O-NaCl (labeled in wt% NaCl) over the temperature range 50° - 125°C. The lower temperature and higher temperature dashed lines represent the maximum temperature of the previous P-T diagram, and the minimum temperature of the following P-T diagram, respectively.

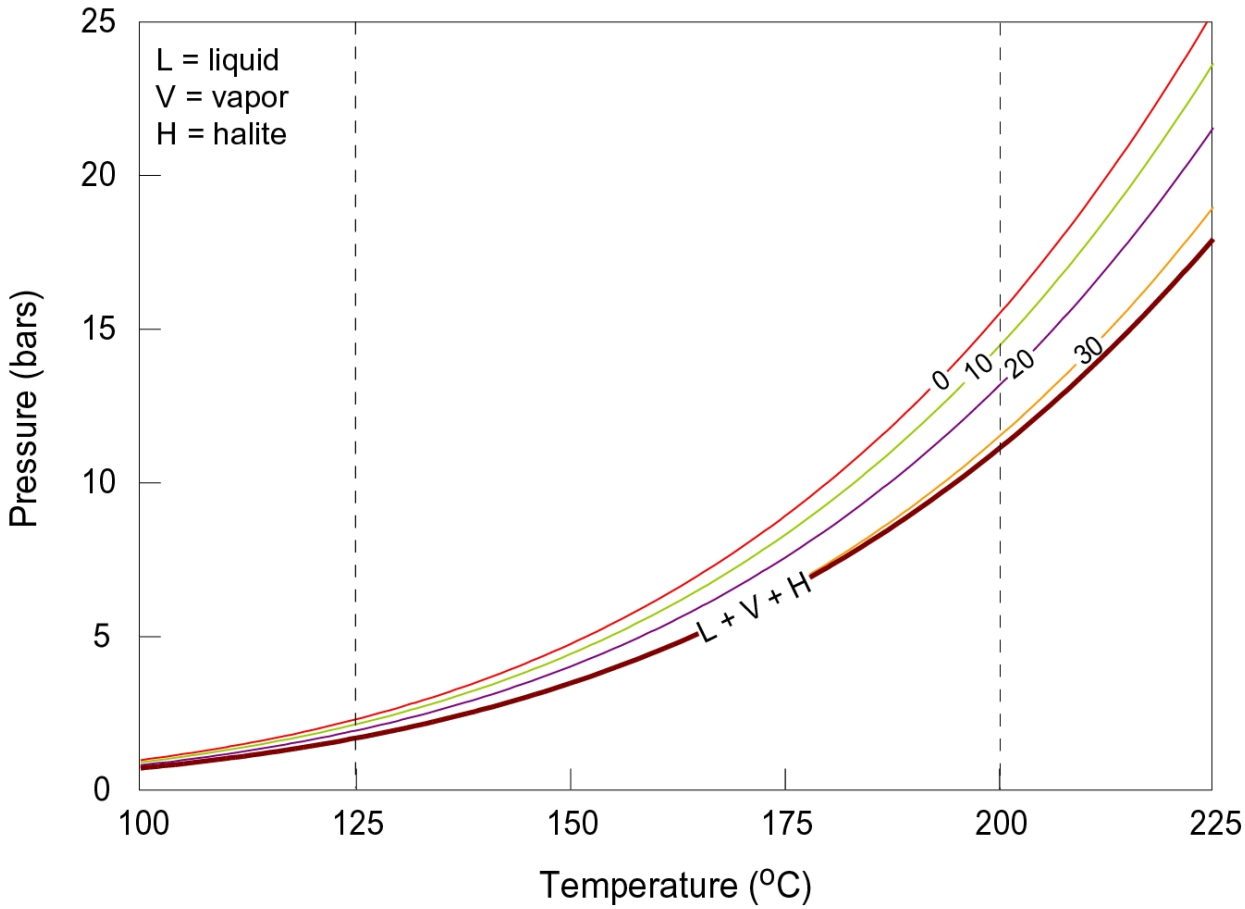

Figure 20. PT projection of isopleths for H_2O-NaCl (labeled in wt% NaCl) over the temperature range 100° - 225°C. The lower temperature and higher temperature dashed lines represent the maximum temperature of the previous P-T diagram, and the minimum temperature of the following P-T diagram, respectively.

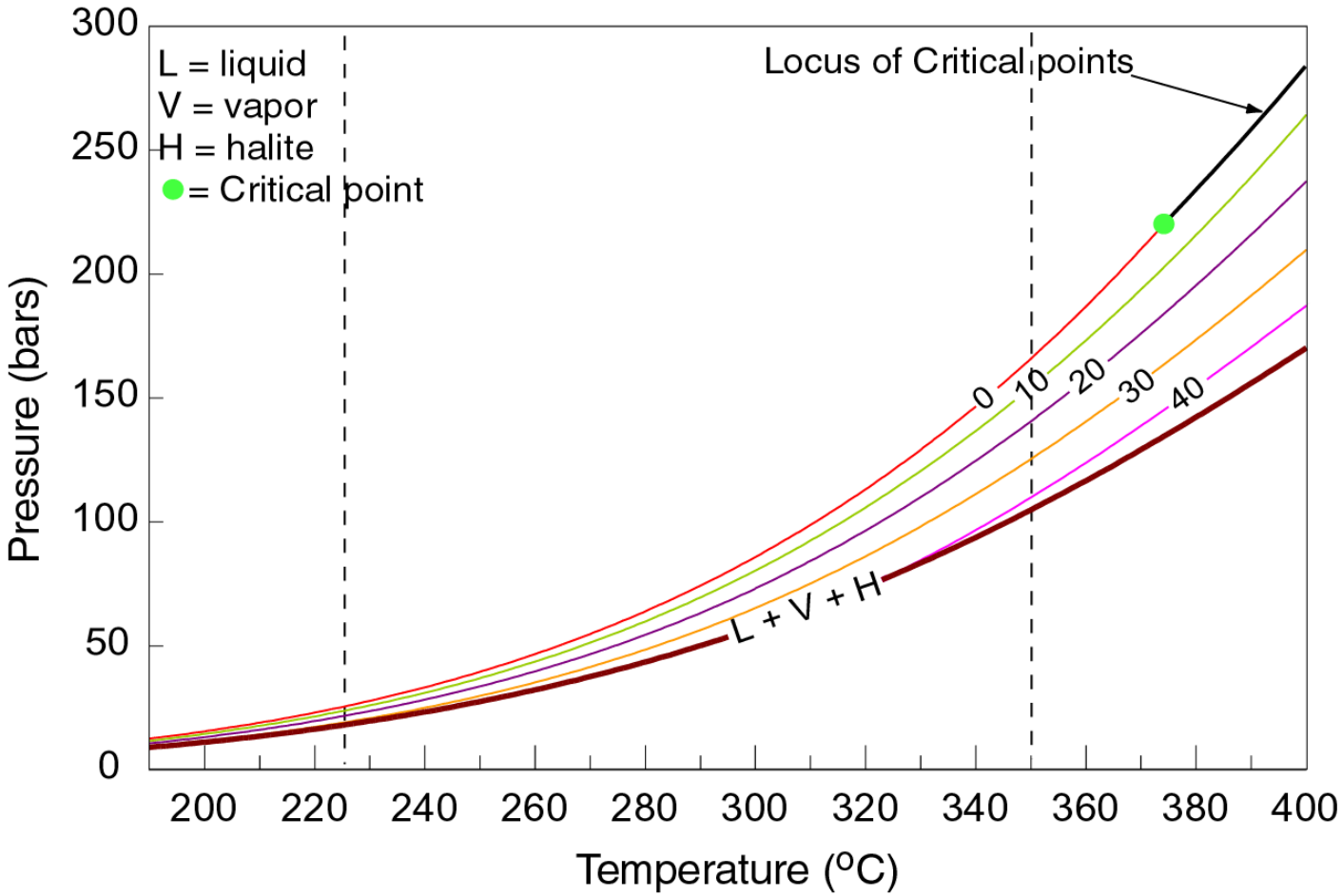

Figure 21. PT projection of isopleths for H_2O-NaCl (labeled in wt% NaCl) over the temperature range 190° - 400°C. The lower temperature and higher temperature dashed lines represent the maximum temperature of the previous P-T diagram, and the minimum temperature of the following P-T diagram, respectively.

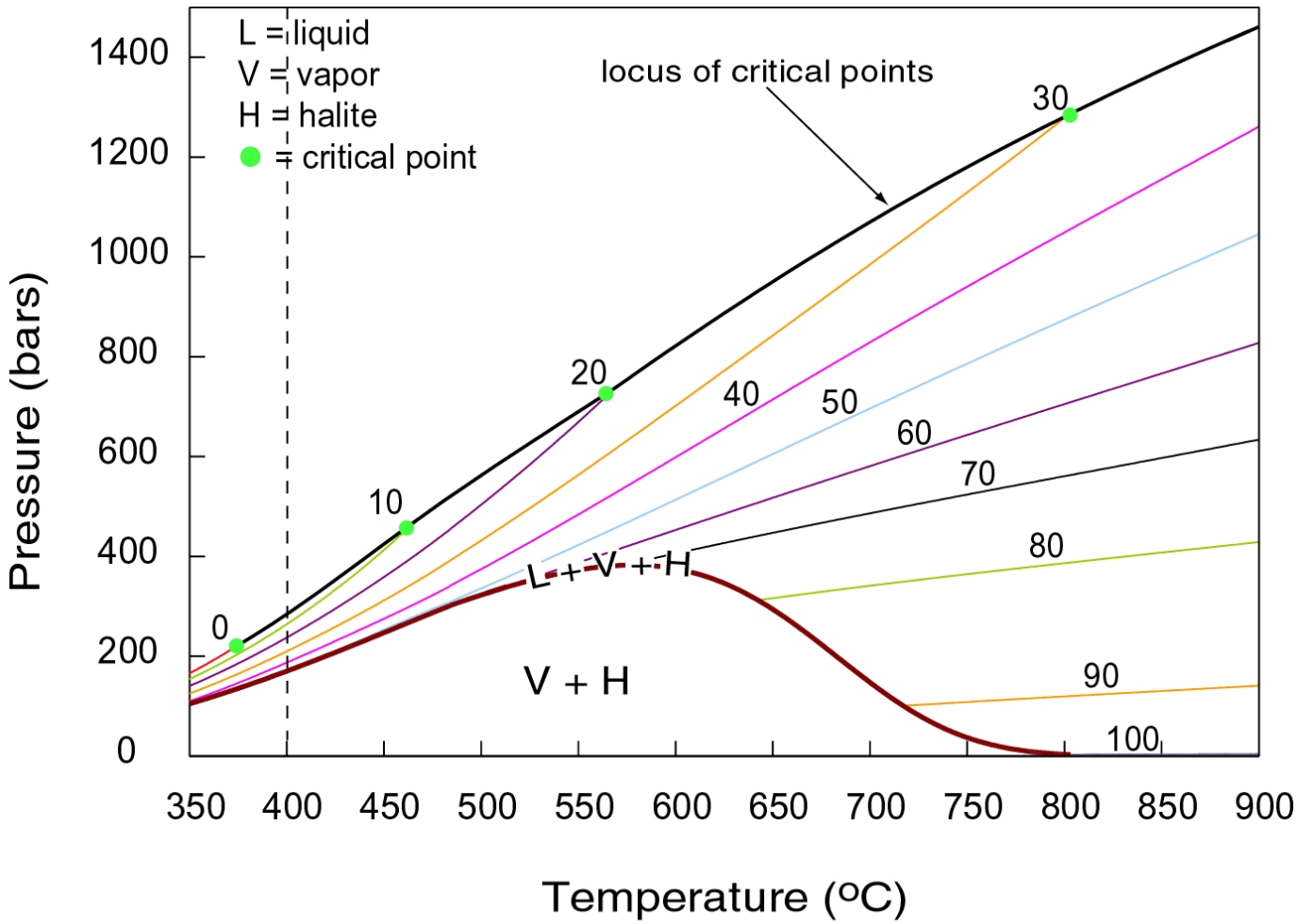

Figure 22. PT projection of isopleths for H_2O-NaCl (labeled in wt% NaCl) over the temperature range 350° - 900°C. The dashed line represents the maximum temperature shown on the previous diagram, and the minimum temperature on the following diagram.

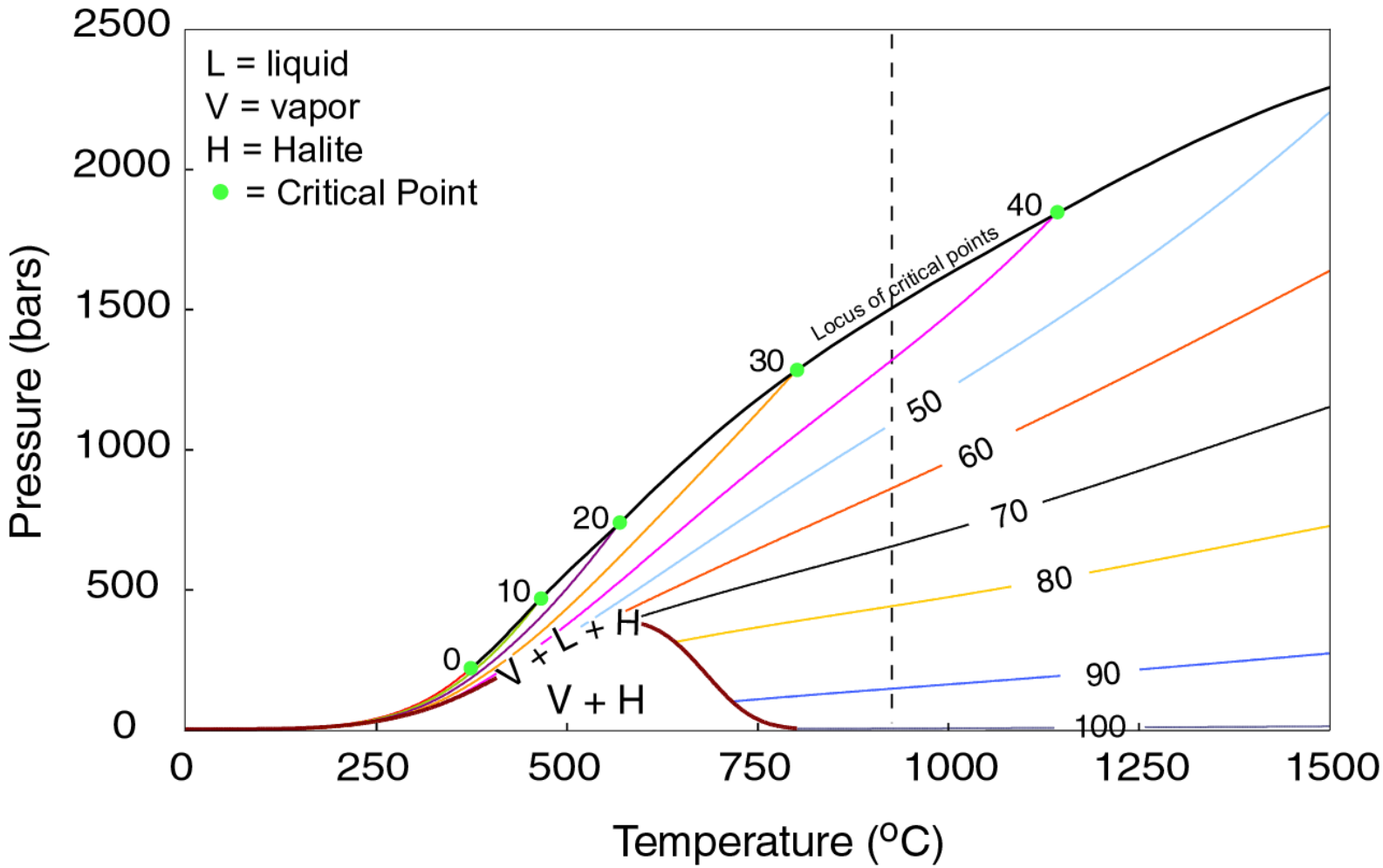

Figure 23. PT projection of H_2O-NaCl liquid-vapor region with isopleths, shown in wt% NaCl, predicted by the model. The dashed line represents the maximum temperature of the previous P-T diagram.

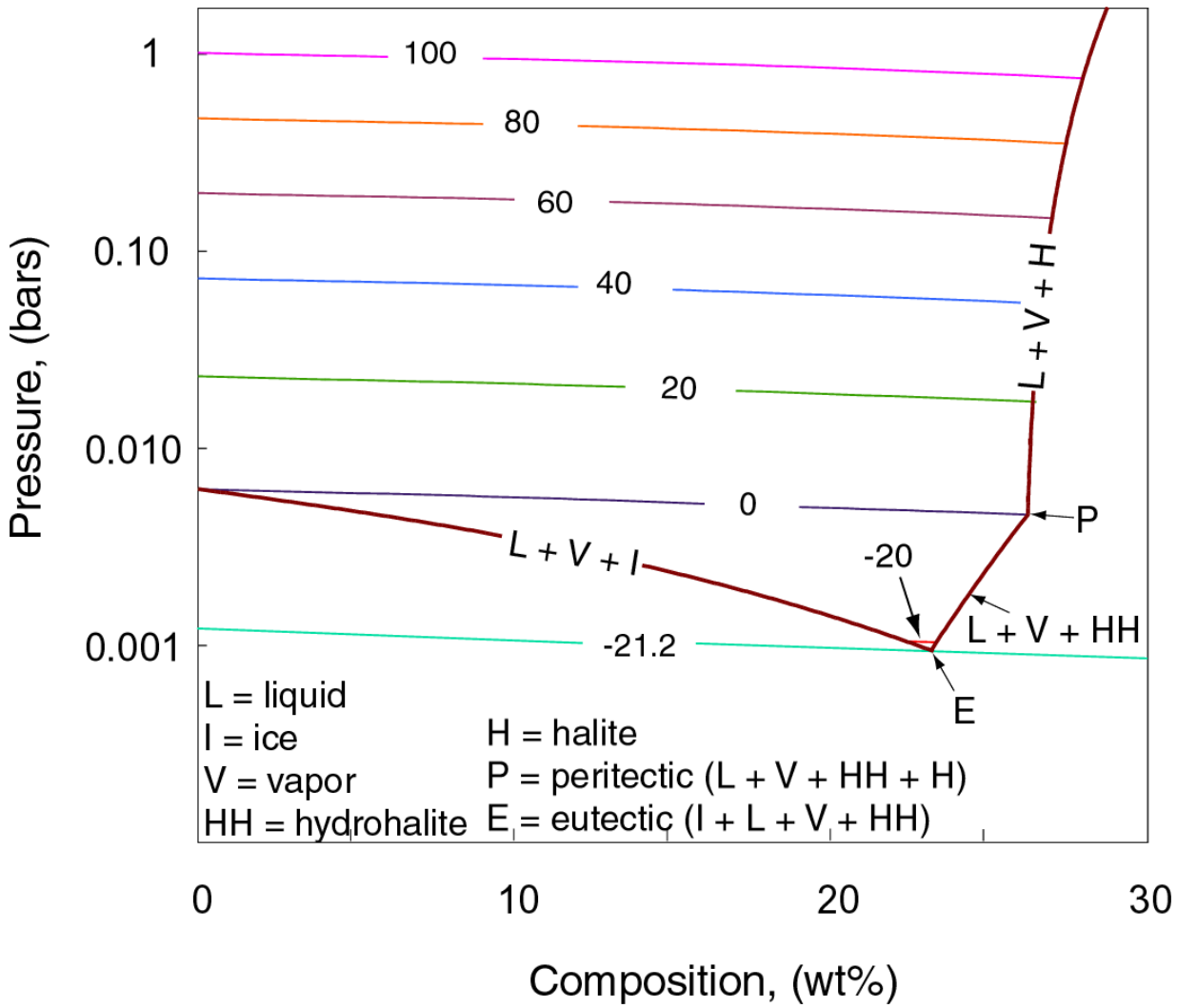

Figure 24. PX projection of the H_2O-NaCl system below 100 °C, predicted by the model.

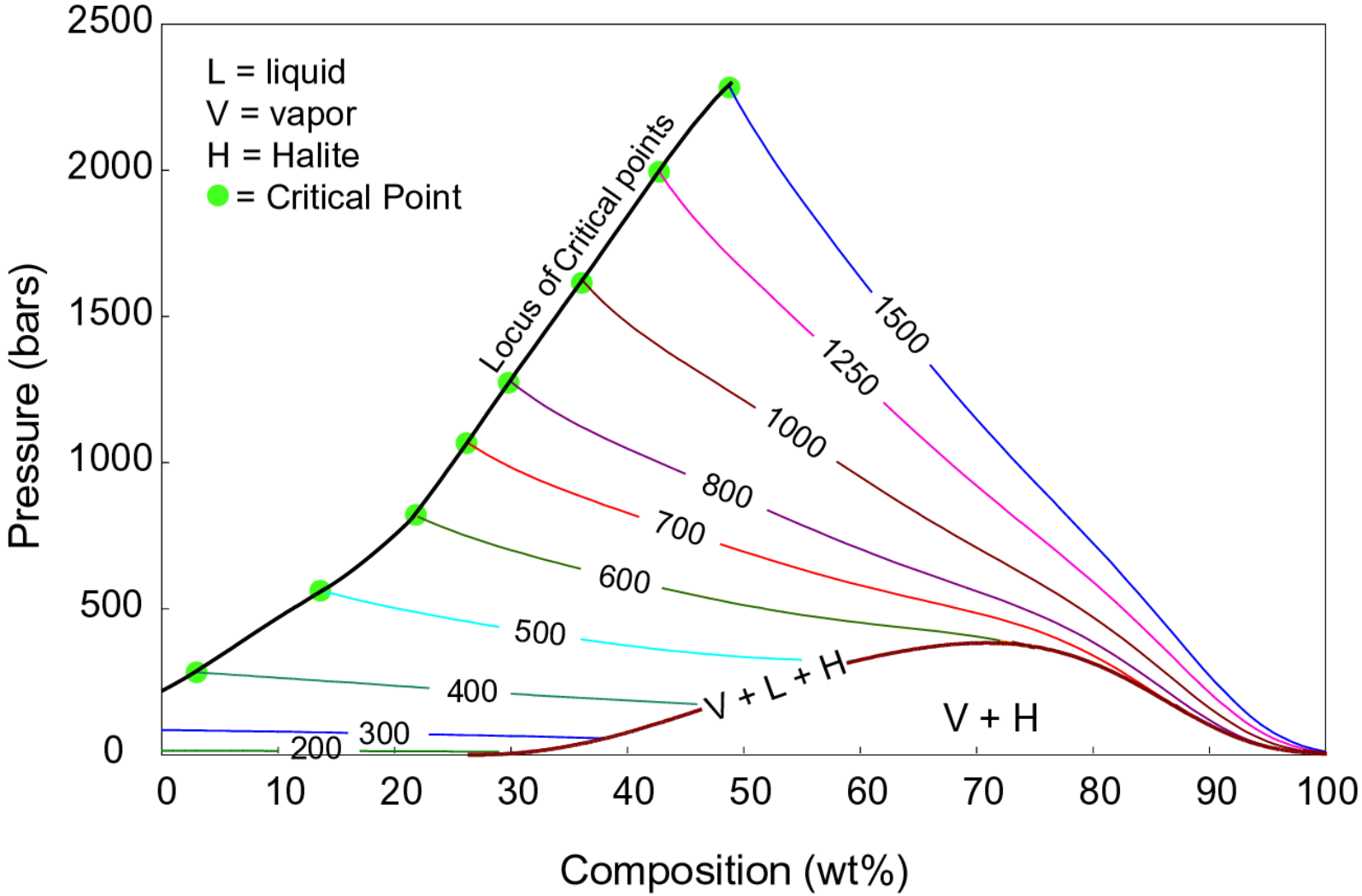

Figure 25. PX projection showing vapor pressures in the liquid region of the H_2O-NaCl system predicted by the model

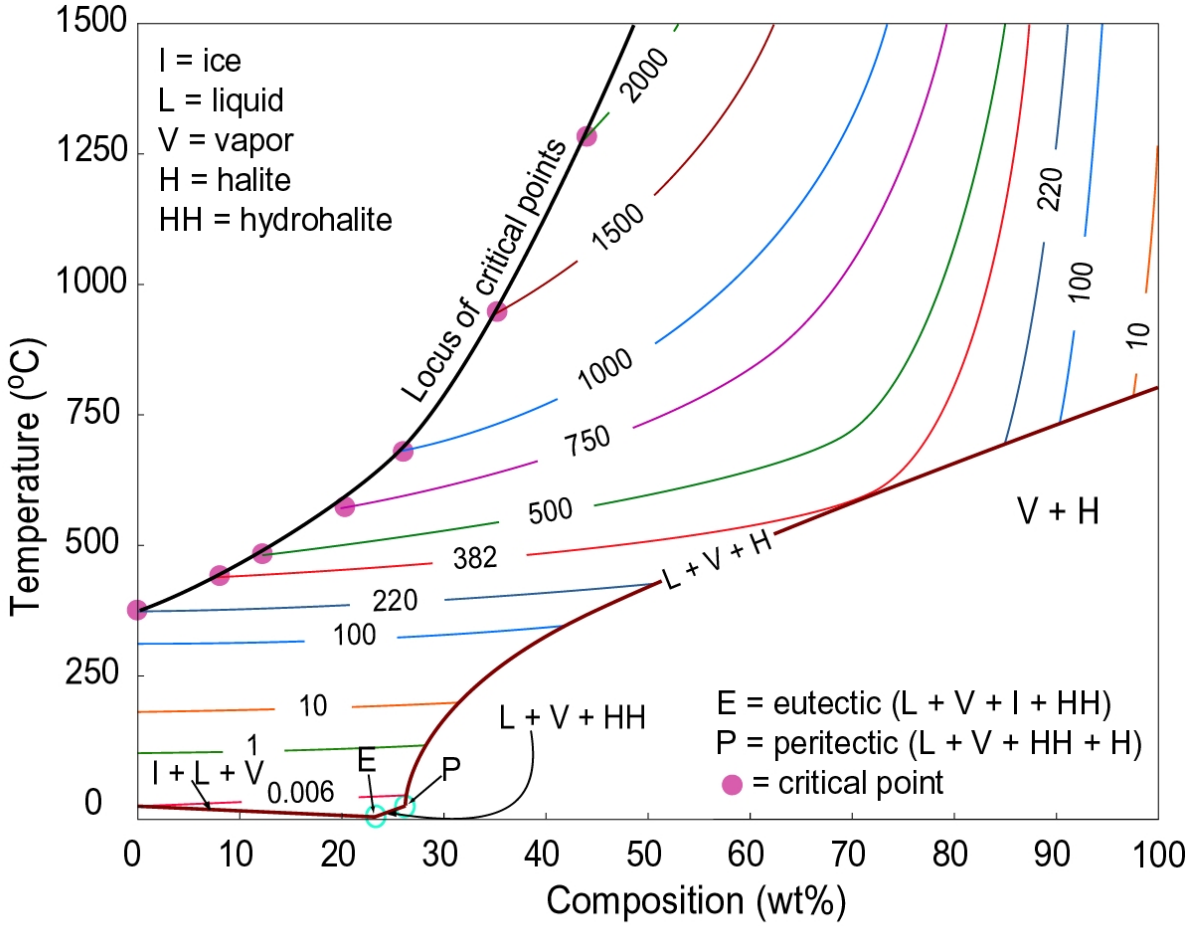

Figure 26. TX projection showing isobars predicted by the model. The .006 bar isobar represents the triple point pressure for pure H_2O, the 220 bar isobar represents the critical pressure of pure H_2O, and the 382 bar isobar represents the maximum pressure on the liquid + vapor + halite (L + V + H) curve.

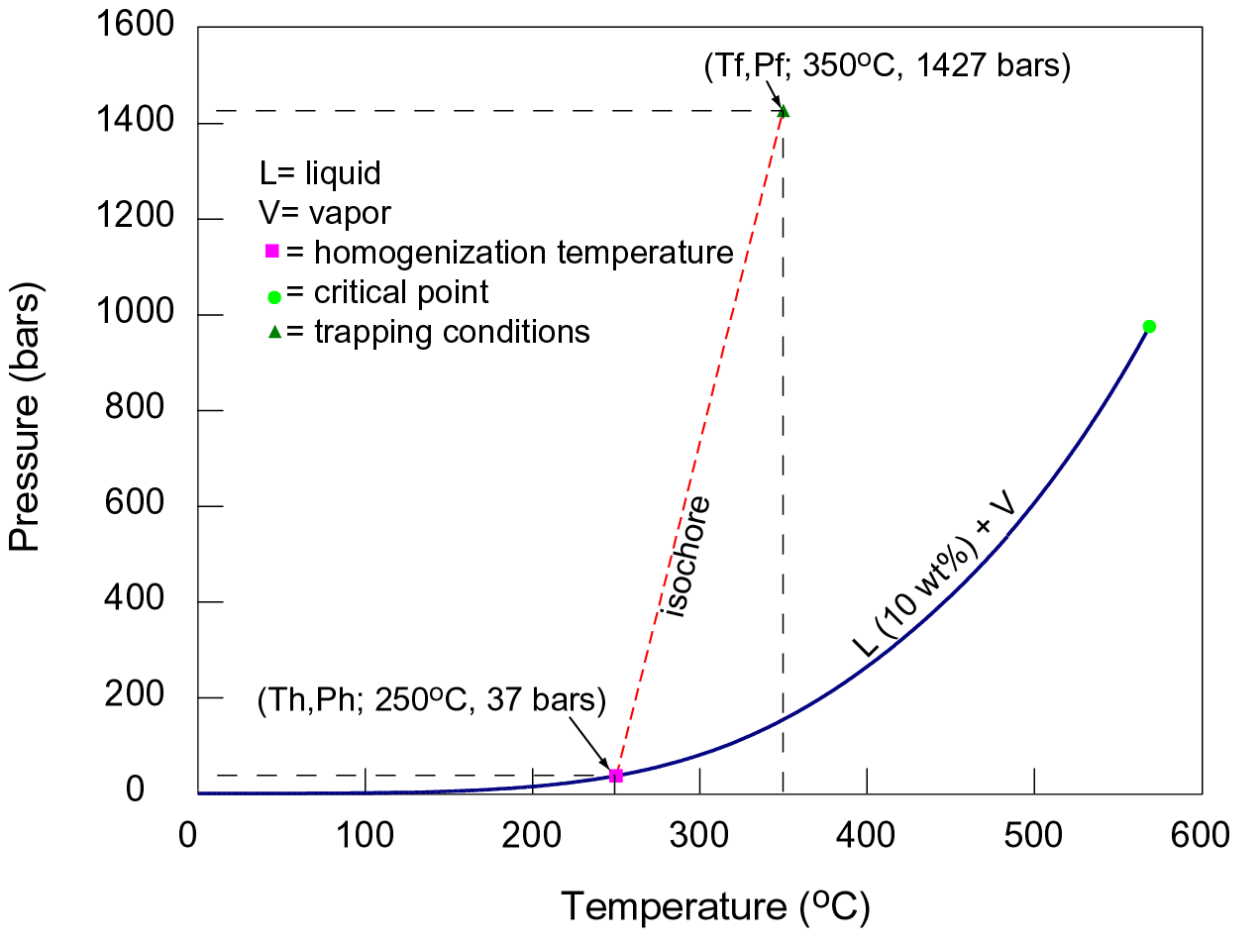

Figure 27. PT projection of the 10 wt% NaCl vapor pressure curve (L +V) predicted by the model showing temperature of homogenization (Th, 250°C) and pressure of homogenization (Ph, 37 bars), isochore and temperature (Tf, 350°C) and pressure of formation (Ph, 1427 bars).

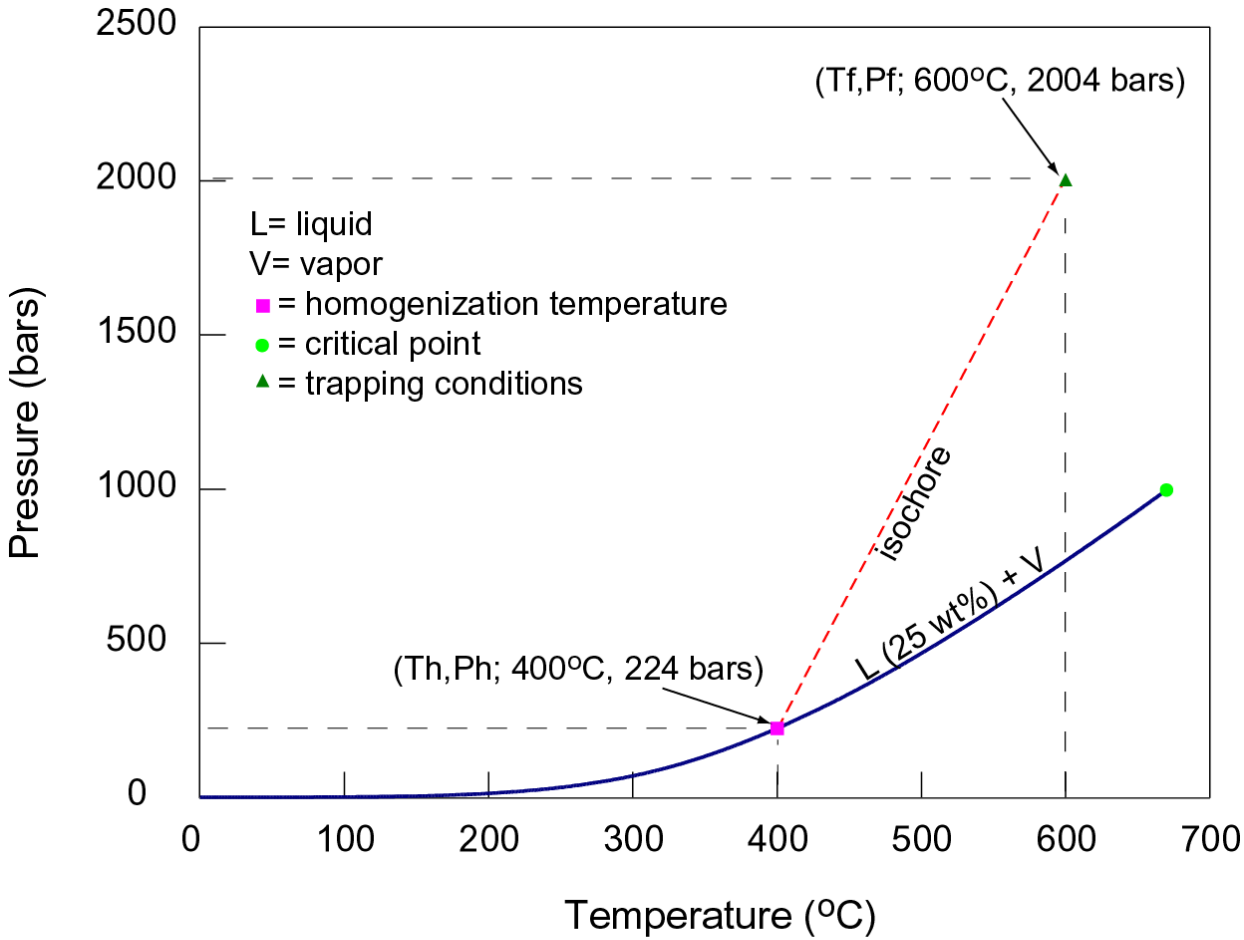

Figure 28. PT projection of the 25 wt% NaCl vapor pressure curve (L + V) predicted by the model showing temperature of homogenization (Th, 400°C) and pressure of homogenization (Ph, 224 bars), isochore and temperature (Tf, 600°C) and pressure of formation (Ph, 2004 bars).

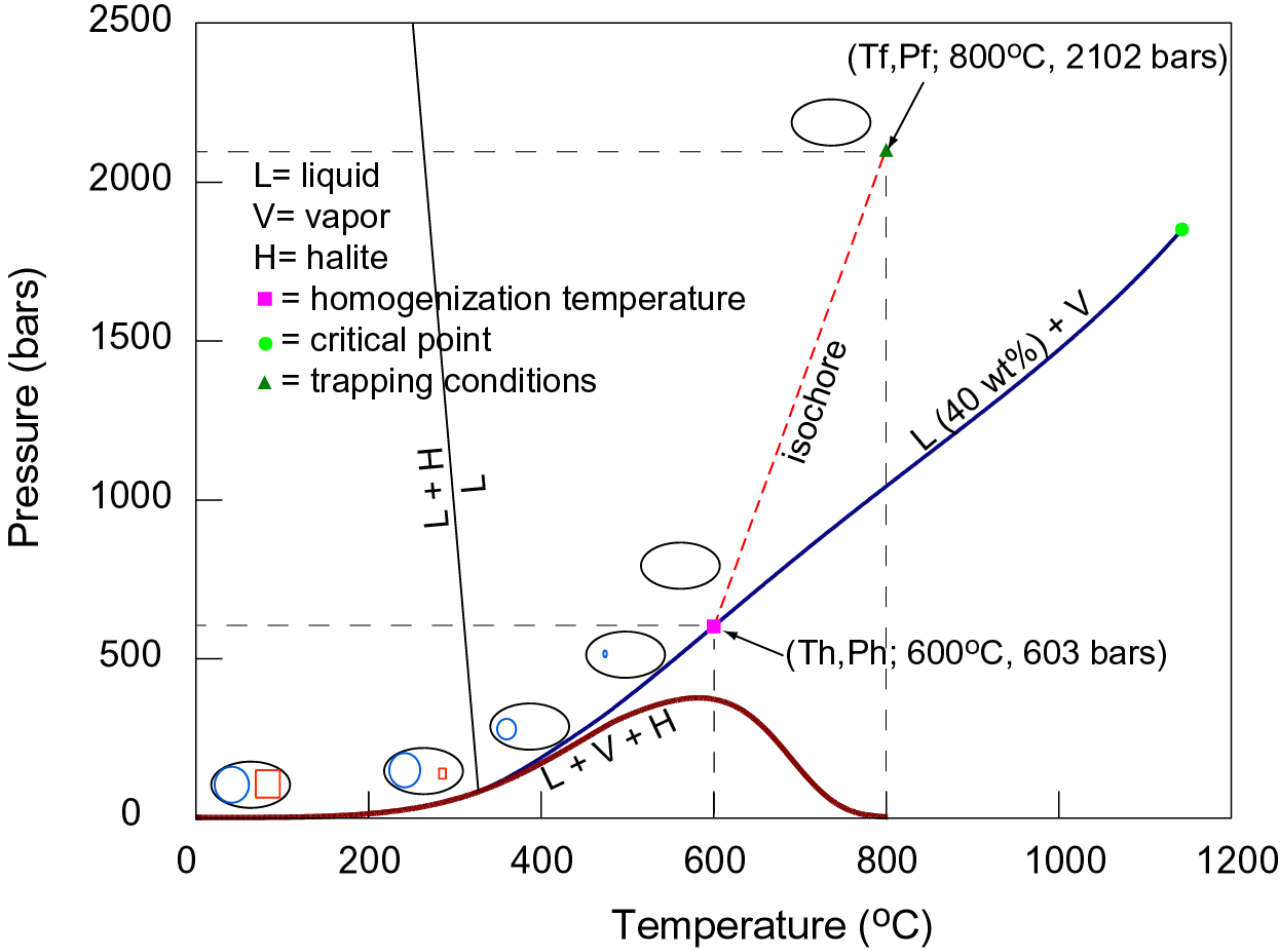

Figure 29. PT projection of the 40 wt% vapor pressure curve (L + V) predicted by the model showing liquid + vapor + halite (L + V + H) curve, temperature (Th, 600ºC) and pressure of homogenization (Ph, 603 bars), isochore and temperature (Tf, 800ºC) and pressure of formation (Ph, 2102 bars).

Table 1. Published data for PTX properties of H_2O-NaCl.

Author	PTX Data Range		
	X (wt% NaCl)	T (°C)	P (bars)
*Bischoff, 1991	0 - 60.7	300 - 500	58 - 580
*Bischoff and Pitzer, 1989	0 - 58.3	300 - 500	58 - 580
*Bischoff and Rosenbauer,1988	3.2	380 - 415	210 - 320
*Bischoff et al., 1986	0.1 - 8.8	373 - 375.5	200 - 225
*Bodnar, 1993	0 - 23	-21.2 - 0	0.006 - 0.001
*Bodnar et al., 1985	44 - 76	500 - 1000	500 - 1300
*Carlson et al., 1960	100	3327	235
*Ewing and Stern, 1974	100	801- 967	0.0005 - 120
*Fabuss and Korosi, 1966	0.5 - 17.3	75 - 150	0.3 - 4.1
*Haar et al., 1984	0	0.01- 374	0.006 - 220
*Haas, 1976	0 - 39.7	80 - 325	.3 - 120
*National Research Council, 1928	26 - 28	0.01 - 110	0.004 - 1.06
*Keevil, 1942	30 - 77	183 - 646	7.3 - 373
*Khaibullin and Borisov, 1966	1 - 25	100 - 440	0.9 - 400
*Knight and Bodnar, 1989	0 - 27.5	374 - 740	220 - 1184
Ölander and Liander,1950	0 - 7	374 - 437.5	221 - 392
*Pitzer and Pabalan, 1986	100	800	0.0005
*Rosenbauer and Bischoff, 1987	10.5 - 25	450 - 500	397 - 582.6
Sourirajan and Kennedy, 1962	0 - 26.4	350 - 700	165 - 1237
Urusova, 1974	3 - 71.7	450 - 550	256 - 740
Urusova, 1975	10 - 59.9	350 - 550	152 - 750
Urusova and Ravich, 1971	10 - 49.5	350 - 400	105 - 223

** denotes data used in model development.*

$$\begin{aligned}\text{Log } P = {} & \beta_{00}*T^0*X^0 + \beta_{01}*T^0*X^1 + \beta_{03}*T^0*X^3 + \beta_{04}*T^0*X^4 + \beta_{05}*T^0*X^5 + \beta_{06}*T^0*X^6 + \beta_{07}*T^0*X^7 + \beta_{10}*T^1*X^0 + \beta_{20}*T^2*X^0 \\ & + \beta_{30}*T^3*X^0 + \beta_{40}*T^4*X^0 + \beta_{50}*T^5*X^0 + \beta_{60}*T^6*X^0 + \beta_{70}*T^7*X^0 + \beta_{11}*T^1*X^1 + \beta_{12}*T^1*X^2 + \beta_{13}*T^1*X^3 + \beta_{15}*T^1*X^5 \\ & + \beta_{16}*T^1*X^6 + \beta_{21}*T^2*X^1 + \beta_{22}*T^2*X^2 + \beta_{23}*T^2*X^3 + \beta_{24}*T^2*X^4 + \beta_{25}*T^2*X^5 + \beta_{31}*T^3*X^1 + \beta_{32}*T^3*X^2 + \beta_{33}*T^3*X^3 \\ & + \beta_{34}*T^3*X^4 + \beta_{42}*T^4*X^2 + \beta_{43}*T^4*X^3 + \beta_{51}*T^5*X^1\end{aligned}$$

Equation 1. Equation and coefficients for the temperature range -21.2° - 300°C. The subscript i, j on the coefficient β_{ij}, corresponds to the exponent for the T and X terms, respectively, listed in Table 4.

Table 2. Estimated coefficients for Equation 1. Coefficients with no value were were not predicted to be significant by the backwards stepwise regression model.

	X^0	X^1	X^2	X^3
T^0	-27.2444260945847	-3.43823854919821	-	49.6470810423974
T^1	19.6752698743832	2.94599944070388	-5.05958726370657	-78.057932502234
T^2	-6.03987279418686	-1.02712250242286	5.3605248349362	18.9371135629599
T^3	1.05318996126294	0.132241696257544	-1.43460393380215	-0.517812895404853
T^4	-0.107523830798341	-	0.115824432759682	-0.147543794540513
T^5	0.0063216048751384	-0.000792743415349166	-	
T^6	-0.000201391014431089	-		
T^7	0.0000029370853393422			

	X^4	X^5	X^6	X^7
T^0	284.920532084465	-671.468924936888	-306.420824097701	-476.3912831617690
T^1	-	272.541674619991	191.281847960897	
T^2	-27.5731923399911	-43.6261697756668		
T^3	4.28981312806579			
T^4				
T^5				
T^6				
T^7				

$$\begin{aligned}\text{Log P} = {} & \beta_{00}*T^0*X^0 + \beta_{01}*T^0*X^1 + \beta_{02}*T^0*X^2 + \beta_{03}*T^0*X^3 + \beta_{04}*T^0*X^4 + \beta_{06}*T^0*X^6 + \beta_{07}*T^0*X^7 + \beta_{10}*T^1*X^0 + \beta_{20}*T^2*X^0 \\ & + \beta_{30}*T^3*X^0 + \beta_{60}*T^6*X^0 + \beta_{11}*T^1*X^1 + \beta_{12}*T^1*X^2 + \beta_{13}*T^1*X^3 + \beta_{14}*T^1*X^4 + \beta_{15}*T^1*X^5 + \beta_{16}*T^1*X^6 + \beta_{21}*T^2*X^1 \\ & + \beta_{22}*T^2*X^2 + \beta_{23}*T^2*X^3 + \beta_{24}*T^2*X^4 + \beta_{31}*T^3*X^1 + \beta_{32}*T^3*X^2 + \beta_{43}*T^4*X^3 + \beta_{51}*T^5*X^1 + \beta_{61}*T^6*X^1\end{aligned}$$

Equation 2. Equation and coefficients for the temperature range 300º - 484ºC. The subscript i, j on the coefficient β_{ij}, corresponds to the exponent for the T and X terms, respectively, listed in Table 3.

Table 3. Estimated coefficients for Equation 2. Coefficients with no value were were not predicted to be significant by the backwards stepwise regression model.

	X^0	X^1	X^2	X^3	X^4
T^0	-7.25091694178014	52.7356253268118	-95.139589091999	237.001333358832	-270.853923550159
T^1	2.91847163119225	-30.0742277771278	41.0055099275695	-82.6121950337547	86.8864476861164
T^2	-0.282727704099067	5.98143068258883	-5.87588111777108	7.89995198785004	-10.886118260654
T^3	0.00898343968706551	-0.436696998416016	0.27654361988714	-	-
T^4	-	-	-	-0.0074586977134027	
T^5	-	0.000828114542697018	-		
T^6	0.0000015228510009732	-			
T^7	-				

	X^5	X^6	X^7
T^0	-	-645.843502315573	411.125432162485
T^1	85.0303689746524	-24.1431916305905	
T^2	-		
T^3			
T^4			
T^5			
T^6			
T^7			

$$
\begin{aligned}
\text{Log } P = {} & \beta_{00}*T^0*X^0 + \beta_{02}*T^0*X^2 + \beta_{03}*T^0*X^3 + \beta_{04}*T^0*X^4 + \beta_{05}*T^0*X^5 + \beta_{06}*T^0*X^6 + \beta_{07}*T^0*X^7 + \beta_{10}*T^1*X^0 + \beta_{20}*T^2*X^0 \\
& + \beta_{30}*T^3*X^0 + \beta_{40}*T^4*X^0 + \beta_{50}*T^5*X^0 + \beta_{60}*T^6*X^0 + \beta_{70}*T^7*X^0 + \beta_{11}*T^1*X^1 + \beta_{12}*T^1*X^2 + \beta_{14}*T^1*X^4 + \beta_{15}*T^1*X^5 \\
& + \beta_{16}*T^1*X^6 + \beta_{21}*T^2*X^1 + \beta_{22}*T^2*X^2 + \beta_{23}*T^2*X^3 + \beta_{24}*T^2*X^4 + \beta_{31}*T^3*X^1 + \beta_{32}*T^3*X^2 + \beta_{33}*T^3*X^3 + \beta_{41}*T^4*X^1 \\
& + \beta_{43}*T^4*X^3 + \beta_{51}*T^5*X^1
\end{aligned}
$$

Equation 3. Equation and coefficients for the temperature range 484º - 1500ºC. The subscript i, j on the coefficient β_{ij}, corresponds to the exponent for the T and X terms, respectively, listed in Table 4.

Table 4. Estimated coefficients for Equation 3. Coefficients with no value were were not predicted to be significant by the backwards stepwise regression model.

	X^0	X^1	X^2	X^3
T^0	-10.1708289018151	-	11.2757426837744	-36.8724870227751
T^1	4.7809083340614	-0.40967075242513	-4.54787095348135	-
T^2	-0.739844995911952	0.253297767997384	0.47135407604605	-0.945923182349318
T^3	0.06103819662666580000	-0.0345961482768031	0.0366507031096144	-0.0221690359176769
T^4	-0.00273833143331212000	0.000309690020876693	-	0.000111317870749135
T^5	0.00008040575345729920	-0.000005651762407103	-	
T^6	-0.00000127759502052200	-		
T^7	0.00000000897506220730			

	X^4	X^5	X^6	X^7
T^0	194.960961125252	-412.422321803683	386.510614816185	-139.824224670799
T^1	7.95552629364737	-6.37018268058654	0.988511643702363	
T^2	0.546929925768266	-		
T^3	-			
T^4				
T^5				
T^6				
T^7				

APPENDIX A

Published PTX Data on H_2O-NaCl Phase Equilibria Used in Regression.

Bischoff and Pitzer (1989)

Temperature (ºC)	Pressure (bars)	Composition (wt% NaCl)
300	58	37.5
300	60	35.23
300	65	29.88
300	70	24.19
300	75	17.49
300	80	9.83
300	83	5.04
300	84	3.18
300	85	1.1
300	85.8	0
310	67	38.4
310	70	35.14
310	75	30.28
310	80	25.42
310	85	19.49
310	90	13
310	95	5.77
310	97	2.55
310	98.6	0
320	76	39.3
320	80	35.69
320	85	31.29
320	90	27.01
320	95	22.09
320	100	16.66
320	105	10.81
320	110	3.95
320	112.8	0
330	86	40.2
330	90	36.97
330	95	33.11
330	100	29.16
330	105	25.26

330	110	20.6
330	115	15.64
330	120	10.26
330	125	4.25
330	128.5	0
340	95	41.2
340	100	37.86
340	105	34.67
340	110	31.29
340	120	24.31
340	125	20.12
340	130	15.89
340	135	11.23
340	140	6.21
340	145	0.5
340	145.9	0
350	105	42.2
350	110	39.25
350	115	36.61
350	120	33.73
350	125	30.79
350	130	28.01
350	135	24.75
350	140	21.08
350	145	17.42
350	150	13.54
350	155	9.41
350	157	7.68
350	160	4.71
350	163	2
350	165.2	0
360	117	43
360	120	41.28
360	125	38.8
360	130	36.5
360	135	34
360	140	31.3
360	145	28.4
360	150	25.5
360	155	22.5
360	160	19.4

360	165	16
360	170	12.4
360	175	8.6
360	177	7
360	180	5
360	183	2.5
360	185	0.6
360	186.5	0
370	130	44
370	135	41.5
370	140	39.3
370	145	37.1
370	150	34.75
370	155	32.5
370	160	30
370	165	27.2
370	170	24.7
370	175	22
370	180	18.9
370	185	15.9
370	190	12.5
370	195	9.1
370	200	6
370	202	5
370	205	3.2
370	208	1.1
370	210.3	0
373	134	44.3
373	140	41.25
373	145	39
373	150	36.7
373	155	34.5
373	160	32.1
373	165	29.9
373	170	27.4
373	175	25
373	180	22.3
373	185	19.5
373	190	16.6
373	195	13.3
373	200	10

373	205	6.75
373	210	3.9
373	215	1.2
373	216	0.55
373	217	0.25
373	217.5	0.18
373	217.9	0
375.5	137	44.5
375.5	140	43.07
375.5	145	41
375.5	150	38.9
375.5	155	36.7
375.5	160	34.52
375.5	165	32.2
375.5	170	29.8
375.5	175	27.4
375.5	180	24.8
375.5	185	22.25
375.5	190	19.6
375.5	195	17
375.5	200	14
375.5	205	10.75
375.5	210	7.5
375.5	215	4.5
375.5	217	3.4
375.5	220	1.75
375.5	222	0.69
375.5	223.5	0.09
380	143	44.75
380	150	41.69
380	155	39.77
380	160	37.86
380	165	35.78
380	170	33.63
380	175	31.39
380	180	29.05
380	185	26.73
380	190	24.19
380	195	21.66
380	200	19.15
380	205	16.4

380	210	13.54
380	215	10.39
380	220	7.39
380	225	4.56
380	230	1.92
380	232	1.05
380	233.2	0.35
390	156	45.7
390	160	44.49
390	165	42.75
390	170	41.28
390	175	39.5
390	180	37.6
390	185	36.06
390	190	33.8
390	195	31.8
390	200	29.75
390	205	27.5
390	210	25.4
390	215	23.25
390	220	20.85
390	225	18.5
390	230	16
390	235	13.35
390	240	10.6
390	245	7.75
390	250	5.1
390	255	2.4
390	257	1.18
400	172	46.5
400	180	44.18
400	185	42.5
400	190	41
400	195	39.5
400	200	38
400	205	36.1
400	210	34.25
400	215	32.4
400	220	30.5
400	225	28.6
400	230	26.6

400	235	24.7
400	240	23.5
400	245	20.5
400	250	18.35
400	255	16.15
400	260	13.7
400	265	11.5
400	270	8.6
400	275	6.15
400	280	3.45
400	280.7	2.22
410	186	47.4
410	190	46.32
410	195	45.11
410	200	43.79
410	205	42.43
410	210	41.12
410	215	39.68
410	220	38.3
410	225	36.79
410	230	35.23
410	235	33.63
410	240	31.98
410	245	30.28
410	250	28.64
410	255	26.83
410	260	24.86
410	265	23.06
410	270	21.08
410	275	18.78
410	280	16.91
410	285	14.86
410	290	12.4
410	295	10
410	300	8
410	305	5
410	306	3.56
420	202	48.8
420	205	48
420	210	46.92
420	215	45.8

420	220	44.65
420	225	43.39
420	230	42.1
420	235	40.87
420	240	39.51
420	245	38.12
420	250	36.79
420	255	35.32
420	260	33.82
420	265	32.37
420	270	30.89
420	275	29.26
420	280	27.58
420	285	25.86
420	290	24.08
420	295	22.37
420	300	20.6
420	305	18.66
420	310	16.66
420	315	14.7
420	320	12.5
420	325	10.5
420	330	8.2
420	334	4.75
430	218	50
430	220	49.58
430	225	48.52
430	230	47.51
430	235	46.47
430	240	45.42
430	245	44.18
430	250	43.23
430	255	41.94
430	260	40.78
430	265	39.6
430	270	38.39
430	275	36.97
430	280	35.69
430	285	34.39
430	290	33.05
430	295	31.59

430	300	30.08
430	305	28.64
430	310	27.16
430	315	25.64
430	320	24.08
430	325	22.37
430	330	20.6
430	335	18.5
430	340	17
430	345	15
430	350	13.1
430	355	11.5
430	360	9.5
430	363	6.1
440	235	51.1
440	240	50
440	245	49.23
440	250	48.23
440	255	47.36
440	260	46.4
440	265	45.26
440	270	44.18
440	275	43.23
440	280	42.19
440	285	41.12
440	290	39.94
440	295	38.91
440	300	37.68
440	305	36.52
440	310	35.32
440	315	34.2
440	320	32.86
440	325	31.49
440	330	30.28
440	335	28.84
440	340	27.37
440	345	26.08
440	350	24.53
440	355	23.17
440	360	21.55
440	365	19.88

440	370	18.2
440	375	16.5
440	380	15
440	385	13.5
440	390	11.2
440	394	7.5
450	250	52.5
450	255	51.5
450	260	50.8
450	265	49.93
450	270	49.09
450	275	48.23
450	280	47.36
450	285	46.47
450	290	45.57
450	295	44.65
450	300	43.71
450	305	42.75
450	310	41.78
450	315	40.78
450	320	39.77
450	325	38.74
450	330	37.5
450	335	36.42
450	340	35.32
450	345	34.2
450	350	33.05
450	355	31.88
450	360	30.69
450	365	29.47
450	370	28.22
450	375	26.94
450	380	25.42
450	385	24.08
450	390	22.5
450	395	21.31
450	400	20
450	405	18.5
450	410	17.1
450	415	15.4
450	420	12.6

450	423	8.8
475	286	56.2
475	290	55.8
475	295	55
475	300	54.31
475	305	53.54
475	310	52.9
475	315	52.24
475	320	51.44
475	325	50.76
475	330	50.07
475	335	49.23
475	340	48.52
475	345	47.8
475	350	46.92
475	355	46.17
475	360	45.42
475	365	44.49
475	370	43.71
475	375	42.75
475	380	41.94
475	385	41.12
475	390	40.11
475	395	39.25
475	400	38.21
475	405	37.33
475	410	36.42
475	415	35.51
475	420	34.39
475	425	33.44
475	430	32.28
475	435	31.29
475	440	30.28
475	445	29.26
475	450	28.01
475	455	26.94
475	460	25.7
475	465	24.8
475	470	23.5
475	475	22
475	480	21

475	485	19
475	490	17
475	495	13.6
475	496.8	11.3
500	324	60.7
500	330	60
500	335	59.4
500	340	58.99
500	345	58.3
500	350	57.72
500	355	57.25
500	360	56.65
500	365	56.05
500	370	55.31
500	375	54.69
500	380	54.18
500	385	53.54
500	390	52.9
500	395	52.24
500	400	51.64
500	405	50.9
500	410	50.21
500	415	49.51
500	420	48.81
500	425	48.09
500	430	47.51
500	435	46.62
500	440	46.02
500	445	45.26
500	450	44.49
500	455	43.71
500	460	42.91
500	465	42.1
500	470	41.28
500	475	40.45
500	480	39.6
500	485	38.74
500	490	37.86
500	495	36.97
500	500	36.06
500	505	35.14

500	510	34.2
500	515	33.25
500	520	32.47
500	525	31.29
500	530	30.18
500	535	29.16
500	540	28.1
500	545	27.2
500	550	26.3
500	555	25
500	560	23.6
500	565	22.5
500	570	21
500	575	19
500	580	16.35
500	581.8	13.6

Bodnar (1993) with Fisher (1988)

Temperature (ºC)	Pressure (bars)	Composition (wt% NaCl)
0	0.00611	0
-1	0.00563	1.74
-2	0.00518	3.39
-3	0.00476	4.96
-4	0.00437	6.45
-5	0.00402	7.86
-6	0.00369	9.21
-7	0.00338	10.49
-8	0.0031	11.7
-9	0.00284	12.85
-10	0.0026	13.94
-11	0.00237	14.97
-12	0.00217	15.96
-13	0.00198	16.89
-14	0.00181	17.79
-15	0.00165	18.63
-16	0.0015	19.45
-17	0.00137	20.22
-18	0.00125	20.97
-19	0.00113	21.68

-20	0.00103	22.38
-21	0.00094	23.05

Bodnar et al. (1985)

Temperature (ºC)	Pressure (bars)	Composition (wt% NaCl)
550	500	48.95
600	500	58.7
650	500	66.5
700	500	69.8
750	500	70.8
775	500	71.85
800	500	75.9
825	500	76.15
625	750	48.65
700	750	59.6
775	750	66.3
800	750	67.25
650	1000	35.65
700	1000	48.85
750	1000	56
800	1000	60.85
825	1000	63.25
850	1000	66.35
900	1000	68
1000	1000	72.35
700	1100	44.2
800	1100	58.6
800	1200	52.95
800	1300	50.6
850	1300	57.2

Carlson et al. (1960)

Temperature (ºC)	Pressure (bars)	Composition (wt% NaCl)
3327	230.9466075	100

Ewing and Stern (1974)

Temperature (ºC)	Pressure (bars)	Composition (wt% NaCl)
807	0.000593816	100
827	0.000857394	100
847	0.001220296	100
867	0.001713188	100
887	0.002371798	100
907	0.003246391	100
927	0.00439296	100
947	0.0058795	100
967	0.007784672	100

Fabuss and Korosi (1966)

Temperature (ºC)	Pressure (bars)	Composition (wt% NaCl)
75	0.38416	0.58187
75	0.37163	5.52916
75	0.35736	10.47826
75	0.34977	12.76315
75	0.33361	17.15640
100	1.00976	0.58314
100	0.97804	5.54089
100	0.94157	10.49858
100	0.92242	12.78693
100	0.87946	17.18535
125	2.30943	0.58586
125	2.24098	5.56362
125	2.15676	10.54079
125	2.11315	12.83203
125	2.01872	17.24150
150	4.73674	0.59065
150	4.59355	5.60576
150	4.41944	10.61182
150	4.33048	12.91654
150	4.14495	17.34376

Haar et al. (1984)

Temperature (ºC)	Pressure (bars)	Composition (wt% NaCl)
0.01	0.00612	0.0
1	0.00657	0.0
2	0.00706	0.0
3	0.00758	0.0
4	0.00814	0.0
5	0.00873	0.0
6	0.00935	0.0
7	0.01002	0.0
8	0.01073	0.0
9	0.01148	0.0
10	0.01228	0.0
11	0.01313	0.0
12	0.01403	0.0
13	0.01498	0.0
14	0.01599	0.0
15	0.01706	0.0
16	0.01819	0.0
17	0.01938	0.0
18	0.02064	0.0
19	0.02198	0.0
20	0.02339	0.0
21	0.02488	0.0
22	0.02645	0.0
23	0.02810	0.0
24	0.02985	0.0
25	0.03169	0.0
26	0.03363	0.0
27	0.03567	0.0
28	0.03782	0.0
29	0.04008	0.0
30	0.04246	0.0
31	0.04495	0.0
32	0.04758	0.0
33	0.05034	0.0
34	0.05323	0.0
35	0.05627	0.0

36	0.05945	0.0
37	0.06280	0.0
38	0.06630	0.0
39	0.06997	0.0
40	0.07381	0.0
41	0.07784	0.0
42	0.08205	0.0
43	0.08646	0.0
44	0.09108	0.0
45	0.09590	0.0
46	0.10094	0.0
47	0.10621	0.0
48	0.11171	0.0
49	0.11745	0.0
50	0.12344	0.0
51	0.12970	0.0
52	0.13623	0.0
53	0.14303	0.0
54	0.15012	0.0
55	0.15752	0.0
56	0.16522	0.0
57	0.17324	0.0
58	0.18159	0.0
59	0.19028	0.0
60	0.19932	0.0
61	0.20873	0.0
62	0.21851	0.0
63	0.22868	0.0
64	0.23925	0.0
65	0.25022	0.0
66	0.26163	0.0
67	0.27347	0.0
68	0.28576	0.0
69	0.29852	0.0
70	0.31176	0.0
71	0.32549	0.0
72	0.33972	0.0
73	0.35448	0.0
74	0.36978	0.0
75	0.38563	0.0
76	0.40205	0.0

77	0.41905	0.0
78	0.43665	0.0
79	0.45487	0.0
80	0.47373	0.0
81	0.49324	0.0
82	0.51342	0.0
83	0.53428	0.0
84	0.55585	0.0
85	0.57815	0.0
86	0.60119	0.0
87	0.62499	0.0
88	0.64958	0.0
89	0.67496	0.0
90	0.70117	0.0
91	0.72823	0.0
92	0.75614	0.0
93	0.78495	0.0
94	0.81465	0.0
95	0.84529	0.0
96	0.87688	0.0
97	0.90945	0.0
98	0.94301	0.0
99	0.97759	0.0
100	1.01320	0.0
101	1.04990	0.0
102	1.08770	0.0
103	1.12660	0.0
104	1.16670	0.0
105	1.20790	0.0
106	1.25030	0.0
107	1.29390	0.0
108	1.33880	0.0
109	1.38500	0.0
110	1.43240	0.0
111	1.48120	0.0
112	1.53130	0.0
113	1.58290	0.0
114	1.63580	0.0
115	1.69020	0.0
116	1.74610	0.0
117	1.80340	0.0

118	1.86230	0.0
119	1.92280	0.0
120	1.98480	0.0
121	2.04850	0.0
122	2.11390	0.0
123	2.18090	0.0
124	2.24960	0.0
125	2.32010	0.0
126	2.39240	0.0
127	2.46660	0.0
128	2.54250	0.0
129	2.62040	0.0
130	2.70020	0.0
131	2.78200	0.0
132	2.86570	0.0
133	2.95150	0.0
134	3.03930	0.0
135	3.12930	0.0
136	3.22140	0.0
137	3.31570	0.0
138	3.41220	0.0
139	3.51090	0.0
140	3.61190	0.0
141	3.71530	0.0
142	3.82110	0.0
143	3.92920	0.0
144	4.03980	0.0
145	4.15290	0.0
146	4.26850	0.0
147	4.38670	0.0
148	4.50750	0.0
149	4.63100	0.0
150	4.75720	0.0
151	4.88610	0.0
152	5.01780	0.0
153	5.15230	0.0
154	5.28960	0.0
155	5.42990	0.0
156	5.57320	0.0
157	5.71940	0.0
158	5.86870	0.0

159	6.02110	0.0
160	6.17660	0.0
161	6.33530	0.0
162	6.49730	0.0
163	6.66250	0.0
164	6.83100	0.0
165	7.00290	0.0
166	7.17830	0.0
167	7.35700	0.0
168	7.53940	0.0
169	7.72520	0.0
170	7.91470	0.0
171	8.10780	0.0
172	8.30470	0.0
173	8.50530	0.0
174	8.70980	0.0
175	8.91800	0.0
176	9.13030	0.0
177	9.34640	0.0
178	9.56660	0.0
179	9.79090	0.0
180	10.01900	0.0
181	10.25200	0.0
182	10.48900	0.0
183	10.73000	0.0
184	10.97500	0.0
185	11.22500	0.0
186	11.47900	0.0
187	11.73800	0.0
188	12.00100	0.0
189	12.26900	0.0
190	12.54200	0.0
191	12.81900	0.0
192	13.10100	0.0
193	13.38800	0.0
194	13.68000	0.0
195	13.97600	0.0
196	14.27800	0.0
197	14.58500	0.0
198	14.89700	0.0
199	15.21400	0.0

200	15.53700	0.0
201	15.86400	0.0
202	16.19700	0.0
203	16.53600	0.0
204	16.88000	0.0
205	17.22900	0.0
206	17.58400	0.0
207	17.94500	0.0
208	18.31100	0.0
209	18.68400	0.0
210	19.06200	0.0
211	19.44600	0.0
212	19.83600	0.0
213	20.23200	0.0
214	20.63400	0.0
215	21.04200	0.0
216	21.45700	0.0
217	21.87800	0.0
218	22.30500	0.0
219	22.73800	0.0
220	23.17800	0.0
221	23.62500	0.0
222	24.07800	0.0
223	24.53800	0.0
224	25.00500	0.0
225	25.47900	0.0
226	25.95900	0.0
227	26.44600	0.0
228	26.94100	0.0
229	27.44200	0.0
230	27.95100	0.0
231	28.46700	0.0
232	28.99000	0.0
233	29.52100	0.0
234	30.05900	0.0
235	30.60400	0.0
236	31.15700	0.0
237	31.71800	0.0
238	32.28600	0.0
239	32.86300	0.0
240	33.44700	0.0

241	34.03900	0.0
242	34.63900	0.0
243	35.24700	0.0
244	35.86300	0.0
245	36.48800	0.0
246	37.12100	0.0
247	37.76200	0.0
248	38.41200	0.0
249	39.07000	0.0
250	39.73700	0.0
251	40.41200	0.0
252	41.09600	0.0
253	41.78900	0.0
254	42.49100	0.0
255	43.20200	0.0
256	43.92200	0.0
257	44.65100	0.0
258	45.39000	0.0
259	46.13700	0.0
260	46.89500	0.0
261	47.66100	0.0
262	48.43700	0.0
263	49.22300	0.0
264	50.01800	0.0
265	50.82300	0.0
266	51.63800	0.0
267	52.46300	0.0
268	53.29800	0.0
269	54.14300	0.0
270	54.99900	0.0
271	55.86400	0.0
272	56.74000	0.0
273	57.62700	0.0
274	58.52400	0.0
275	59.43100	0.0
276	60.35000	0.0
277	61.27900	0.0
278	62.21900	0.0
279	63.17000	0.0
280	64.13200	0.0
281	65.10500	0.0

282	66.08900	0.0
283	67.08500	0.0
284	68.09200	0.0
285	69.11100	0.0
286	70.14100	0.0
287	71.18300	0.0
288	72.23700	0.0
289	73.30300	0.0
290	74.38000	0.0
291	75.47000	0.0
292	76.57200	0.0
293	77.68600	0.0
294	78.81300	0.0
295	79.95200	0.0
296	81.10300	0.0
297	82.26800	0.0
298	83.44500	0.0
299	84.63500	0.0
300	85.83800	0.0
301	87.05400	0.0
302	88.28300	0.0
303	89.52600	0.0
304	90.78200	0.0
305	92.05100	0.0
306	93.33400	0.0
307	94.63100	0.0
308	95.94200	0.0
309	97.26700	0.0
310	98.60500	0.0
311	99.95800	0.0
312	101.32600	0.0
313	102.70700	0.0
314	104.10400	0.0
315	105.51000	0.0
316	106.94000	0.0
317	108.38000	0.0
318	109.84000	0.0
319	111.31000	0.0
320	112.79000	0.0
321	114.29000	0.0
322	115.81000	0.0

323	117.34000	0.0
324	118.89000	0.0
325	120.46000	0.0
326	122.04000	0.0
327	123.64000	0.0
328	125.25000	0.0
329	126.88000	0.0
330	128.52000	0.0
331	130.19000	0.0
332	131.87000	0.0
333	133.57000	0.0
334	135.28000	0.0
335	137.01000	0.0
336	138.76000	0.0
337	140.53000	0.0
338	142.32000	0.0
339	144.12000	0.0
340	145.94000	0.0
341	147.78000	0.0
342	149.64000	0.0
343	151.52000	0.0
344	153.42000	0.0
345	155.33000	0.0
346	157.27000	0.0
347	159.22000	0.0
348	161.20000	0.0
349	163.20000	0.0
350	165.21000	0.0
351	167.25000	0.0
352	169.31000	0.0
353	171.38000	0.0
354	173.48000	0.0
355	175.61000	0.0
356	177.75000	0.0
357	179.92000	0.0
358	182.11000	0.0
359	184.32000	0.0
360	186.55000	0.0
361	188.81000	0.0
362	191.10000	0.0
363	193.40000	0.0

364	195.74000	0.0
365	198.09000	0.0
365.5	199.28000	0.0
366	200.48000	0.0
366.5	201.68000	0.0
367	202.89000	0.0
367.5	204.11000	0.0
368	205.33000	0.0
368.5	206.56000	0.0
369	207.80000	0.0
369.5	209.05000	0.0
370	210.30000	0.0
370.5	211.56000	0.0
371	212.83000	0.0
371.5	214.11000	0.0
372	215.39000	0.0
372.5	216.69000	0.0
373	217.99000	0.0
373.5	219.30000	0.0
373.976	220.55000	0.0

Haas (1976)

Temperature (ºC)	Pressure (bars)	Composition (wt% NaCl)
80	0.474	0
85	0.578	0
90	0.701	0
95	0.845	0
100	1.013	0
105	1.208	0
110	1.433	0
115	1.691	0
120	1.985	0
125	2.321	0
130	2.701	0
135	3.131	0
140	3.614	0
145	4.155	0
150	4.76	0
155	5.433	0
160	6.18	0
165	7.008	0
170	7.92	0
175	8.925	0
180	10.027	0
185	11.234	0
190	12.552	0
195	13.989	0
200	15.551	0
205	17.245	0
210	19.08	0
215	21.063	0
220	23.201	0
225	25.504	0
230	27.979	0
235	30.635	0
240	33.48	0
245	36.524	0
250	39.776	0
255	43.245	0

260	46.94	0
265	50.872	0
270	55.051	0
275	59.487	0
280	64.192	0
285	69.175	0
290	74.449	0
295	80.025	0
300	85.917	0
305	92.136	0
310	98.697	0
315	105.612	0
320	112.899	0
325	120.571	0
80	0.459	5.0000
85	0.560	5.0000
90	0.679	5.0000
95	0.819	5.0000
100	0.982	5.0000
105	1.171	5.0000
110	1.388	5.0000
115	1.638	5.0000
120	1.924	5.0000
125	2.249	5.0000
130	2.618	5.0000
135	3.034	5.0000
140	3.502	5.0000
145	4.027	5.0000
150	4.613	5.0000
155	5.266	5.0000
160	5.991	5.0000
165	6.792	5.0000
170	7.677	5.0000
175	8.651	5.0000
180	9.719	5.0000
185	10.889	5.0000
190	12.167	5.0000
195	13.559	5.0000
200	15.073	5.0000
205	16.715	5.0000
210	18.493	5.0000

215	20.415	5.0000
220	22.487	5.0000
225	24.718	5.0000
230	27.116	5.0000
235	29.689	5.0000
240	32.446	5.0000
245	35.395	5.0000
250	38.544	5.0000
255	41.904	5.0000
260	45.483	5.0000
265	49.290	5.0000
270	53.336	5.0000
275	57.631	5.0000
280	62.184	5.0000
285	67.007	5.0000
290	72.110	5.0000
295	77.505	5.0000
300	83.203	5.0000
305	89.218	5.0000
310	95.561	5.0000
315	102.245	5.0000
320	109.286	5.0000
325	116.697	5.0000
80	0.44200	10.0000
85	0.54000	10.0000
90	0.65500	10.0000
95	0.79000	10.0000
100	0.94700	10.0000
105	1.12900	10.0000
110	1.33800	10.0000
115	1.57900	10.0000
120	1.85500	10.0000
125	2.16800	10.0000
130	2.52400	10.0000
135	2.92500	10.0000
140	3.37600	10.0000
145	3.88200	10.0000
150	4.44700	10.0000
155	5.07600	10.0000
160	5.77400	10.0000
165	6.54700	10.0000

170	7.39900	10.0000
175	8.33700	10.0000
180	9.36700	10.0000
185	10.49400	10.0000
190	11.72500	10.0000
195	13.06600	10.0000
200	14.52400	10.0000
205	16.10600	10.0000
210	17.81900	10.0000
215	19.67000	10.0000
220	21.66500	10.0000
225	23.81400	10.0000
230	26.12300	10.0000
235	28.60100	10.0000
240	31.25400	10.0000
245	34.09300	10.0000
250	37.12400	10.0000
255	40.35700	10.0000
260	43.80100	10.0000
265	47.46400	10.0000
270	51.35600	10.0000
275	55.48700	10.0000
280	59.86500	10.0000
285	64.50200	10.0000
290	69.40700	10.0000
295	74.59200	10.0000
300	80.06700	10.0000
305	85.84400	10.0000
310	91.93500	10.0000
315	98.35200	10.0000
320	105.10800	10.0000
325	112.21800	10.0000
80	0.42300	15.0000
85	0.51600	15.0000
90	0.62600	15.0000
95	0.75500	15.0000
100	0.90500	15.0000
105	1.07900	15.0000
110	1.28000	15.0000
115	1.51100	15.0000
120	1.77400	15.0000

125	2.07400	15.0000
130	2.41400	15.0000
135	2.79800	15.0000
140	3.22900	15.0000
145	3.71300	15.0000
150	4.25400	15.0000
155	4.85600	15.0000
160	5.52400	15.0000
165	6.26300	15.0000
170	7.07900	15.0000
175	7.97600	15.0000
180	8.96100	15.0000
185	10.04000	15.0000
190	11.21700	15.0000
195	12.50100	15.0000
200	13.89500	15.0000
205	15.40900	15.0000
210	17.04700	15.0000
215	18.81700	15.0000
220	20.72600	15.0000
225	22.78100	15.0000
230	24.98900	15.0000
235	27.35800	15.0000
240	29.89500	15.0000
245	32.60900	15.0000
250	35.50700	15.0000
255	38.59700	15.0000
260	41.88900	15.0000
265	45.38900	15.0000
270	49.10800	15.0000
275	53.05300	15.0000
280	57.23500	15.0000
285	61.66300	15.0000
290	66.34600	15.0000
295	71.29500	15.0000
300	76.51900	15.0000
305	82.03000	15.0000
310	87.83900	15.0000
315	93.95800	15.0000
320	100.39700	15.0000
325	107.17100	15.0000

80	0.40000	20.0000
85	0.48800	20.0000
90	0.59200	20.0000
95	0.71400	20.0000
100	0.85600	20.0000
105	1.02100	20.0000
110	1.21100	20.0000
115	1.42900	20.0000
120	1.67900	20.0000
125	1.96300	20.0000
130	2.28500	20.0000
135	2.64900	20.0000
140	3.05900	20.0000
145	3.51800	20.0000
150	4.03100	20.0000
155	4.60200	20.0000
160	5.23600	20.0000
165	5.93700	20.0000
170	6.71200	20.0000
175	7.56400	20.0000
180	8.49900	20.0000
185	9.52300	20.0000
190	10.64200	20.0000
195	11.86100	20.0000
200	13.18600	20.0000
205	14.62300	20.0000
210	16.17900	20.0000
215	17.86100	20.0000
220	19.67500	20.0000
225	21.62700	20.0000
230	23.72500	20.0000
235	25.97600	20.0000
240	28.38700	20.0000
245	30.96600	20.0000
250	33.71900	20.0000
255	36.65500	20.0000
260	39.78200	20.0000
265	43.10800	20.0000
270	46.64000	20.0000
275	50.38800	20.0000
280	54.36000	20.0000

285	58.56500	20.0000
290	63.01200	20.0000
295	67.71000	20.0000
300	72.66900	20.0000
305	77.89900	20.0000
310	83.41100	20.0000
315	89.21400	20.0000
320	95.32100	20.0000
325	101.74200	20.0000
80	0.37000	25.0000
85	0.45300	25.0000
90	0.55000	25.0000
95	0.66300	25.0000
100	0.79600	25.0000
105	0.95000	25.0000
110	1.12800	25.0000
115	1.33200	25.0000
120	1.56600	25.0000
125	1.83200	25.0000
130	2.13400	25.0000
135	2.47600	25.0000
140	2.86000	25.0000
145	3.29100	25.0000
150	3.77300	25.0000
155	4.31000	25.0000
160	4.90700	25.0000
165	5.56700	25.0000
170	6.29600	25.0000
175	7.09900	25.0000
180	7.98000	25.0000
185	8.94600	25.0000
190	10.00100	25.0000
195	11.15100	25.0000
200	12.40100	25.0000
205	13.75900	25.0000
210	15.22900	25.0000
215	16.81800	25.0000
220	18.53200	25.0000
225	20.37800	25.0000
230	22.36300	25.0000
235	24.49200	25.0000

240	26.77300	25.0000
245	29.21400	25.0000
250	31.82000	25.0000
255	34.60100	25.0000
260	37.56200	25.0000
265	40.71200	25.0000
270	44.05800	25.0000
275	47.60900	25.0000
280	51.37300	25.0000
285	55.35700	25.0000
290	59.57200	25.0000
295	64.02400	25.0000
300	68.72500	25.0000
305	73.68200	25.0000
310	78.90500	25.0000
315	84.40500	25.0000
320	90.19200	25.0000
325	96.27700	25.0000
160	4.52300	30.0000
165	5.13800	30.0000
170	5.81800	30.0000
175	6.56800	30.0000
180	7.39200	30.0000
185	8.29500	30.0000
190	9.28300	30.0000
195	10.36100	30.0000
200	11.53500	30.0000
205	12.81000	30.0000
210	14.19200	30.0000
215	15.68700	30.0000
220	17.30200	30.0000
225	19.04200	30.0000
230	20.91400	30.0000
235	22.92500	30.0000
240	25.08000	30.0000
245	27.38800	30.0000
250	29.85500	30.0000
255	32.48700	30.0000
260	35.29300	30.0000
265	38.28000	30.0000
270	41.45500	30.0000

275	44.82600	30.0000
280	48.40100	30.0000
285	52.18800	30.0000
290	56.19500	30.0000
295	60.42100	30.0000
300	64.90500	30.0000
305	69.62500	30.0000
310	74.60100	30.0000
315	79.84200	30.0000
320	85.35900	30.0000
325	91.16100	30.0000
80	0.465	2.8400
85	0.568	2.8400
90	0.689	2.8400
95	0.831	2.8400
100	0.996	2.8400
105	1.187	2.8400
110	1.408	2.8400
115	1.662	2.8400
120	1.951	2.8400
125	2.281	2.8400
130	2.655	2.8400
135	3.077	2.8400
140	3.552	2.8400
145	4.084	2.8400
150	4.679	2.8400
155	5.341	2.8400
160	6.076	2.8400
165	6.889	2.8400
170	7.786	2.8400
175	8.773	2.8400
180	9.857	2.8400
185	11.044	2.8400
190	12.340	2.8400
195	13.752	2.8400
200	15.287	2.8400
205	16.953	2.8400
210	18.756	2.8400
215	20.705	2.8400
220	22.808	2.8400
225	25.071	2.8400

230	27.504	2.8400
235	30.114	2.8400
240	32.911	2.8400
245	35.902	2.8400
250	39.098	2.8400
255	42.507	2.8400
260	46.138	2.8400
265	50.002	2.8400
270	54.108	2.8400
275	58.466	2.8400
280	63.088	2.8400
285	67.983	2.8400
290	73.163	2.8400
295	78.640	2.8400
300	84.426	2.8400
305	90.533	2.8400
310	96.974	2.8400
315	103.763	2.8400
320	110.914	2.8400
325	118.444	2.8400
80	0.457	5.5200
85	0.558	5.5200
90	0.677	5.5200
95	0.816	5.5200
100	0.979	5.5200
105	1.167	5.5200
110	1.384	5.5200
115	1.633	5.5200
120	1.917	5.5200
125	2.241	5.5200
130	2.609	5.5200
135	3.024	5.5200
140	3.490	5.5200
145	4.013	5.5200
150	4.597	5.5200
155	5.248	5.5200
160	5.969	5.5200
165	6.768	5.5200
170	7.650	5.5200
175	8.620	5.5200
180	9.685	5.5200

185	10.850	5.5200
190	12.124	5.5200
195	13.511	5.5200
200	15.019	5.5200
205	16.655	5.5200
210	18.427	5.5200
215	20.342	5.5200
220	22.407	5.5200
225	24.630	5.5200
230	27.019	5.5200
235	29.583	5.5200
240	32.329	5.5200
245	35.267	5.5200
250	38.405	5.5200
255	41.752	5.5200
260	45.318	5.5200
265	49.111	5.5200
270	53.142	5.5200
275	57.421	5.5200
280	61.957	5.5200
285	66.762	5.5200
290	71.845	5.5200
295	77.220	5.5200
300	82.896	5.5200
305	88.887	5.5200
310	95.206	5.5200
315	101.864	5.5200
320	108.877	5.5200
325	116.259	5.5200
80	0.449	8.0600
85	0.548	8.0600
90	0.665	8.0600
95	0.802	8.0600
100	0.961	8.0600
105	1.146	8.0600
110	1.359	8.0600
115	1.603	8.0600
120	1.883	8.0600
125	2.201	8.0600
130	2.562	8.0600
135	2.969	8.0600

140	3.427	8.0600
145	3.941	8.0600
150	4.514	8.0600
155	5.153	8.0600
160	5.862	8.0600
165	6.646	8.0600
170	7.512	8.0600
175	8.464	8.0600
180	9.510	8.0600
185	10.654	8.0600
190	11.904	8.0600
195	13.266	8.0600
200	14.746	8.0600
205	16.353	8.0600
210	18.092	8.0600
215	19.971	8.0600
220	21.998	8.0600
225	24.180	8.0600
230	26.525	8.0600
235	29.041	8.0600
240	31.737	8.0600
245	34.620	8.0600
250	37.699	8.0600
255	40.983	8.0600
260	44.481	8.0600
265	48.203	8.0600
270	52.157	8.0600
275	56.354	8.0600
280	60.803	8.0600
285	65.515	8.0600
290	70.500	8.0600
295	75.770	8.0600
300	81.335	8.0600
305	87.208	8.0600
310	93.401	8.0600
315	99.926	8.0600
320	106.797	8.0600
325	114.029	8.0600
80	0.441	10.4700
85	0.538	10.4700
90	0.653	10.4700

95	0.787	10.4700
100	0.943	10.4700
105	1.124	10.4700
110	1.333	10.4700
115	1.573	10.4700
120	1.848	10.4700
125	2.160	10.4700
130	2.514	10.4700
135	2.914	10.4700
140	3.363	10.4700
145	3.867	10.4700
150	4.430	10.4700
155	5.057	10.4700
160	5.752	10.4700
165	6.522	10.4700
170	7.371	10.4700
175	8.306	10.4700
180	9.331	10.4700
185	10.454	10.4700
190	11.681	10.4700
195	13.017	10.4700
200	14.469	10.4700
205	16.045	10.4700
210	17.751	10.4700
215	19.595	10.4700
220	21.583	10.4700
225	23.723	10.4700
230	26.024	10.4700
235	28.491	10.4700
240	31.135	10.4700
245	33.962	10.4700
250	36.982	10.4700
255	40.202	10.4700
260	43.633	10.4700
265	47.281	10.4700
270	51.158	10.4700
275	55.272	10.4700
280	59.633	10.4700
285	64.251	10.4700
290	69.137	10.4700
295	74.300	10.4700

300	79.753	10.4700
305	85.506	10.4700
310	91.572	10.4700
315	97.963	10.4700
320	104.691	10.4700
325	111.771	10.4700
80	0.432	12.7500
85	0.528	12.7500
90	0.640	12.7500
95	0.771	12.7500
100	0.925	12.7500
105	1.102	12.7500
110	1.307	12.7500
115	1.543	12.7500
120	1.812	12.7500
125	2.118	12.7500
130	2.456	12.7500
135	2.857	12.7500
140	3.298	12.7500
145	3.792	12.7500
150	4.344	12.7500
155	4.959	12.7500
160	5.641	12.7500
165	6.396	12.7500
170	7.229	12.7500
175	8.145	12.7500
180	9.151	12.7500
185	10.252	12.7500
190	11.454	12.7500
195	12.765	12.7500
200	14.189	12.7500
205	15.734	12.7500
210	17.407	12.7500
215	19.215	12.7500
220	21.164	12.7500
225	23.262	12.7500
230	25.517	12.7500
235	27.936	12.7500
240	30.528	12.7500
245	33.299	12.7500
250	36.259	12.7500

255	39.416	12.7500
260	42.777	12.7500
265	46.353	12.7500
270	50.152	12.7500
275	54.183	12.7500
280	58.456	12.7500
285	62.980	12.7500
290	67.766	12.7500
295	72.823	12.7500
300	78.163	12.7500
305	83.797	12.7500
310	89.736	12.7500
315	95.992	12.7500
320	102.578	12.7500
325	109.506	12.7500
80	0.423	14.9200
85	0.517	14.9200
90	0.627	14.9200
95	0.756	14.9200
100	0.906	14.9200
105	1.080	14.9200
110	1.281	14.9200
115	1.512	14.9200
120	1.775	14.9200
125	2.076	14.9200
130	2.416	14.9200
135	2.800	14.9200
140	3.232	14.9200
145	3.716	14.9200
150	4.257	14.9200
155	4.860	14.9200
160	5.528	14.9200
165	6.268	14.9200
170	7.084	14.9200
175	7.983	14.9200
180	8.968	14.9200
185	10.048	14.9200
190	11.226	14.9200
195	12.510	14.9200
200	13.907	14.9200
205	15.421	14.9200

210	17.061	14.9200
215	18.832	14.9200
220	20.742	14.9200
225	22.799	14.9200
230	25.009	14.9200
235	27.380	14.9200
240	29.919	14.9200
245	32.635	14.9200
250	35.535	14.9200
255	38.628	14.9200
260	41.922	14.9200
265	45.425	14.9200
270	49.147	14.9200
275	53.096	14.9200
280	57.281	14.9200
285	61.712	14.9200
290	66.399	14.9200
295	71.352	14.9200
300	76.581	14.9200
305	82.096	14.9200
310	87.910	14.9200
315	94.034	14.9200
320	100.479	14.9200
325	107.258	14.9200
80	0.414	16.9800
85	0.506	16.9800
90	0.613	16.9800
95	0.740	16.9800
100	0.887	16.9800
105	1.057	16.9800
110	1.254	16.9800
115	1.480	16.9800
120	1.738	16.9800
125	2.032	16.9800
130	2.365	16.9800
135	2.742	16.9800
140	3.165	16.9800
145	3.639	16.9800
150	4.169	16.9800
155	4.759	16.9800
160	5.414	16.9800

165	6.139	16.9800
170	6.939	16.9800
175	7.819	16.9800
180	8.785	16.9800
185	9.842	16.9800
190	10.997	16.9800
195	12.256	16.9800
200	13.624	16.9800
205	15.108	16.9800
210	16.714	16.9800
215	18.450	16.9800
220	20.322	16.9800
225	22.337	16.9800
230	24.502	16.9800
235	26.825	16.9800
240	29.314	16.9800
245	31.975	16.9800
250	34.816	16.9800
255	37.846	16.9800
260	41.073	16.9800
265	44.505	16.9800
270	48.151	16.9800
275	52.019	16.9800
280	56.119	16.9800
285	60.459	16.9800
290	65.049	16.9800
295	69.900	16.9800
300	75.020	16.9800
305	80.420	16.9800
310	86.112	16.9800
315	92.106	16.9800
320	98.415	16.9800
325	105.049	16.9800
80	0.405	18.9500
85	0.494	18.9500
90	0.600	18.9500
95	0.723	18.9500
100	0.867	18.9500
105	1.034	18.9500
110	1.226	18.9500
115	1.448	18.9500

120	1.700	18.9500
125	1.988	18.9500
130	2.314	18.9500
135	2.682	18.9500
140	3.097	18.9500
145	3.561	18.9500
150	4.080	18.9500
155	4.658	18.9500
160	5.300	18.9500
165	6.009	18.9500
170	6.793	18.9500
175	7.655	18.9500
180	8.601	18.9500
185	9.637	18.9500
190	10.768	18.9500
195	12.001	18.9500
200	13.341	18.9500
205	14.795	18.9500
210	16.369	18.9500
215	18.070	18.9500
220	19.904	18.9500
225	21.879	18.9500
230	24.001	18.9500
235	26.277	18.9500
240	28.715	18.9500
245	31.323	18.9500
250	34.107	18.9500
255	37.076	18.9500
260	40.238	18.9500
265	43.601	18.9500
270	47.173	18.9500
275	50.963	18.9500
280	54.980	18.9500
285	59.232	18.9500
290	63.729	18.9500
295	68.480	18.9500
300	73.495	18.9500
305	78.785	18.9500
310	84.359	18.9500
315	90.229	18.9500
320	96.406	18.9500

325	102.901	18.9500
80	0.395	20.8200
85	0.483	20.8200
90	0.586	20.8200
95	0.706	20.8200
100	0.847	20.8200
105	1.010	20.8200
110	1.198	20.8200
115	1.414	20.8200
120	1.662	20.8200
125	1.943	20.8200
130	2.262	20.8200
135	2.623	20.8200
140	3.028	20.8200
145	3.483	20.8200
150	3.991	20.8200
155	4.557	20.8200
160	5.185	20.8200
165	5.880	20.8200
170	6.647	20.8200
175	7.491	20.8200
180	8.418	20.8200
185	9.432	20.8200
190	10.541	20.8200
195	11.748	20.8200
200	13.061	20.8200
205	14.486	20.8200
210	16.028	20.8200
215	17.695	20.8200
220	19.492	20.8200
225	21.427	20.8200
230	23.507	20.8200
235	25.738	20.8200
240	28.128	20.8200
245	30.683	20.8200
250	33.412	20.8200
255	36.323	20.8200
260	39.422	20.8200
265	42.718	20.8200
270	46.220	20.8200
275	49.935	20.8200

280	53.872	20.8200
285	58.040	20.8200
290	62.447	20.8200
295	67.104	20.8200
300	72.020	20.8200
305	77.203	20.8200
310	82.666	20.8200
315	88.418	20.8200
320	94.470	20.8200
325	100.834	20.8200
80	0.385	22.6100
85	0.470	22.6100
90	0.571	22.6100
95	0.689	22.6100
100	0.826	22.6100
105	0.986	22.6100
110	1.169	22.6100
115	1.381	22.6100
120	1.622	22.6100
125	1.898	22.6100
130	2.210	22.6100
135	2.562	22.6100
140	2.959	22.6100
145	3.404	22.6100
150	3.901	22.6100
155	4.454	22.6100
160	5.069	22.6100
165	5.750	22.6100
170	6.501	22.6100
175	7.328	22.6100
180	8.235	22.6100
185	9.229	22.6100
190	10.315	22.6100
195	11.498	22.6100
200	12.785	22.6100
205	14.181	22.6100
210	15.692	22.6100
215	17.326	22.6100
220	19.088	22.6100
225	20.985	22.6100
230	23.023	22.6100

235	25.211	22.6100
240	27.554	22.6100
245	30.060	22.6100
250	32.736	22.6100
255	35.590	22.6100
260	38.630	22.6100
265	41.863	22.6100
270	45.297	22.6100
275	48.941	22.6100
280	52.803	22.6100
285	56.891	22.6100
290	61.214	22.6100
295	65.782	22.6100
300	70.603	22.6100
305	75.688	22.6100
310	81.046	22.6100
315	86.687	22.6100
320	92.622	22.6100
325	98.863	22.6100
80	0.375	24.3200
85	0.458	24.3200
90	0.556	24.3200
95	0.671	24.3200
100	0.805	24.3200
105	0.961	24.3200
110	1.140	24.3200
115	1.346	24.3200
120	1.583	24.3200
125	1.851	24.3200
130	2.156	24.3200
135	2.501	24.3200
140	2.889	24.3200
145	3.324	24.3200
150	3.810	24.3200
155	4.352	24.3200
160	4.954	24.3200
165	5.620	24.3200
170	6.355	24.3200
175	7.165	24.3200
180	8.054	24.3200
185	9.027	24.3200

190	10.091	24.3200
195	11.251	24.3200
200	12.512	24.3200
205	13.880	24.3200
210	15.362	24.3200
215	16.964	24.3200
220	18.691	24.3200
225	20.552	24.3200
230	22.551	24.3200
235	24.697	24.3200
240	26.996	24.3200
245	29.455	24.3200
250	32.081	24.3200
255	34.882	24.3200
260	37.865	24.3200
265	41.038	24.3200
270	44.409	24.3200
275	47.986	24.3200
280	51.777	24.3200
285	55.791	24.3200
290	60.035	24.3200
295	64.520	24.3200
300	69.254	24.3200
305	74.246	24.3200
310	79.507	24.3200
315	85.046	24.3200
320	90.874	24.3200
325	97.002	24.3200
80	0.364	25.9600
85	0.445	25.9600
90	0.540	25.9600
95	0.652	25.9600
100	0.783	25.9600
105	0.935	25.9600
110	1.110	25.9600
115	1.311	25.9600
120	1.542	25.9600
125	1.804	25.9600
130	2.102	25.9600
135	2.439	25.9600
140	2.818	25.9600

145	3.244	25.9600
150	3.719	25.9600
155	4.249	25.9600
160	4.838	25.9600
165	5.490	25.9600
170	6.210	25.9600
175	7.003	25.9600
180	7.873	25.9600
185	8.827	25.9600
190	9.870	25.9600
195	11.006	25.9600
200	12.242	25.9600
205	13.584	25.9600
210	15.037	25.9600
215	16.608	25.9600
220	18.303	25.9600
225	20.129	25.9600
230	22.091	25.9600
235	24.198	25.9600
240	26.454	25.9600
245	28.869	25.9600
250	31.448	25.9600
255	34.199	25.9600
260	37.129	25.9600
265	40.246	25.9600
270	43.558	25.9600
275	47.073	25.9600
280	50.798	25.9600
285	54.742	25.9600
290	58.914	25.9600
295	63.322	25.9600
300	67.976	25.9600
305	72.884	25.9600
310	78.055	25.9600
315	83.501	25.9600
320	89.231	25.9600
325	95.256	25.9600
85	0.432	27.5300
90	0.524	27.5300
95	0.633	27.5300
100	0.761	27.5300

105	0.908	27.5300
110	1.079	27.5300
115	1.275	27.5300
120	1.500	27.5300
125	1.756	27.5300
130	2.047	27.5300
135	2.376	27.5300
140	2.746	27.5300
145	3.162	27.5300
150	3.627	27.5300
155	4.145	27.5300
160	4.721	27.5300
165	5.359	27.5300
170	6.064	27.5300
175	6.840	27.5300
180	7.693	27.5300
185	8.628	27.5300
190	9.649	27.5300
195	10.764	27.5300
200	11.976	27.5300
205	13.292	27.5300
210	14.718	27.5300
215	16.260	27.5300
220	17.923	27.5300
225	19.716	27.5300
230	21.643	27.5300
235	23.712	27.5300
240	25.929	27.5300
245	28.301	27.5300
250	30.835	27.5300
255	33.540	27.5300
260	36.420	27.5300
265	39.486	27.5300
270	42.743	27.5300
275	46.200	27.5300
280	49.865	27.5300
285	53.746	27.5300
290	57.851	27.5300
295	62.189	27.5300
300	66.769	27.5300
305	71.600	27.5300

310	76.692	27.5300
315	82.053	27.5300
320	87.695	27.5300
325	93.628	27.5300
135	2.311	29.0300
140	2.673	29.0300
145	3.079	29.0300
150	3.533	29.0300
155	4.040	29.0300
160	4.603	29.0300
165	5.227	29.0300
170	5.917	29.0300
175	6.677	29.0300
180	7.513	29.0300
185	8.428	29.0300
190	9.430	29.0300
195	10.522	29.0300
200	11.711	29.0300
205	13.002	29.0300
210	14.402	29.0300
215	15.915	29.0300
220	17.549	29.0300
225	19.310	29.0300
230	21.203	29.0300
235	23.237	29.0300
240	25.416	29.0300
245	27.749	29.0300
250	30.242	29.0300
255	32.902	29.0300
260	35.737	29.0300
265	38.754	29.0300
270	41.961	29.0300
275	45.365	29.0300
280	48.974	29.0300
285	52.797	29.0300
290	56.841	29.0300
295	61.116	29.0300
300	65.630	29.0300
305	70.392	29.0300
310	75.412	29.0300
315	80.698	29.0300

320	86.262	29.0300
325	92.113	29.0300
170	5.768	30.4700
175	6.512	30.4700
180	7.330	30.4700
185	8.227	30.4700
190	9.209	30.4700
195	10.280	30.4700
200	11.446	30.4700
205	12.713	30.4700
210	14.087	30.4700
215	15.573	30.4700
220	17.178	30.4700
225	18.908	30.4700
230	20.770	30.4700
235	22.769	30.4700
240	24.913	30.4700
245	27.209	30.4700
250	29.662	30.4700
255	32.282	30.4700
260	35.074	30.4700
265	38.046	30.4700
270	41.205	30.4700
275	44.560	30.4700
280	48.119	30.4700
285	51.889	30.4700
290	55.878	30.4700
295	60.096	30.4700
300	64.550	30.4700
305	69.250	30.4700
310	74.206	30.4700
315	79.426	30.4700
320	84.920	30.4700
325	90.699	30.4700
200	11.178	31.8600
205	12.421	31.8600
210	13.769	31.8600
215	15.229	31.8600
220	16.806	31.8600
225	18.506	31.8600
230	20.337	31.8600

235	22.304	31.8600
240	24.413	31.8600
245	26.673	31.8600
250	29.090	31.8600
255	31.670	31.8600
260	34.421	31.8600
265	37.351	31.8600
270	40.467	31.8600
275	43.777	31.8600
280	47.289	31.8600
285	51.010	31.8600
290	54.949	31.8600
295	59.114	31.8600
300	63.515	31.8600
305	68.160	31.8600
310	73.058	31.8600
315	78.219	31.8600
320	83.653	31.8600
325	89.369	31.8600
225	18.098	33.1900
230	19.898	33.1900
235	21.833	33.1900
240	23.909	33.1900
245	26.134	33.1900
250	28.514	33.1900
255	31.057	33.1900
260	33.770	33.1900
265	36.660	33.1900
270	39.734	33.1900
275	43.001	33.1900
280	46.468	33.1900
285	50.144	33.1900
290	54.037	33.1900
295	58.154	33.1900
300	62.506	33.1900
305	67.100	33.1900
310	71.947	33.1900
315	77.055	33.1900
320	82.435	33.1900
325	88.096	33.1900
250	27.925	34.4700

255	30.431	34.4700
260	33.105	34.4700
265	35.955	34.4700
270	38.989	34.4700
275	42.215	34.4700
280	45.639	34.4700
285	49.271	34.4700
290	53.119	34.4700
295	57.191	34.4700
300	61.497	34.4700
305	66.044	34.4700
310	70.842	34.4700
315	75.902	34.4700
320	81.233	34.4700
325	86.844	34.4700
260	32.813	35.0000
265	35.646	35.0000
270	38.663	35.0000
275	41.870	35.0000
280	45.277	35.0000
285	48.891	35.0000
290	52.719	35.0000
295	56.772	35.0000
300	61.058	35.0000
305	65.586	35.0000
310	70.365	35.0000
315	75.404	35.0000
320	80.715	35.0000
325	86.306	35.0000
270	38.213	35.7000
275	41.396	35.7000
280	44.778	35.7000
285	48.366	35.7000
290	52.170	35.7000
295	56.197	35.7000
300	60.456	35.7000
305	64.957	35.7000
310	69.710	35.7000
315	74.722	35.7000
320	80.006	35.7000
325	85.570	35.7000

290	51.156	36.8900
295	55.136	36.8900
300	59.348	36.8900
305	63.801	36.8900
310	68.505	36.8900
315	73.469	36.8900
320	78.704	36.8900
325	84.220	36.8900
80	0.353	27.47200
85	0.431	27.59600
90	0.522	27.72500
95	0.629	27.85900
100	0.754	27.99800
105	0.897	28.14300
110	1.063	28.29300
115	1.253	28.44800
120	1.470	28.60800
125	1.716	28.77400
130	1.994	28.94500
135	2.308	29.12200
140	2.659	29.30400
145	3.053	29.49100
150	3.491	29.68300
155	3.978	29.88100
160	4.516	30.08400
165	5.111	30.29200
170	5.765	30.50500
175	6.483	30.72400
180	7.268	30.94800
185	8.125	31.17800
190	9.058	31.41300
195	10.072	31.65300
200	11.170	31.89800
205	12.357	32.14900
210	13.639	32.40500
215	15.019	32.66600
220	16.502	32.93200
225	18.093	33.20400
230	19.797	33.4810
235	21.619	33.76400
240	23.564	34.05200

245	25.636	34.34500
250	27.841	34.64300
255	30.183	34.94700
260	32.668	35.25600
265	35.301	35.57000
270	38.086	35.88900
275	41.029	36.21400
280	44.133	36.54400
285	47.404	36.88000
290	50.845	37.22100
295	54.461	37.56700
300	58.253	37.91800
305	62.226	38.27500
310	66.379	38.63700
315	70.713	39.00400
320	75.227	39.37600
325	79.918	39.75400

National Research Council (1928)

Temperature (ºC)	Pressure (bars)	Composition (wt% NaCl)
0.01	0.00467	26.25
10	0.00920	26.3
20	0.01760	26.4
30	0.03187	26.5
40	0.05547	26.65
50	0.09267	26.85
60	0.14934	27.05
70	0.23334	27.3
80	0.35361	27.6
90	0.52215	27.85
100	0.75202	28.15
108.67	1.01336	28.4
110	1.06003	28.45

Keevil (1942)

Temperature (ºC)	Pressure (bars)	Composition (wt% NaCl)
183	7.36633	30.66
205.1	11.91582	31.46
230.2	19.54559	32.64
246.7	25.41231	33.61
254.6	27.87451	34.18
299.3	56.77240	37.30
327.3	79.54013	39.74
344.4	97.56584	41.25
354.3	107.80980	42.08
385.7	146.92125	45.54
410	181.27043	47.33
442.5	233.14883	50.32
467.5	272.56425	52.08
485.5	298.30080	54.53
514.2	339.54008	56.38
550.5	375.00383	62.03
600	393.85028	69.35
646.2	373.38263	76.79

Khaibullin and Borisov (1966)

Temperature (ºC)	Pressure (bars)	Composition (wt% NaCl)
100	0.98067	1
110	1.45138	1
120	1.99075	1
130	2.70664	1
140	3.59904	1
150	4.71700	1
160	6.11935	1
170	7.89435	1
180	9.90472	1
190	12.35638	1
200	15.39644	1
210	18.92683	1
220	22.84949	1
230	28.83155	1
240	33.34261	1
250	39.52080	1
260	46.48352	1
270	54.52497	1
280	63.64516	1
290	72.07888	1
300	85.31786	1
310	97.57617	1
320	111.79581	1
330	127.48645	1
340	144.94229	1
350	164.45752	1
360	185.14955	1
370	207.90098	1
380	232.90794	1
386	248.59858	1
100	1.01008	2
110	1.42196	2
120	1.97114	2
130	2.68702	2
140	3.56962	2
150	4.68758	2

160	6.08012	2
170	7.84532	2
180	9.90472	2
190	12.25831	2
200	15.39644	2
210	18.73070	2
220	22.75143	2
230	27.55669	2
240	33.14648	2
250	39.32467	2
260	46.18932	2
270	54.13271	2
280	63.25289	2
290	73.54988	2
300	84.82752	2
310	96.79164	2
320	110.81515	2
330	126.50579	2
340	144.15776	2
350	162.59426	2
360	182.50176	2
370	206.42998	2
380	230.84854	2
390	256.93423	2
392	262.32789	2
100	0.99047	3.5
110	1.39254	3.5
120	1.89268	3.5
130	2.65760	3.5
140	3.53039	3.5
150	4.64835	3.5
160	6.03109	3.5
170	7.76687	3.5
180	9.79684	3.5
190	12.16025	3.5
200	15.20031	3.5
210	18.53457	3.5
220	22.45723	3.5
230	27.26249	3.5
240	32.85228	3.5
250	38.93240	3.5

260	45.60092	3.5
270	53.34818	3.5
280	62.37029	3.5
290	72.56921	3.5
300	83.84686	3.5
310	95.32064	3.5
320	109.34415	3.5
330	125.03479	3.5
340	142.19643	3.5
350	161.02519	3.5
360	181.52109	3.5
370	204.95899	3.5
380	228.00461	3.5
390	253.50190	3.5
400	280.96052	3.5
402.5	288.31551	3.5
100	0.98067	5
110	1.37293	5
120	1.91230	5
130	2.62818	5
140	3.49117	5
150	4.59932	5
160	5.98206	5
170	7.68841	5
180	9.70858	5
190	12.06218	5
200	15.10224	5
210	18.33844	5
220	22.35916	5
230	27.06635	5
240	32.46001	5
250	38.54013	5
260	45.01252	5
270	52.56364	5
280	61.58576	5
290	71.68661	5
300	82.86619	5
310	94.33997	5
320	108.06928	5
330	123.56379	5
340	140.72543	5

350	159.35806	5
360	179.16750	5
370	202.01699	5
380	224.86648	5
390	250.06958	5
400	278.50886	5
410	306.45781	5
417.5	331.17057	5
100	0.91202	7.5
110	1.34351	7.5
120	1.88288	7.5
130	2.56934	7.5
140	3.43233	7.5
150	4.52087	7.5
160	5.89380	7.5
170	7.58054	7.5
180	9.58110	7.5
190	11.86605	7.5
200	14.80804	7.5
210	18.04424	7.5
220	21.86883	7.5
230	26.47796	7.5
240	31.87161	7.5
250	37.85367	7.5
260	44.22799	7.5
270	51.58298	7.5
280	50.30811	7.5
290	70.11755	7.5
300	81.39520	7.5
310	92.67284	7.5
320	105.71569	7.5
330	121.11213	7.5
340	137.78343	7.5
350	156.71027	7.5
360	175.53904	7.5
370	196.62333	7.5
380	219.86509	7.5
390	244.67592	7.5
400	271.74227	7.5
410	299.69122	7.5
420	331.85704	7.5

430	360.98279	7.5
435	389.81434	7.5
100	0.93163	10
110	1.32390	10
120	1.84365	10
130	2.52031	10
140	3.37349	10
150	4.45222	10
160	5.81534	10
170	7.47267	10
180	9.46342	10
190	11.76798	10
200	14.51384	10
210	17.55390	10
220	21.37850	10
230	25.88956	10
240	31.18515	10
250	37.16720	10
260	43.44346	10
270	50.60231	10
280	58.93797	10
290	68.64655	10
300	79.72806	10
310	91.00571	10
320	101.89109	10
330	118.85660	10
340	135.52790	10
350	153.47407	10
360	171.91057	10
370	192.79874	10
380	215.35403	10
390	239.28226	10
400	264.77955	10
410	293.41497	10
420	324.99238	10
430	358.13886	10
100	0.88260	15
110	1.25525	15
120	1.76520	15
130	2.45166	15
140	3.27542	15

150	4.31493	15
160	5.63882	15
170	7.25692	15
180	9.20844	15
190	11.47378	15
200	14.02351	15
210	17.06357	15
220	20.59397	15
230	25.88956	15
240	30.00835	15
250	35.79427	15
260	41.77633	15
270	48.54292	15
280	56.38824	15
290	65.60649	15
300	76.29574	15
310	87.86758	15
320	99.83170	15
330	114.24747	15
340	129.74198	15
350	146.70748	15
360	164.55559	15
370	185.05149	15
380	207.31258	15
390	230.45628	15
400	254.97290	15
410	281.94119	15
420	312.04760	15
430	342.64435	15
440	374.31983	15
100	0.83357	20
110	1.17680	20
120	1.70636	20
130	2.35360	20
140	3.13813	20
150	4.11879	20
160	5.42308	20
170	7.01175	20
180	8.86521	20
190	10.98345	20
200	13.53318	20

210	16.47517	20
220	20.00557	20
230	24.22243	20
240	29.02768	20
250	34.51941	20
260	40.30533	20
270	46.97385	20
280	54.62304	20
290	63.35096	20
300	73.45181	20
310	84.53332	20
320	96.30130	20
330	110.03061	20
340	124.74059	20
350	140.52929	20
360	158.37740	20
370	178.28490	20
380	199.85953	20
390	221.33609	20
400	244.18559	20
410	271.84034	20
420	298.80863	20
430	328.03244	20
440	357.94273	20
100	0.78453	25
110	1.11796	25
120	1.61810	25
130	2.25553	25
140	3.00083	25
150	3.93247	25
160	5.20733	25
170	6.72736	25
180	8.51217	25
190	10.59118	25
200	12.84671	25
210	15.88677	25
220	19.31910	25
230	23.33983	25
240	27.94895	25
250	33.34261	25
260	39.12853	25

270	45.60092	25
280	52.95591	25
290	61.48770	25
300	71.09821	25
310	81.39520	25
320	92.18251	25
330	104.14662	25
340	117.67980	25
350	133.37044	25
360	151.51274	25
370	170.34151	25
380	191.72001	25
390	212.80431	25
400	235.35960	25
410	260.36656	25
420	288.11938	25
430	316.95093	25
440	347.84188	25

Knight and Bodnar (1989)

Temperature (ºC)	Pressure (bars)	Composition (wt% NaCl)
374	220	0
405	298	3.2
404	298	3.2
421	337	5
421	337	5
467	458	10
466	458	10
513	598	15
514	598	15
566	755	20
565	755	20
611	840	22.5
668	945	25
664	945	25
730	1184	27.5
729	1184	27.5

Pitzer and Pabalan (1986)

Temperature (ºC)	Pressure (bars)	Composition (wt% NaCl)
800	0.0005	100

APPENDIX B

Input Code Used by SAS for Regression

```
options ls=85;

data d1;
 infile 'C:X.txt'  dlm='09'x firstobs=2 missover;
 input t p x;
 t=t;
 t2=t*t;
 t3=t2*t;
 t4=t3*t;
 t5=t4*t;
 t6=t5*t;
 t7=t6*t;
 t8=t7*t;
 t9=t8*t;
 t10=t9*t;
 x=x;
 x2=x*x;
 x3=x2*x;
 x4=x3*x;
 x5=x4*x;
 x6=x5*x;
 x7=x6*x;
 x8=x7*x;
 xt=x*t;
 xxt=x2*t;
 xtt=x*t2;
 xxxt=x3*t;
 xxtt=x2*t2;
 xttt=x*t3;
 xxxxt=x4*t;
 xxxtt=x3*t2;
 xxttt=x2*t3;
 xtttt=x*t4;
 xxxxxt=x5*t;
 xxxxtt=x4*t2;
 xxxttt=x3*t3;
 xxtttt=x2*t4;
 xttttt=x*t5;
 xxxxxxt=x6*t;
 xxxxxtt=x5*t2;
 xxxxttt=x4*t3;
 xxxttttt=x3*t4;
```

```
 xxttttt=x2*t5;
 xtttttt=x*t6;
 xxxxxxxt=x7*t;
 xxxxxxtt=x6*t2;
 xxxxxttt=x5*t3;
 xxxxtttt=x4*t4;
 xxxttttt=x3*t5;
 xxtttttt=x2*t6;
 xtttttttt=x*t7;
 logp=log10(p);
 w1=(((1.0001-x)/1.0001)*(2.5/t));
 index=_n_;
run;

title1 'Regression model with weight w1';
*----------------------------------------;
PROC reg data=d1 outest=param1;
model logp=t t2 t3 t4 t5 t6 t7 x x2 x3 x4 x5 x6 x7 xt xxt
xtt xxxt xxtt xttt xxxxt xxxtt xxttt xtttt xxxxxt xxxxtt
xxxttt xxtttt xttttt xxxxxxt xxxxxtt xxxxttt xxxtttt
xxttttt xtttttt / selection=backward;
weight w1;
 output out=bw1 r=resid1 p=yhatw1;
run;
data predw1;
 set bw1 (keep=  x t p logp yhatw1 resid1 index);
 phatw1=10**yhatw1;
 resw1=p-phatw1;
 res_p1=(resw1/p)*100;
run;
proc print data=param1;
format intercept t t2 t3 t4 t5 t6 t7 t8 x x2 x3 x4 x5 x6 x7
x8 xt xxt xtt xxxt xxtt xttt xxxxt xxxtt xxttt xtttt xxxxxt
xxxxtt xxxttt xxtttt xttttt xxxxxxt xxxxxtt xxxxttt xxxtttt
xxttttt xtttttt comma20.19;
run;


title1 ' ';

*               begin merging the residual from all models
;
*
_____________________________________________;
data b4b4w1;
 merge predw1;
 by index;
```

```
run;

data all;
 merge b4b4w1;
 by index;
run;


*                begin creating categories for levels of x
and t ;
*
_____________________________________________________;
data all_cat;
 set all;
if (t<100) then do;
   t_plot=1;
   t_cat='<100';
   end;
  else if (t<150) then do ;
   t_plot=2;
   t_cat='<150';
  end;
  else if (t<200) then do;
   t_plot=3;
   t_cat='<200';
  end;
  else if (t<250) then do;
   t_plot=4;
   t_cat='<250';
  end;
  else if (t<300) then do;
   t_plot=5;
   t_cat='<300';
  end;
  else if (t<350) then do;
   t_plot=6;
   t_cat='<350';
  end;
  else if (t<400) then do;
   t_plot=7;
   t_cat='<400';
  end;
  else do ;
   t_plot=8;
   t_cat='>=400';
  end;
```

```
if (x=0) then do;
   x_plot=1;
   x_cat='=0   ';
  end;
  else if (x<0.25) then do;
   x_plot=2;
   x_cat='<.25  ';
  end;
  else if (x<0.5) then do;
   x_plot=3;
   x_cat='<.5  ';
  end;
  else if (x<10) then do;
   x_plot=4;
   x_cat='<10  ';
  end;
  else if (x<15) then do;
   x_plot=5;
   x_cat='<15  ';
  end;
  else if (x<25) then do;
   x_plot=6;
   x_cat='<25  ';
  end;
  else do;
   x_plot=7;
   x_cat='>=25  ';
  end;
run;

PROC FREQ ;
  TABLES t_cat / norow nocol nopct;
RUN;
PROC FREQ ;
  TABLES x_cat / norow nocol nopct;
RUN;
data test;
set all_cat (keep=t p x phatw1 resw1 res_p1);
run;
Proc sort;
by descending x;
run;
* To print the residuals;
proc print;
run;
*                        begin residual plots;
```

```
*                          ____________________;
data short;
set all_cat;
if t<1100;
run;
title1 'Residual Plots';
* --------------------;
data short;
set all_cat;
if t<1100;
run;

title1 'Residual Plots';
* --------------------;
proc plot data=all_cat;
 plot resw1  * (x t)/VREF=0;
 plot resw1*x=t_plot /VREF=0;
 plot resw1*t=x_plot/VREF=0;
run;
proc plot data=short;
 plot resw1  *  t/VREF=0;
 plot resw1*t=x_plot/VREF=0;
run;
title1 'Residual in percent Plots';
* -------------------------------;

title1 'Residual in logarithm Plots';
* ----------------------------------;
proc plot data=all_cat;
 plot residw1  * (x t)/VREF=0;
 plot resid*x=t_plot/VREF=0 ;
 plot resid*t=x_plot/VREF=0;
run;
data datax5;
set test;
if x=.0000;
run;
proc plot data=datax5;
 plot resw1 * t/VREF=0;
run;
proc plot data=datax5;
 plot res_p1 * t/VREF=0;
run;
quit;
```

VITA

Allen Bradley Atkinson Jr "Brad"

aatkinso@vt.edu
Virginia Tech
4060A Derring Hall
Blacksburg, Virginia 24061
(540) 231-8829

Education

August 2000- July 2002
Master of Science Candidate
Virginia Polytechnic Institute and State University Blacksburg, Virginia

- Thesis title: A Model for the PTX Properties of H_2O-NaCl
- Thesis completion date: July 2002 (in process of submission)
- Advisor: Dr. Robert J. Bodnar
- Research in PTX (pressure, temperature and composition) properties and phase equilibria of NaCl-H_2O system with emphasis on developing a statistical model to predict the vapor pressure of water as a function of temperature and salinity.
- Defended thesis on July 16 2002.

May 1997-Dec 1999
Bachelor of Science, Geology
Virginia Polytechnic Institute and State University Blacksburg, Virginia

- GPA: 2.9, 3.0 in Major
- Specialized studies in Advanced Structural Geology Field Methods, Environmental Geology, Geographic Information Systems, and Remote Sensing.

August 1994 – May 1997
Virginia Western Community College Roanoke, Virginia

- General Science Major

Relevant Experience

January 2001-May 2002
Graduate Teaching Assistant, Resource Geology
Department of Geological Sciences, Virginia Tech

- **Responsible for preparing and lecturing three laboratory sections per week.**

June 2000 – December 2000
Laboratory Technician, Fluid Inclusions Research Lab

Department of Geological Sciences, Virginia Tech
Supervisor: Dr. Robert J. Bodnar

- **Prepared doubly polished thin-section rock samples for fluid inclusion studies.**
- **Fabricated test tubes used in synthetic fluid inclusion studies.**

March 2000 – June 2000
Computer Technician, Volunteer
Department of Computer Engineering, Virginia Tech Blacksburg, Virginia
Supervisor: Allison Barth

- **Provided computer hardware and software support.**
- **Built and maintained local area network systems.**

January 2000 – May 2000
Teaching Assistant-Assistant
Department of Geological Sciences, Virginia Tech Blacksburg, Virginia

- **Assisted with laboratory instruction for a physical geology section.**

September 1999 – March 2000
Under Graduate Researcher
Department of Geological Sciences, Virginia Tech Blacksburg, Virginia

- **Studied NaCl-H_2O systems with computer modeling to derive a previously unknown relationship where vapor pressure is a function of temperature and salinity.**

November 1999 - April 2000
Assistant Geologist, Orndorf Consulting **Blacksburg, Virginia**
Supervisor: William Orndorf

- **Participated in project to evaluate karst areas of Southwest Virginia.**
- **Surveyed land and sub-terrain spaces.**
- **Entered survey-point data gathered by fellow surveyors into three-dimensional mapping/modeling program.**
- **Collected soil and ground water samples.**
- **Performed dye traces to analyze ground water flow.**

February 2000 – July 2000
Level I and II Rescue Training: National Cave Rescue Commission

- Situational group problem solving associated with injured party extraction methods.

Computer and Software: Experienced user of Windows, Excel, Word, Access, Statistica, SAS, Arcview, ERDAS, Mathematica, Illustrator, and Photoshop.

Professional Meeting Abstracts:

Atkinson, A.B., 2001, Energy release during explosive eruptions: a look into the thermodynamics of water in silicate melts; Virginia Tech 6th annual Geological Sciences Student Research Symposium, Abstracts with Programs.

Atkinson, A.B., 2002, Development of a model for the PTX properties of H2O-NaCl; Virginia Tech 7th annual Geological Sciences Student Research Symposium, Abstracts with Programs.

Atkinson, A.B., Bodnar, R.J., Anderson-Cook, C.M. and Zahran, A., 2002, A Model for the PTX Properties of H_2O-NaCl; Eighth Biennial Pan-American Conference on Research on Fluid Inclusions, Program with Abstracts; Halifax, Nova Scotia.